Universität Rostock Traditio et Innovatio

Low-Cost Adsorptive Technologies: Batch Reactor and Fixed-Bed Column Experiments for the Removal of Phosphate from Wastewater

Cumulative dissertation

For obtaining the academic degree of Doctor of Engineering (Dr.-Ing.)

at the Faculty of Agricultural and Environmental Sciences of the University of Rostock

Submitted by:

Dereje Tadesse Mekonnen (BSc, M.Sc.)

Rostock, 2023

https://doi.org/10.18453/rosdok_id00004293

Scientific Supervisors:

Prof. Dr. Bernd Lennartz, Faculty of Agriculture and Environmental Sciences, University of Rostock, Justus Von Liebig Weg 6, 18051 Rostock, Germany.

Prof. Dr.-Ing Esayas Alemayehu, Faculty of Civil and Environmental Engineering, Jimma Instituted of Technology, Jimma University, P. O. Box 378, Jimma, Ethiopia.

Reviewers:

Prof. Dr. Bernd Lennartz, Faculty of Agriculture and Environmental Sciences, University of Rostock, Justus Von Liebig Weg 6, 18051 Rostock, Germany.

Prof. Dr.ir. Bart Van Der Bruggen, Katholieke Universiteit Leuven Department of Chemical Engineering Celestijnenlaan 200f B-3001 Heverlee (Leuven) Belgium

Prof. Dr.-Ing Esayas Alemayehu, Faculty of Civil and Environmental Engineering, Jimma Instituted of Technology, Jimma University, P. O. Box 378, Jimma, Ethiopia.

Date of Submission: March 1, 2022

Date of Defense: March 31, 2023

Eidesstattliche Erklärung

Hiermit erkläre ich durch eigenhändige Unterschrift, die vorliegende Dissertation selbstständig verfasst und keine anderen als die angegebenen Quellen und Hilfsmittel verwendet zu haben. Die aus den Quellen direkt oder indirekt übernommenen Gedanken sind als solche kenntlich gemacht. Die Dissertation ist in dieser Form noch keiner anderen Prüfungsbehörde vorgelegt worden.

Jimma, 05.01.2022 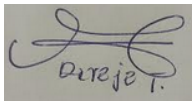

Ort, Datum Unterschrift der Doktorandin/des Doktoranden

Dedication

I am dedicating this Ph.D. thesis to four beloved people who have meant and continue to mean so much to me. First and foremost, my beloved wife, Yeamanuelwork Anbessei (BSc in Nursing), who has been a constant source of support and encouragement during the challenges of PhD work. Without your constant support this thesis paper was not possible. I am truly thankful for having you in my life. Next, my lovely kids Emanda Dereje and, (the twins: Mariyamawit (Nani) and Abigiya (Koki) Dereje), who I always love you unconditionally and that your childhood happiness has encouraged me to work hard for the things that I aspire to achieve.

Preface

The work reported in this thesis, including three manuscripts published in peer-reviewed journals, form the basis for the application for the PhD - degree of doctor engineer (Dr.-Ing) at the University of Rostock, Faculty of Agricultural and Environmental Sciences, Chair of Soil Physics. The manuscripts and materials presented in this dissertation describe the phosphate removal methods from aqueous solution employing readily available and low-cost adsorbents. In low-income countries like Ethiopia, where advanced phosphate removal technologies are not affordable, the use of low-cost adsorbents may pave the way for an effective wastewater treatment.

The dissertation starts with a brief introduction and background to water pollution and, appropriate phosphate removal methods. Next, phosphate contamination of surface water bodies and its impact on aquatic lives has been discussed. In the following chapters (Chapter 2, 3, and 4), the sustainability of phosphate removal techniques using low-cost (i.e., leftover coal, pumice, and scoria) adsorbents by slurry batch and fixed-bed column adsorption experiments were analyzed. Further, the effects of competitive anions on phosphate removal have been discussed, and the impact of design parameters on the removal capacity of the adsorbent are, likewise, considered. Finally, Chapter 5 summarizes the findings obtained from the study drawing definite conclusion and suggesting future works.

Acknowledgments

First and above all, I would like to thank my Almighty God for giving me the potential and strength to finish all my works during my ups and downs. Then, I would like to express my sincere appreciation and thanks to the people who have supported me throughout my Ph.D. research journey.

First and foremost, I would like to thank and acknowledge my supervisors Prof. Dr. Bernd Lennartz (Professor of Soil physics at Faculty of Agricultural and Environmental Sciences University of Rostock, Germany) and Prof. Dr.-Ing Esayas Alemayehu (Professor of water and Environmental Engineering at the Faculty of Civil and Environmental Engineering, Jimma Institute of Technology, Jimma University, Ethiopia) for their trust and providing me the opportunity to continue my Ph.D. research work under their supervision. I admire their technical guidance and close personal support from the beginning to the end of this work. Without their guidance, my research work would not be actual.

Next, I use this chance to acknowledge my families, friends, colleagues, and those individuals who were with me during laboratory experiments, especially Miss Evelyn Boltzmann, Dr. Stefan Koehler, and other staff members in the laboratory at the University of Rostock, Germany, for their kind assistance and supports.

Besides, I would like to thank MoE and DAAD for sponsoring me during my study and Jimma University Jimma Institute of Technology community, School of Chemical Engineering, for the direct and indirect support they made for me. Special thank also goes to Dr. Asnakech Demissie (Jimma University, JU) and Dr. Wakene Chawaka (University of Rostock) for their kind assistance in reading my document.

Last but not least, I would like to extend my heartfelt thanks to my dearest wife, S/r Yeamanuelwork Anbessie (BSc. Nursing & MSc candidate at JU), my lovely Kids Emanda (8), Mariyamawit-Nani (4), and Abigiya-Koki (4) for their precious supports and countless tolerances even in the hard time they spend without me. My wife pays a lot to my dream to become true, and without her supports, appreciation, and confidence, my dream couldn't be true.

Summary

Using low-cost and locally available raw materials to remove phosphate instead of high-cost phosphate removal techniques is one of the viable solutions to prevent aquatic life from excess phosphate discharges. Unfortunately, the widespread use of commercially available activated carbon as an adsorbent for phosphate removal is not economically feasible due to its high operating cost. Therefore, this research aimed to study the possibilities of using low-cost carbon-based (i.e., leftover coal materials) and natural adsorbents (volcanic rocks, i.e., pumice- VPum and scoria-VSco) for the removal of phosphate from synthesized wastewater. The study evaluated the three low-cost and locally available sorbents: coal leftover, VPum, and VSco, using batch and fixed-bed column experiments under various environmental conditions.

Numerous experiments were conducted, and the effects of significant design parameters such as solution pH, initial concentration of phosphate ion, contact time, and adsorbents dose for batch adsorption onto leftover coal, VPum, and VSco were examined. Effects of major parameters (Bed height, influent solution concentration, and solution flow rate) on fixed-bed column adsorption are also investigated via breakthrough curve analysis. Design of experiment (DoE) software based on the response surface method (RSM) using central composite design (CCD) was used to investigate the effect of two parameters at a time such as initial phosphate concentration, contact time, pH, and adsorbent dose at a time on the adsorption performance of the selected material.

The structure, surface morphology, and chemical compositions of the adsorbents' materials were characterized before and after adsorption. When the crystallinity and amorphousness of the adsorbents were examined using an XRD machine, it was found that the adsorbent used in this study was both crystalline and amorphous. The functional groups found in the adsorbent materials were obtained and identified using the Fourier Transform Infrared (FT-IR) method. The FT-IR spectrum result after adsorption confirmed the interaction with phosphate ions.

The findings from batch adsorptions revealed that the maximum amount of phosphate removed onto leftover coal material was 198mg/kg at a pH of 2.3, while for VPum and VSco were 294 and 169mg/kg at the solution pH of 6.5 and 5.5, respectively. This maximum phosphate removal capacity was obtained at the contact time of 200 min for leftover coal and 420min both for VPum and VSco. Furthermore, the effects of the adsorbents size on phosphate adsorption from aqueous solution was investigated, and it was obtained that the removal efficiency of phosphate onto leftover coal increased from 66 to 94.5%, from 64 to 91.8%, and from 74 to 92.1% for particle

size 0.075 – 0.425mm, less than 0.075mm, and for 0.425 to 2mm respectively. Thus, all the adsorption experiments, both for batch and fixed-bed column experiments, other than on particle size effect, were performed at a particle size of 0.075 – 0.425mm.

Several adsorption kinetic and isotherm models that describe the adsorption process were also applied. The pseudo-second-order equation best described the experimental data, with a correlation value of $R^2 = 0.99$ for all adsorbents used in this study. However, the phosphate removal process on the adsorbents' surface was found to be complex. Intraparticle diffusion, with the thickness of boundary layer constants of 180 to 209 mg/kg, contributed to the rate determining step. The adsorption equilibrium data for phosphate removal onto adsorbents materials were followed by Langmuir, Freundlich, and Dubinin-Radushkevich isotherms at the constant temperature of 20 ºC and solution pH examined for this research. The calculated values of the dimensionless separation factor (i.e., 0.03 to 0.87) from the Langmuir constant revealed favorable phosphate adsorption onto the adsorbents' materials.

The effects of competitive anions on the phosphate removal onto the volcanic rock materials, on the other hand, were also studied by applying several anions into the synthesized wastewater usin g a batch mode experimental setup. The study findings revealed that the presence of competitive anions markedly reduced the removal efficiency of phosphate from the aqueous solution. The adsorptive removal of phosphate was affected by competitive anions in the order: $HCO_3^- > F^- > SO_4^{-2} > NO_3^- > Cl^-$ for VPum, and $HCO_3^- > F^- > Cl^- > SO_4^{-2} > NO_3^-$ for VSco.

The adsorption of phosphate onto leftover coal material by continuous-flow fixed-bed column experiments has shown that the breakthrough curve time increased from 190 to 348min with increasing bed height from 5 to 8cm but decreased from 348 to 187min with increasing solution flow rate from 1 to 2 mL/min. The longer the bed height, the longer the time phosphate ions interact with the adsorbent surface. The amount of phosphate removed onto the leftover coal material was also increasing from 190 to 243mg/kg with increasing influent initial phosphate concentration from 10 to 25mg/L which agrees with the previously obtained results from batch experiments. The Adams-Bohart adsorption model with a higher correlation factor (R^2) of 0.98 described the continuous flow fixed-bed column phosphate adsorption better than Thomas and Yoon-Nelson model.

In general, the research findings showed that the adsorbents used have an excellent capacity for p hosphate recovery because of their high removal efficiency, especially at the optimum phosphate

concentration, and medium particle sizes (0.75 mm to 0.425 mm). Overall, the methods look co mfortable in preliminary and operating stages as they have relatively low operational and invest ment costs as the adsorbents are easily accessible and found at low or no cost. In addition, the results have shown that leftover coal, VPum, and VSco materials have great potential for phosphate removal. However, further research is needed before the generated data can be applied at field scale, and also regenerable adsorbents for further benefits are highly recommended. Furthermore, to increase the removal efficiencies of the adsorbent materials as economically viable adsorbents for phosphate removal, chemical and physical modification of the adsorbents is highly recommended by considering the cost of modification.

List of Figures

Figure 1.1: River pollution by (a) agricultural runoff and (b) domestic activities 6
Figure 1.2: Surface water pollution from the release of industries and municipal drainages..... 7
Figure 1.3: Location of coal occurrence in the world (*Image: Encyclopedia Britannica, Inc*).... 11
Figure 1.4: Formation and classification of rock materials 12
Figure 1.5: Experimental Setup and conceptualization 16

Figure 2. 1: Scanning electron microscope (SEM) images (a) before adsorption, (b) after adsorption; energy dispersive X-ray (EDX) elemental spectra (c) before adsorption and (d) after adsorption. 26
Figure 2. 2: Kinetic of phosphate adsorption process: (a) Effect of contact time on phosphate removal and (b) linear regression of t/q vs. time (pseudo second-order) 28
Figure 2. 3: Effect of particle size on removal of phosphate (temperature: 20 °C; Co: 10 mg/L; dose 40 g/L; contact time 240 min) 30
Figure 2. 4: The plot of Langmuir and Freundlich adsorption isotherm (Temperature: 20 °C; contact time 1440 min; dose 40 g/L; adsorbent size 0.075–0.425 mm) 32
Figure 2. 5: The plot of predicted versus measured values for: (a) % removal and (b) removal capacity, q 34
Figure 2. 6: The combined effect of (a) contact time and initial concentration, (b) contact time and pH, and (c) initial concentration and solution pH on % removal of phosphate 35

Figure 3. 1: Scanning electron microscope (SEM) and energy dispersive X-ray (EDX) patterns of Vpum (a,b) and Vsco (c,d), respectively 46
Figure 3. 2: Effect of contact time on the removal efficiency of phosphate..... 47
Figure 3. 3: Pseudo-second-order kinetic plot for VPum and VSco..... 49
Figure 3. 4: Kinetics of phosphate adsorption on VPum and VSco, and data fitting for pseudo-first-order, pseudo-second-order, and intra-particle diffusion 50
Figure 3. 5: Intra-particle diffusion plot for VPum and VSco with two different slopes 50
Figure 3. 6: Nonlinear phosphate adsorption isotherms for VPum and Vsco 53
Figure 3. 7: Effects of competitive anions on phosphate removal: (a) pumice and (b) scoria 56

Figure 4. 1: FT-IR results for leftover coal material (a) before and (b) after adsorption 65

Figure 4. 2: XRD pattern of leftover coal material (a) before and (b) after adsorption..... 66
Figure 4. 3: Effects of adsorbent bed height 67
Figure 4. 4: Effects of influents concentrations on phosphate behavior 68
Figure 4. 5: Effects of influent flow rate on phosphate breakthrough 69
Figure 4.6: Experimental and calculated breakthrough curve values for Adams-Bohart model at different values of adsorbent bed height..... 72

List of Tables

Table 2.1: Adsorption kinetics constants 27

Table 2.2: Freundlich and Langmuir isotherm constants..... 31

Table 3. 1: Chemical compositions of pumice (VPum) and scoria (VSco)..... 41

Table 3. 2: Calculated and experimental values of parameters for pseudo-first order, pseudo-second order, and the intra-particle diffusion kinetics model for phosphate adsorption onto volcanic rocks 51

Table 3. 3: Adsorption isotherm parameters for the adsorption of phosphate onto volcanic rocks 53

Table 4. 1: Obtained parameters from breakthrough curves for phosphate adsorption onto leftover coal material with different bed heights, initial phosphate concentrations, and flow rates... 70

Table 4. 2: Parameters for Thomas, Adam-Bohart, and Yoon-Nelson models at different parameters..... 70

Abbreviations

A-B	Adams Bohart
ANOVA	Analysis of Variance
AGR	Analytical Grade Reagents
BDST	Bed Depth Service Time
BET	Brunuer-Emmett-Teller
CCD	Central Composite Design
CFA	Continuous Flow Analyzer
DAAD	Deutscher Akademischer Austauschdienst
DoE	Design of Experiments
D-R	Dubinin-Radushkevich
EDX	Energy Dispersive X-Ray
EBCT	Empty Bed Contact Time
FTIR	Fourier-Transform Infrared Spectroscopy
FWHM	Full Width at Half Maximum
MDPI	Multidisciplinary Digital Publishing Institute
MoE	Ministry of Education
MTZ	Mass Transfer Zone
NZVI	Nano-scale Zero-valent Iron
pHpzc	pH Zero Point Charges
RSM	Response Surface Methodology
SEM	Scanning Electron Microscope
TP	Total Phosphorus
UNEP	United Nations Environmental Protections
UNIDO	United Nations Industrial Development Organization
UV	Ultra violet
VPum	Virgin Pumice
VSco	Virgin Scoria
XRD	X-Ray Diffraction
Y-N	Yoon-Nelson

Table of Contents

Dedication i
Preface ii
Acknowledgments iii
Summary iv
List of Figures vii
List of Tables ix
Abbreviations x
Table of Contents xi
1. Introduction 1
1.1 Motivation 1
1.2 Background 3
1.2.1 Water pollution and pollutants 5
1.2.2 Overall surface water pollution problems 6
1.2.3 History, source, advantages, and disadvantages of phosphate 7
1.2.4 Application areas of phosphate 9
1.2.5 Carbon based adsorbent 10
1.2.5.1 Coal and its application 10
1.2.6 Natural adsorbent materials 11
1.2.6.1 Volcanic rocks 13
1.3 Research Objectives 14
1.4 Significance of the Study 14
1.5 Scope of the study 15
1.6 Experimental setups and conceptualization 15
1.7 Outline of the Thesis 16
2. Removal of Phosphate Ions from Aqueous Solutions by Adsorption onto Leftover Coal (Paper 1) 18
2.1 Introduction 18
2.2 Materials and Methods 21
2.2.1 Adsorbent Preparation and Characterization 21
2.2.2 Reagents Used and Adsorbate Preparation 21

2.2.3 Experimental Set-Up 22
2.2.4 Effects of Particle Size 23
2.2.5 Effects of Temperature 23
2.2.6 Adsorption Kinetics 23
2.2.7 Adsorption Isotherm 24
2.2.8 Statistical Analysis—Central Composite Design (CCD) 25
2.3 Results and Discussion 26
2.3.1 Raw Material Characterization 26
2.3.2 Effect of Contact Time and Adsorption Kinetics 26
2.3.3 Effect of Initial pH 28
2.3.4 Effect of Adsorbent Dose 29
2.3.5 Effect of Particle Size 29
2.3.6 Effect of Initial Concentration 30
2.3.7 Adsorption Isotherm and Thermodynamics 31
2.3.8 Central Composite Design (CCD) 32
2.4 Conclusions 35
3. Adsorptive Removal of Phosphate from Aqueous Solutions Using Low-Cost Volcanic Rocks: Kinetics and Equilibrium Approaches (Paper 2) 37
3.1 Introduction 37
3.2 Materials and Methods 40
3.2.1 Materials Preparation and Characterization 40
3.2.2 Batch Adsorption Studies 41
3.2.3 Adsorption Equilibrium Studies 42
3.2.4 Adsorption Kinetics 44
3.3 Results and Discussions 45
3.3.1 Adsorbents Characterization 45
3.3.2 Effects of Contact Time 46
3.3.3 Adsorption Kinetics 47
3.3.4 Effects of Initial Concentration 51
3.3.5 Adsorption Isotherm 52
3.3.6 Effects of Competitive Anions 54

3.4 Conclusions 56
4. Fixed-Bed Column Technique for the Removal of Phosphate from Water Using Leftover Coal (Paper 3) 57
4.1 Introduction 58
4.2 Materials and methods 59
4.2.1 Adsorbent Preparation and Characterization 59
4.2.2 Phosphate Adsorption in a Fixed Bed Column 60
4.2.3 Theory and Column Data Evaluation 61
4.2.4 Theoretical Breakthrough Curve Models 62
4.3 Results and discussions 64
4.3.1 Adsorbent characterization 64
4.3.2 Effects of operational parameters 66
4.3.2.1 Effects of Adsorbent Bed Height 66
4.3.2.2 Effects of Influent Concentration 67
4.3.2.3 Effects of influent flow rate 68
4.3.3 Prediction of breakthrough curves using adsorption models 71
4.4 Conclusions 73
5. Synthesis 74
5.1 General Overview 74
5.2 Synthesis and general conclusions 75
5.2.1 Batch adsorption experiments 75
5.2.1.1 Effects of contact time 75
5.2.1.2 Effects of Particle size 75
5.2.1.3 Effects of solution pH 76
5.2.1.4 Effects of initial concentration 76
5.2.1.5 Effects of adsorbent dose 77
5.2.1.6 Adsorption kinetics 77
5.2.1.7 Adsorption isotherms 77
5.2.2 Fixed-Bed Column Experiments 78
5.2.2.1 Effects of adsorbent bed height 78
5.2.2.2 Effects of influent concentration 78

5.3 Recommendations for future work 81
References 83
Appendices: Supplementary materials 106

1. Introduction

1.1 Motivation

Ethiopia is gifted with natural resources and has large areas suitable for the development of a chemical industry. With increasing industrialization and urbanization, the Ethiopian government has recently focused on developing chemical and food-related industries. According to statistics, there are about 2,610 processing and manufacturing plants, of which 670 belong to the food and beverage industry (UNIDO, 2019). Several industries in the country produce and manufacture detergents and food related products. Most industrial products, i.e., detergents and food products contain a lot of phosphate as an ingredient. In addition, some of the industries use phosphate as a raw material in production and return it to wastewater treatment after use. Most industrial wastewater treatment plants release phosphate nutrients into nearby rivers, and high phosphate levels in water bodies cause eutrophication (An et al., 2019) and require further treatment.

Phosphate is one of the most abundant nutrients and very important for living organisms (Ajmal et al., 2018). However, when it occurs in excessive amounts, it causes serious environmental problems such as increased eutrophication of surface waters. It occurs in combination with other elements in the earth's crust in the forms of phosphate rock. Phosphate is increasingly consumed with a large amount of spent phosphate eventually entering waterways as diluted waste, often resulting in pollution of water ways.

A number of techniques have been proposed for the removal of phosphate from water and wastewater. Biological, and chemical precipitations treatment methods are widely accepted methods for removing phosphate from water and wastewater on an industrial scale (Srinivasan, 2011). However, these two treatment methods have several limitations, such as the cost of chemicals, large sludge generation and sensitive process operating conditions (Lemraski & Sharafinia, 2016; Nageeb, 2013; Pan et al., 2020). There are also techniques that can remove phosphate from water even at very low concentrations (less than 0.15 mg/L). These include wetland, microalgal biofilms, precipitation combined with reactive filtration, coagulation, or precipitation with ultrafiltration (Mitchell & Ullman, 2016; Newcombe et al., 2008). However, each technology has its own drawbacks: e.g. optimal nutrient loading and elimination, the need for large operating areas, fouling, or large sludge formation due to the addition of metal salts.

Therefore, there is a need for better technologies that remove phosphate from water with less effort and, minimal waste generation, and where phosphate recovery is possible. Of the methods listed, adsorption is a powerful and efficient technique for removing pollutants such as phosphate from industrial wastewater. However, commercial activated carbons are costly, and losses during manufacture limit their application (Vassileva et al., 2013), which has sparked interest in using low-cost adsorbents generated from locally available materials. Thus, extensive research has been conducted to facilitate the maintenance, stable operation, and removal efficiency of adsorbents (Wang et al., 2017). Therefore, several research efforts have been directed towards the fabrication of low-cost and efficient adsorbents from readily available materials, such as natural, and carbon-based materials (Cheng et al., 2018; Sud et al., 2008).

Leftover coal, and volcanic rock materials can be used as filter media because of their physical and chemical properties and mineral composition. Although they are abundant in Ethiopia, they have not been commercialized as adsorbents for the removal of phosphate from water. However, studies have indicated that coal, and volcanic rocks are carbon and silica rich materials that can be used as adsorbents to remove heavy metals and color from water solutions (Samarghandi et al., 2018; Willett, 2015). In addition, volcanic rocks are used as adsorbents to remove heavy metals (Alemayehu & Lennartz, 2009) and fluoride ions (Geleta et al., 2021) from aqueous solutions, and coal ash materials are used to remove pollutants from the wastewater in batch reactors. However, in Ethiopia, the use of coal leftover and volcanic rocks as adsorbents for phosphate removal has received little attention until recently.

In the present study, the coal residues and volcanic rocks (pumice -VPum and scoria-VSco) for the removal of phosphate from simulated phosphate containing water by adsorption was investigated under different operational design parameters. Slurry batch experiments and fixed bed column experiments were conducted to evaluate the removal efficiency of the selected adsorbents. The mechanisms of phosphate removal from water solutions at different pH values were investigated. The effects of competing anions on phosphate removal were also investigated in selected removal processes. Based on the results, fixed-bed column experiments were performed and the effects of various parameters such as adsorbent bed height, influent concentration, and flow rate were investigated in a breakthrough analysis.

1.2 Background

Pollution is a serious problem for life all over the world, and water pollution is one of the deadliest threats to healthy aquatic ecosystems. Water, without which no life is possible, is the most critical resource that nature provides us (Gupta et al., 2009). However, with advanced technologies for industrialization and urbanization, water quality is deteriorating, mainly due to population growth, unplanned urbanization and improper use of water resources (Adeogun et al., 2013; Gisi et al., 2016). Therefore, the sustainable livelihood of the aquatic ecosystem can be affected by water pollution. Water bodies can be polluted by various factors, i.e., natural and anthropogenic activities, with the latter playing a major role. Anthropogenic activities, particularly the discharge of chemicals into water from point sources, have negative impacts on aquatic life when untreated water is used (UNEP, 1997). However, some water pollutants that are highly toxic in excessive concentrations are needed in trace amounts. Copper, zinc, manganese, boron and phosphorus, for example, can be toxic or otherwise adversely affect aquatic life when presented above specific concentrations, even though their presence in small amounts is essential to support and maintain functions in aquatic ecosystems (UNEP, 1997).

The consequences of contaminated water directly or indirectly affect the health of those who use it, including aquatic life. Therefore, one of the major causes of health problems worldwide is due to poor water management. Studies have shown that more than 1 billion people in the world do not have adequate access to safe drinking water, and in Africa, 115 people die every hour because of contaminated water (Eriksson & Sigvant, 2019; Matsuo, 2001).

Preventing water pollution is generally a top priority in low-income countries like Ethiopia. Accordingly, prevention of pollution at source, the precautionary principle, and the prior approval of wastewater discharges by relevant authorities have become vital elements of a successful policy to prevent, control, and reduce inputs of pollutants and other water contaminants from a point source into aquatic ecosystems.

In Ethiopia, surface water quality is deteriorating due to uncontrolled urbanization and inadequate sanitation infrastructure as a result of population growth (Yohannes & Elias, 2017). Nowadays, water pollution from industrial wastewater disposal, domestic activities, and agricultural operations is becoming an environmental concern in Ethiopia (Ademe, 2014). In addition, fresh surface water is polluted by effluents from sources where the amount and nature of pollutants are not well known

(Angello et al., 2020). Several toxic and harmful nutrients enter nearby waterways via agricultural run-off or uncontrolled municipal wastewater discharges. One of these nutrients entering waterways is phosphate. Phosphate is an essential nutrient for plants and animals that live in the earth's crust. It is also very important for life and an essential component in fertilizer production (Kumar, 2018). However, even in very low concentrations, it can threaten aquatic ecosystems once it enters into water bodies. The presence of such nutrients, even at lower concentrations, is sufficient for microbial growth, resulting a condition known as eutrophication. Clear, well-treated water for drinking and other operational purposes is a top priority for humankind and other life forms. Therefore, the removal of these contaminants (i.e., phosphate) from water and wastewater has been a major concern of many researchers around the world and particularly in Ethiopia in recent decades.

To regulate uncontrolled phosphate discharges from various sources, new and current treatment technologies are being proposed worldwide. Several techniques such as chemical precipitations, electrochemical treatments, enhanced biological treatments, etc., have been used to remove phosphate from water and wastewater. However, these techniques are not suitable for the low phosphate concentrations in water and wastewater, that are harmful to the environment (Uddin, 2017).

Chemical precipitation and enhanced biological phosphate treatment are the main advanced techni ques for removing phosphate from domestic and industrial wastewater (Lalley et al., 2016). Biological removal processes are sometimes referred to as secondary treatment methods. These technologies have great difficulty in removing very low phosphate concentration with chemical treatment being the one in which the use of chemical agents is a major criterion, and it can remove lower phosphate concentration even below 0.5 mg/L (Bui et al., 2018). However, the required amount of metals ions, the cost of chemical additives, and environmental problems associated with disposing of a large amount of chemical sludge make these treatment methods deficient. Biological treatment uses naturally occurring microorganisms to convert dissolved organic matter into dense biomass that can be separated from treated wastewater through the sedimentation process. In fact, the microorganisms utilize the dissolved organic matter as food for themselves, while the resulting sludge is much less suitable for chemical treatment. Therefore, in practice, the biological process is combined with a chemical process to remove toxic compounds. These limitations lead to the search

for a better and more effective method of removing pollutants such as phosphate, of which adsorption is the best.

Adsorption is a surface-based phenomenon that occurs when various ions and molecules of gases or liquids attached to the surface of a solid (Králik, 2014). It can also be defined as a mass transfer process involving the accumulation of substances at the interface between two phases, i.e., between liquid and solid or liquid and gaseous phases. Generally, this involves the use of a solid material the adsorbent, to remove the substance of interest the adsorbate, in this case phosphate. Nowadays, adsorption is a widely used method for separating and purifying organic and inorganic pollutants from the aqueous phases. Therefore, adsorption is a superior technique compared to other treatment methods because it is initially inexpensive, simple to design, flexible, easy to handle, insensitive to toxic pollutants, and forms little or no waste (Largitte & Pasquier, 2016; Saki et al., 2019; Uddin, 2017). Based on the interactions between the surface and the species being adsorbed (adsorbate), adsorption can be categorized as chemical sorption or physical sorption. Both physical and chemical forces act from the solvent adsorption. Physical forces include Vander Waals forces and electrostatic forces, while chemical forces result from the formation of internal compounds which exchange bonds (Mhemeed, 2018).

The most common factors affecting the adsorption performance are initial adsorbate concentration, solution pH, contact time, adsorbent dose, temperature, and particle size of adsorbents. In addition, pore size, surface area, and agitation speed also determine the adsorption capacity of the adsorbents (Peng et al., 2018).

1.2.1 Water pollution and pollutants

Water pollution is the process by which water is contaminated by certain pollutants. Surface waters can be polluted by a variety of human and natural processes, with human activities being one of the main causes of water pollution. There are two types of water pollutions, point sources, pollution that originates from single places and non-point source pollution that originates from many places at the same time. Typically, point sources include industrial chemicals, sewage treatment plants, domestic activities, and municipal waste that is discharged directly into water bodies. Non-point sources are pollutants emitted to water bodies indirectly through natural activities such as flooding and agricultural runoff (Angello et al., 2020). The main sources of water pollution are agriculture, mining, deforestation, urbanization, and poor sanitation.

Agriculture: agricultural activities play a significant role in water contamination, as agriculture releasees large amounts of organic and inorganic matter. The use of fertilizers and pesticides on farms releases phosphate into water bodies, leading to eutrophication (Sellner et al., 2019).

Mining: as mining is substantial economic activity in low-income countries like Ethiopia, it negatively impacts the living environment. For example, coal and phosphate rock mining can pollute nearby water ways and the air in general (Wolela, 2007).

Deforestation: deforestation causes soil erosion, which in turn can release nutrients from the soil into water bodies.

Urbanization: an increasing population leads people to migrate to urban areas, where the large volume of used water discharged to wastewater treatment plants and the lack of funding from the local governments is the main factor in the treatment of the wastewater, which is often discharged to water bodies with or without treatment (Figure 1.1) (Yohannes & Elias, 2017).

Figure 1.1: River pollution by (a) agricultural runoff and (b) domestic activities (Yohannes & Elias, 2017)

1.2.2 Overall surface water pollution problems

Water pollution is the contamination of streams, lakes, rivers, oceans, and other watercourses that degrade water quality and becomes toxic to the environment and human beings (Figure 1.2).

Surface water bodies can be polluted in many ways, with organic pollution and chemical pollution being the main types of water pollution.

Organic pollution: this type of pollution is mainly caused by microorganisms such as bacteria and viruses, which are produced by animal waste and plant wastes in waters.

Chemical pollution: chemical pollution is caused by nitrates and **phosphates** from pesticides, human and animal medication, household activities, heavy metals, acids, and hydrocarbons used in industry.

These pollutants can affect both surface and groundwater reservoirs. Groundwater is the deepest form of accumulated water that is not visible to the eye. When rains fall and seep deep into the earth, it can be accumulated as groundwater, one of the least visible but most critical natural resources. Surface water is what fills out the oceans, lakes, rivers, and all other water bodies. Surface water covers about 70 % of the earth. Unfortunately, ground and surface water in low-income countries is highly polluted by agricultural runoff, domestic and institutional activities (Sellner et al., 2019).

Figure 1.2: Surface water pollution from the release of industries and municipal drainages

(Source: https://www.nrdc.org/stories/water-pollution-everything-you-need-know)

1.2.3 History, source, advantages, and disadvantages of phosphate

History of Phosphorus: phosphorus is one of the most common elements found in the environment, and it is essential to all life on earth. Phosphorus (P) is an unusual element that does

not occur in nature as a free element due to its high reactivity. Therefore, it has been a defining element in modern human history. The elemental form of P was first discovered by the German alchemist Hennig Brandt in 1669 (Ashley et al., 2011). It is a very important macronutrient for plants and animals that is present only in a limited amount. In the form of phosphate-PO_4 excess P can promote eutrophication in water bodies (Nguyen et al., 2015). Wastewater discharged from various sources is considered the primary source of phosphate concentration in water ecosystems. Phosphate is a compound that contains phosphorus (P) and oxygen. Phosphorus is a vital element for algal growth, and P loads discharged to water bodies increase, exceptional growth of algae and aquatic plants occurs. As algae and aquatic plants die and decompose, the decomposing organisms consume the dissolved oxygen. This causes a phenomenon called eutrophication, which is deterioration of water quality (Fu et al., 2018). Therefore, there should be water quality criteria for phosphorus compounds, such as phosphate, because it can lead significant changes in community structure if enters aquatic ecosystems in excessive amounts.

Source of Phosphate: Phosphate is a nutrient that is taken up by plants and animals from a variety of sources. Phosphorus (P) is found in large amounts in protein foods such as dairy products, meats, and alternatives such as beans, lentils, and nuts. In addition, whole grains provide P, while vegetables contain a small amount of P. Phosphate polluting water bodies can come from different groups and it can be categorized as a point source (i.e., untreated municipal wastewater and industrial wastes) and non-point sources (i.e., agricultural runoff) (Kim et al., 2015). A point source is a pollutant whose source has been identified, e.g., households, industries, institutions, etc. A non-point source is from an unknown source, such as agricultural runoff.

Advantages and Disadvantages of Phosphate: Eutrophication is the enrichment of water with nutrients (primarily nitrogen (N) and P), that results in excessive growth of algae or floating plant mats and higher forms of plant life, causing an undesirable disturbance to the balance of organisms present in the water and to water quality. A thick floating algal material prevents light from reaching plants below the water surface during algal blooms. As the algae organisms die, they settle to the bottom and are digested by bacteria living in the sediments. This mechanism, in conjunction with an algal bloom, leads to a bacteria bloom and thus increased oxygen consumption, which leads to anoxia in poorly mixed bottom waters. Over time, sediments release phosphate, which reinforces eutrophication (Kagalou et al., 2008).

Plants need various things to grow, such as water, sunlight, carbon dioxide, and various nutrients such as nitrogen and phosphate. Normally, plants absorb the required nutrients from the soil through their roots. However, when the soil is inadequate or unsuitable, people introduce unknown amounts of fertilizer into the soil. As a result, plants do not absorb all of the soils nutrients. Instead of remaining in soil for years, most excess nutrients are carried away by rain or other forms of runoff and are mixed into nearby rivers, resulting in eutrophication (Li et al., 2013). In addition, phosphate can pollute surface water and groundwater if it exceeds the required amount.

1.2.4 Application areas of phosphate

Phosphate is used as an essential nutrient for plants and aquatic life. A single phosphate compound can be used in a variety of applications, including pharmaceuticals, personal care products, industrial cleaners, and fire extinguishers (Arshadi et al., 2018). In addition to being a nutrient, phosphate can be used in many applications. The following is an example of applications of phosphate in a various form of compounds.

- The fertilizer industry uses about 85% of the phosphates available on earth in the form of superphosphate ($CaH_4P_2O_8$), triple superphosphate ($Ca(H_2PO_4)_2.H_2O$), and ammonium phosphate $(NH_4)_3PO_4$.
- 5% phosphate is used in the detergent industry mainly to give beverages a sour taste and as an emulsifier (in processed cheese, dried milk, etc.).
- 2.5% phosphate is also used for the treatment of metals in the metal industry.
- 1% phosphate is used in industry for water softening (e.g., Calgon, Na_3PO_4), for the production of buffers (e.g., NaH_2PO_4, Na_2PO_4), for the removal of H_2S from gases, particularly in the petroleum industry (e.g., K_3PO_4) and as a paint stripper (e.g., Na_3PO_4).
- 1% phosphate is used for the production of phosphorus sulfide (e.g., for matches).
- 1% phosphate is also used to produce organo-phosphorus compounds such as plasticizers (e.g., triaryl phosphate), insecticides (e.g., triethyl phosphate), and gasoline additives (e.g., tritolyl phosphate).

- 1% phosphate is used for pharmaceutical products such as fluoride toothpaste (e.g., $CaHPO_4.2H_2O$) and combined baking powder (e.g., $Ca(H_2PO_4)_2$).
- 0.5% phosphate is also used as a flame retardant (e.g., ammonium phosphate and urea phosphate).

1.2.5 Carbon based adsorbents

Numerous treatment methods have been developed to remove phosphate ions from aqueous solutions, including adsorptions. Adsorption with carbon-based materials is one of the most cost-effective methods for phosphate removal. Carbonaceous materials, including activated carbon, biochar, and carbon nanotubes made from different materials, are widely used to remove various environmental pollutants such as phosphate (Yang et al., 2019). Carbonaceous materials used to produce biochar and activated carbons include various agricultural biomasses such as peanut shell, diary manure, coconut shells, and rice husks (Vassileva et al., 2013). These carbonaceous materials can be used as adsorbents in both natural and modified forms.

Coal materials are also among the carbonaceous materials used in their natural form to remove phosphate from aqueous solutions (see chapter 2 and chapter 4 of this thesis work). However, surface modifications of the coal materials are still required to increase the efficiency of the materials.

1.2.5.1 Coal and its application

Coal is a material that has formed naturally from dead plant matter that has decomposed into peat due to the heat and pressure of being buried deep in the ground for millions of years. Coal, also known as fossil fuel, was formed millions of years ago. Because it is formed from peat deposits, it contains energy obtained from the sun through the photosynthetic system of plants. Different types of coal can be formed from different types of plant residues that form peat after decomposition, producing different types of coal with different qualities. Coal materials can be occurred in different locations in the Earth's crust (Figure 1.3)

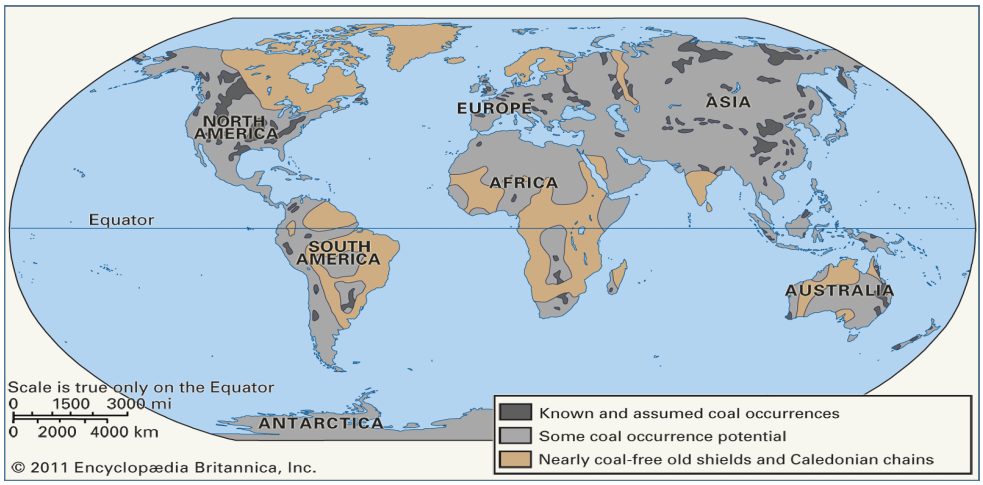

Figure 1.3: Location of coal occurrence in the world (*Image: Encyclopedia Britannica, Inc*).

In ancient times, people began using coal to heat their homes and generate energy for cooking in 1800s. Today, we burn coal to get electricity for heating, cooling, cooking, transportation, lighting, communications, agriculture, and so on. Many countries use coal for power system depending on the coal resources in each area. The United States has more coal deposits than other countries in the world.

Ethiopia is one of the African countries that have significant underground coal deposits. In western and southwestern Ethiopia, there are large coal deposits in the Dilbi Moye, Chilga, Lalo-Sapo, Yayu, Nejo, Wuchale, and Mush valley basins (Wolela, 2007). Coal contains several inorganic minerals such as quartz and clay which are very important for the application of surface adsorption (Kopp, 2021). As described in Chapter 2 of this dissertation, the Yayu coal mine is one of the largest mining areas. The deposited coal material is mined to be used for various purposes. Coal mining in this area produces several residual materials that can have a significant environmental impact (details in Chapter 2). Therefore, the use of these residues as an adsorbent is very versatile for low-income countries such as Ethiopia.

1.2.6 Natural adsorbent materials

There are numerous natural adsorbents that have recently been used to remove pollutants. With or without processing, forest and agricultural wastes are considered as promising adsorbents for the removal of anions and cations from water and wastewater due to their unique properties, such as large surface area, surface chemical properties, and microporous properties (Fernando et al., 2009).

They are also cheap and readily available raw materials where volcanic rocks being one of the naturally occurring materials that can be used for water purification.

Rocks are any naturally occurring solid mass composed of minerals and mineraloid substances. Generally, they can be formed naturally in various manners in the earth's crust. Based on their chemical and mineral composition, rocks can be classified into different categories (Warner, 1990). Igneous, sedimentary, and metamorphic are the three main categories of rocks. Igneous rocks are formed by the cooling of molten magma in the earth's crust and at the earth's surface. Figure 1.4 shows the general formation and classification of rocks and their types. These rocks can be formed only when important elements and minerals are present in them. There are different chemicals and minerals that are mainly responsible for the presence of rock materials; these can be divided into *felsic* and *mafic* minerals. Example of *felsic* minerals are quartz (SiO_3), muscovite ($KAl_2(AlSi_3O_{10}(F, OH)_2$), orthoclase ($KAlSi_3O_8$), and Na-plagioclase/albite ($NaAlSi_3O_8$ where m afic minerals are biotite (K (Fe, $Mg)_3AlSi_3O_{10}(F, OH)_2$), Amphibole ($Ca_2(Mg, Fe, Al)_5(Al, Si)_8O_{22}(OH)_2$), pyroxene ($(Ca,Na)(Mg,Fe,Al)(Al,Si)_2O_6$), Ca-plagioclase ($CaAl_2Si_2O_8$), and olivine ($(Mg,Fe)_2SiO_4$). The studies revealed that of the more than 300 known minerals only the above listed nine minerals and chemicals constitute 95% of the crust (Manville et al., 1998).

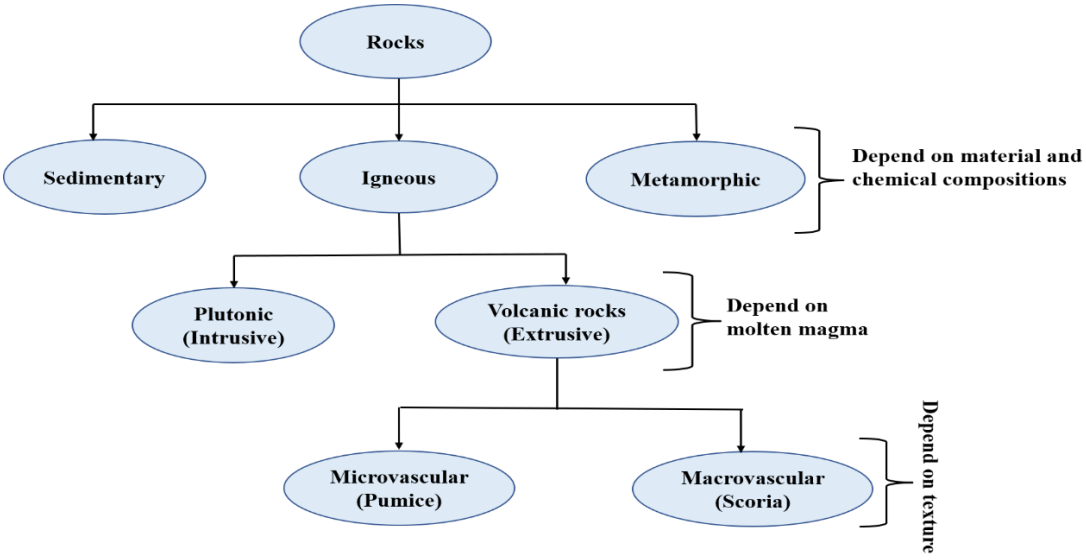

Figure 1.4: Formation and classification of rock materials

1.2.6.1 Volcanic rocks

Volcanic rocks are rocks formed from lava erupted during a volcanic explosion. In other words, they distinguished from other igneous rocks (plutonic rocks) by their volcanic origin from molten magma (Figure 1.4). These microvascular and macrovascular volcanic rocks are mainly classified into two groups: pumice and scoria (Wikipedia, 2021). Thus, volcanic rocks have a vascular texture due to the voids that escape from molten lava.

Pumice is a volcanic rock with a highly vascular, rough texture. Pumice is formed when superheated high pressure rock is ejected from a volcano. Pumice is commonly pale in color ranging from white, cream, blue or grey to green-brown or black. It has a porosity of 64-85% by volume and floats on water until it eventually becomes waterlogged and sinks (Le Bas & Streckeisen, 1991; Venezia et al., 1992). According to observations by the U.S. Geological Survey Cascades, pumice is formed from gray to black fine-grained volcanic basalt which is rich in iron and magnesium.

Scoria is formed from magma that exists from the volcano and condenses on the ground. The highly vascular, dark, black, or purplish red-colored volcanic rock may or may not contain crystals and differs from pumice that it is denser and thicker and sinks rapidly in water. It has a large surface area and high strength for its weight (Wilkinson et al., 2009).

Pumice and scoria are abundant volcanic rock materials found in many parts of the world (Asere et al., 2017). For example, there are large amounts of volcanic rocks deposited in the Ethiopian Main Rift Valley, which occupies about 30% of the country's area (Alemayehu & Lennartz, 2009; Yasin et al., 2015). Pumice and scoria have many applications in the cement industry and are also used as the main ingredients for the supplementary cementitious materials of Portland cement (Mboya et al., 2017). Due to their vascular structure, high content of silica, alumina, iron oxides, alkaline earth metal, and large surface area, both pumice and scoria promote surface fixation of hydroxyl groups, which is a basic requirement for fixation of pollutants (i.e., phosphate) on their surface (Choi et al., 2014; Mboya et al., 2019). Previous studies have demonstrated the adsorption efficiency of volcanic rocks (pumice and scoria) for heavy metals (Alemayehu & Lennartz, 2010; Alemu et al., 2018; Aregu et al., 2018; Kwon et al., 2010) in a single system; in fact adsorption efficiency for phosphate can be significantly enhanced by modifying the adsorbent as there is little

information on how virgin volcanic rocks are used to remove phosphate from aqueous solutions in Ethiopia.

1.3 Research Objectives

The main objective of this study is to apply leftover coal and volcanic rock materials for phosphate removal using slurry batch and fixed-bed continuous flow experiments. Specific objectives are:

- Characterization and analysis of the physicochemical properties of leftover coal and volcanic rocks
- Analyze the effects of key design parameters (solution pH, initial phosphate concentration, adsorbent particle size, and contact time) on the adsorption of phosphate on leftover coal and volcanic rocks.
- Measure the phosphate removal capacity of leftover coal and volcanic rocks by conducting separate slurry batch and continuous flow experiments
- Investigation of the effects of co-existing anions on the adsorption of phosphate on low-cost adsorbents
- Modeling of the adsorption process using various isotherms, kinetic models, and breakthrough models and prediction of the removal rate of the adsorbents
- Investigation of fixed-bed experiments with continuous flow and analysis of breakthrough curve using low-cost adsorbents

1.4 Significance of the Study

This study aimed to investigate the phosphate removal capacity of low-cost adsorbents, namely leftover coal and virgin volcanic rocks (Pumice and Scoria) in slurry batch and fixed bed adsorption experiments. The use of locally available and inexpensive adsorbents for phosphate removal has several advantages. The first benefit is that there is minimal waste in the environment when these materials are used as adsorbents, and they are even environmentally friendly after the adsorption process. The second advantage is that the use of adsorbents from the local reduce costs for local government to use expensive adsorbents from the markets for the adsorption purposes. The third advantage is that the low-cost and locally available materials can be reused to recover phosphate at low desorption costs. Fourth, the findings from this study can serve as a benchmark for the wastewater treatment industry to replace all or part of the expensive materials/adsorbents with low-cost adsorbents regardless of the cost and environmental impact. Finally, the results of

this study can also serve as a benchmark or as secondary data for stockholders, scientists, and researchers interested in further studies on the adsorbent materials used in this study.

1.5 Scope of the study

The experimental investigations conducted in this study were carried out at laboratory scale. The study mainly focused on the measurement of adsorption capacity, illustration of the effects of design parameters on removal capacity, physicochemical analysis, and characterization of the adsorbents used in this study. All three adsorbents (coal leftover, pumice, and scoria) were characterized, and their adsorption capacities were optimized. For this particular study, the effects of the design factors, i.e., contact time, initial adsorbate concentration, pH, adsorbent dose, and adsorbent particle size for the batch experiment; and the effects of adsorbent bed height, flow rate, and influent concentration for the column experiments were examined in detail. In addition, adsorption kinetics and adsorption isotherm models were identified and applied to study the adsorption properties. Finally, the effects of co-existing anions on the removal of phosphate on low-cost adsorbents were investigated.

1.6 Experimental setup and conceptualization

The experiments of the present work were performed in a laboratory scenario. The following diagram (Figure 1.5) shows the general flow of the experiments, starting with sampling and ending with the final discussion.

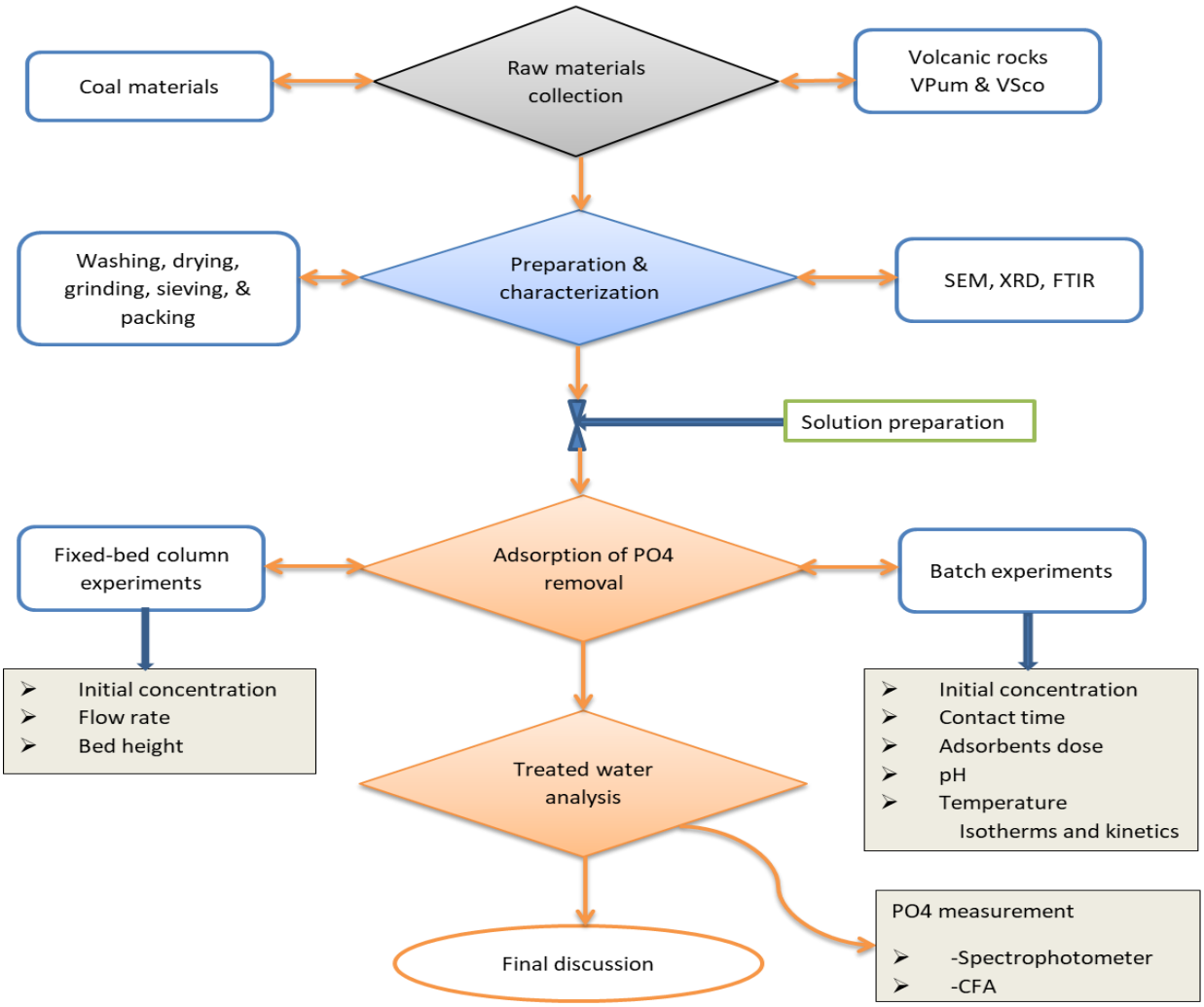

Figure 1.5: Experimental Setup and conceptualization

1.7 Outline of the Thesis

Chapter 1 describes the introduction, motivation for the study, general background of the study, objectives of the study, significance of the study, and scope of the study.

Chapter 2 describes the removal of phosphate ions from an aqueous solution by adsorption onto leftover coal materials. This chapter provided an overview of adsorption and removal techniques. For each specific chapter, the research approaches were discussed and elaborated. The design parameters for phosphate removal of a specific adsorbent were discussed and compared. In addition, the software Response Surface Methodology (RSM) was used to compare the effects of the selected parameters. Adsorption isotherms and kinetic models were discussed, and adsorption

kinetics were predicted accordingly. Finally, the results were summarized in view of future work to improve the adsorption process for the specific adsorbents.

Chapter 3 describes virgin volcanic rocks as adsorptive material for the removal of phosphate from solutions: Kinetics and Equilibrium studies. In this chapter, inorganic or natural adsorbents (pumice and scoria) were used to remove phosphate in batch experiments. For this particular case, isotherm and kinetic adsorption models were elaborated to predict the adsorption mechanism. At the same time, the characterization and removal efficiencies of the two adsorbents were compared. In addition, the effects of competitive anions on phosphate removal were also discussed in this chapter. Finally, the conclusions and recommendations for the future were made at the end of the chapter.

Chapter 4 introduced a fixed-bed column technique for the removal of phosphate from synthetic water using leftover coal as an adsorbent. In this chapter, the total adsorption of phosphate onto the surface of the adsorbent was studied using fixed-bed column experiments. Fixed-bed column experiments were described using breakthrough analysis. Three design parameters, namely influent phosphate concentration, adsorbent bed height, and influent flow rate were compared and manipulated in detail. Known models were analyzed to manipulate the results of the column experiments using breakthrough curve analysis.

Chapter 5 deals with the synthesis of the research results. It contains general discussions, conclusions, and recommendations for future research. The findings of the experiments and future work on the overall research work were addressed.

Appendices: Appendix 1 contains original published papers. **Appendix 2** contains supplementary materials for the published work of chapter 2; **Appendix 3** contains supplementary materials to the published work of chapter 3. **Annex 4** contains the curriculum vitae of the of the candidate

2. Removal of Phosphate Ions from Aqueous Solutions by Adsorption onto Leftover Coal (Paper 1)

Dereje Tadesse Mekonnen, Esayas Alemayehu and Bernd Lennartz

Water/MDPI, https://doi.org/10.3390/w12051381

Abstract: High loadings of wastewater with phosphorus (P) require purification measures, which can be challenging to realize in regions where the technical and financial frame does not allow sophisticated applications. Simple percolation devices employing various kinds of adsorbents might be an alternative. Here, it was investigated the application of leftover coal, which was collected from Ethiopian coal mining areas, as an adsorbent for the removal of phosphate from aqueous solutions in a classical slurry batch set-up. The combined effects of operational parameters such as contact time, initial concentration, and solution pH on P retention efficiency was studied employing the Response Surface Methodology (RSM). The maximum phosphate adsorption (79% removal and 198 mg kg−1 leftover coal) was obtained at a contact time of 200 min, an initial phosphate concentration of 5 mg L^{-1}, and a solution pH of 2.3. The Freundlich isotherm was fitted to the experimental data. The pseudo second-order equation describes the experimental data well, with a correlation value of $R^2 = 0.99$. The effect of temperature on the adsorption reveals that the process is exothermic. The results demonstrate that leftover coal material could potentially be applied for the removal of phosphate from aqueous media, but additional testing in a flow-through set-up using real wastewater is required to draw definite conclusions.

Keywords: leftover coal; phosphate; isotherms; aqueous solution; central composite design

2.1 Introduction

Phosphorus, generally occurring as phosphate (PO_4^{3-}) in aqueous solutions (Xiong et al., 2019a), is an essential amendment and nutrient for many industrial and agricultural applications and often present in water and wastewater at various concentrations (Karageorgiou et al., 2007). For example, phosphate is highly required for the manufacturing of glass products (like glass fiber, military-grade lasers), toothpaste, pesticides and detergent among others (Arshadi et al., 2018). However, the increase of phosphate in water bodies promotes the growth of algae, which results

in eutrophication and eventually consumes dissolved oxygen thereby adversely affects water quality (Ding et al., 2017; Karageorgiou et al., 2007; Kumar & Viswanathan, 2018).

Municipal and industrial wastewaters are the main point sources for phosphate while run-off from agriculture is the dominant non-point source. Studies indicate that 4 to 15 mg/L phosphate may be contained in municipal wastewater, whereas effluent from chemical industries such as detergent manufacturing and metal coating processes may contain 14 to 25 mg/L phosphate (Arshadi et al., 2018; Peleka & Deliyanni, 2009). According to Yadav et al. (2015) the tolerable phosphate level in waters should not exceed 0.05 mg/L to maintain an ecologically sustainable status. In such a case, to lower the phosphate loading in wastewater and runoff especially if local circumstances do not allow for advanced techniques such as membrane filtration became a challenge to local scientists and engineers.

The most widespread wastewater treatment technology for phosphate removal is based on precipitation processes, in which massive amounts of chemicals such as iron and aluminum salts are utilized (Karageorgiou et al., 2007). However, many of the techniques are suffering from either large amount of sludge for disposal, or high operational and maintenance costs with recurring expenses, which are not suitable for many developing countries such as Ethiopia. Therefore, searching cost-effective and environmentally sound phosphate removal alternatives for low-income countries is essential.

A variety of physical, chemical, and biological methods have been developed in recent years for the removal of phosphate from wastewater. Advanced biological methods can remove up to 97% of phosphate and generate low amounts of sludge but the method has limited practical applicability (Karageorgiou et al., 2007). Similarly, physical processes (sedimentation, membrane filtration, etc.) techniques are too expensive and accompanied by a high sludge production and often inefficient in the removal of phosphate from wastewater effluent (Khan et al., 2013; Venkatesan et al., 2016).

Studies on P-laden wastewater treatments have revealed adsorption to be a highly effective and easy method among the physicochemical treatment processes if materials are carefully chosen (Alemayehu & Lennartz, 2009; Mehrabi et al., 2016). Some of these adsorbents are calcite (Karageorgiou et al., 2007), Nano-scale zero-valent iron (NZVI) (Arshadi et al., 2018), rice husk and fruit juice (Yadav et al., 2015), acid-activated red mud (Tor & Cengeloglu, 2006), granulated

coal ash (Asaoka & Yamamoto, 2010), aleppo pine (Benyoucef & Amrani, 2011), zirconium(IV) loaded fibrous (Awual et al., 2011), still slag produced (Meyer et al., 2012), bone charcoal (Ghaneian et al., 2014), Lanthanum hydroxide materials (Xie et al., 2014), aluminum sludge (Nawar et al., 2015), modified multi-walled carbon nanotube with chitosan (Yimin Huang et al., 2018), manganese-laden bio-char (Jiang et al., 2018), marble waste (Bouamra et al., 2018), chitosan composited beads derived from crude oil refinery waste (Cui et al., 2019), iron-coated diatomite (Lyngsie et al., 2019), halloysite nanotubes (Saki et al., 2019), and industrial solid waste bio-char (Qiu & Duan, 2019). Adsorption emerges as a robust process that could solve the aforementioned problems and render the treatment system more economically viable, especially if low-cost adsorbents are involved. Recently, considerable attention has been directed towards naturally occurring and abundantly available carbon-related adsorbents due to the high cost of widely used activated carbon.

Coals, as well as leftover coal, are carbon-rich materials, which could prove suitable for the removal of phosphate from aqueous solutions. Leftover coal is basically a material that was left as waste after mining underground deposited coal. In many parts of the world (including Ethiopia) this leftover coal is abundantly available. Open-pit coal mining is widespread in Ethiopia where there are more than 430 million tons of coal deposits found in the country of which Yayu coal mining being the largest site (Fantaw, 2019). About 200 million tons of coal deposits to be mined in the area, from which more than 0.1% is leftover coal.

The potential of coal to remove phosphate has been reported (Asaoka & Yamamoto, 2010; Regassa et al., 2016; Zhang et al., 2012). Moreover, a variety of carbon-related materials such as coal gangue loaded with zirconium oxide (Xiong et al., 2019), coal bottom ash (Zhou et al., 2019), magnetic coal (William et al., 2019), coal slag (Lam et al., 2020), and coal fly ash (Matsubara, 2018) are used as adsorbents for phosphate removal from aqueous solutions. However, very limited information is available so far on the phosphate adsorption on raw leftover coal. Therefore, the objectives of the present study were to (i) investigate the possible use of raw leftover coal as an adsorbent for the removal of phosphate from aqueous solution by considering various contact times, pH values, initial phosphate concentrations, particle size, adsorbent dose and temperature; (ii) evaluate and optimize the interactive effects of operating parameters using the Central Composite Design (CCD), a common approach of the response surface methodology (RSM); (iii)

elucidate adsorption mechanisms using energy dispersive x-ray spectrometer with the scanning electron microscope (EDX-SEM), as well as kinetics and isotherm models.

2.2 Materials and Methods

2.2.1 Adsorbent Preparation and Characterization

The sample (leftover coal) was obtained from Yayu coal mining, Ethiopia (Figure A2.1 in supplementary data of Appendix 2). The chemical composition of the leftover coal shows that the material has a high potential for phosphate adsorption due to significant amounts of oxides (54.56% SiO_2, 34.17% Al_2O_3, 6.85% Fe_2O_3, 1.42% CaO, 0.9% SO_3, 0.71% MgO) (Regassa et al., 2016).

Images and elemental spectra of the leftover coal, before and after adsorption, were obtained from EDX-SEM (energy dispersive X-ray spectrometer with a scanning electron microscope). Physicochemical properties such as organic matter, moisture content, electrical conductivity and pH zero point of charges (pH_{zpc}) were also measured according to Penn & Bowen (2018). Organic matter, moisture content, electrical conductivity and pH_{zpc} of the coal material were determined to be 28.5%, 0.93%, 0.69 mS cm^{-1} and 4.6, respectively.

Prior to adsorption experiments, the collected raw material was washed thoroughly and repeatedly with de-ionized water to remove dust and small particles adhered to it (Nawar et al., 2015). Then, the wet material was transferred to an oven for drying at a temperature of 105 °C for 1440 min to obtain constant mass (Fiol & Villaescusa, 2009). Subsequently, the sample was grounded to small granules and passed through an appropriate mesh size (75–425 µm). Finally, the well-sieved sample was stored in a desiccator to prevent moisture uptake until the onset of the experiments.

2.2.2 Reagents Used and Adsorbate Preparation

Hydrochloric acid (0.1 M HCl), sulfuric acid (50% H_2SO_4), sodium hydroxide (0.1 M NaOH), ammonium molybdate ($(NH_4)_6Mo_7O_{24}\cdot 4H_2O$), potassium antimony tartrate ($(SbO)K(C_4H_4)_6)\cdot 1/2 H_2O$) and ascorbic acid ($C_6H_8O_6$) were used for the photometric quantification of phosphate. All chemicals and reagents used in this experiment were of analytical grade from Merck Germany unless stated otherwise.

A stock solution of potassium dihydrogen phosphate, KH_2PO_4 with a concentration of 1000 mg/L PO_4^{3-} and 99.9% purity, was diluted to a working solution with concentrations of 0.5 mg/L PO_4^{3-} to 25 mg/L PO_4^{3-} in 1000 mL of de-ionized water then labeled as 'phosphate solution or working solution' and stored in a tightly closed plastic bottle in a cool place (4 °C) until the experiments were commenced.

2.2.3 Experimental Set-Up

All the experiments were conducted in batch mode by adding 25 mL of phosphate solution to 1 g of leftover coal (initial solution concentration ranging from 0.5 mg/L to 25 mg/L, the temperature at 20 °C and pH = 3.5) in 100 mL Erlenmeyer flasks. The flasks were shaken using a horizontal shaker (Edmund Buhler 7400 Tubingen, SM 25, Germany) operating at 200 rpm for 1440 min. After the shaking of the slurries, the suspensions were centrifuged using a centrifuge apparatus (HERAEUS MULTIFUGE 3RS+ Centrifuge, Kendro GmbH, Hanau, Germany) operating at 3000 rpm for 10 min and immediately filtered by means of a vacuum filtration pump employing 0.45 µm filter (Whatman, Carl Roth GmbH, Karsruhe, Germany) to obtain a clear supernatant aliquot. The supernatant solution obtained from filtration was then treated with ammonium molybdate and ascorbic acid solution prior to the phosphate analysis (molybdenum-blue ascorbic acid method) (Krishna et al., 2017). Finally, the phosphate concentration of the solution was analyzed using a spectrophotometer (UV-SPECTROD 40, Analytik Jena AG, Jena, Germany). The adsorbed and % removal of phosphate was computed using Equations (2.1) and (2.2) as indicated below:

$$q_t = \frac{(C_o - C_t)V}{M} \tag{2.1}$$

$$\% = \left(\frac{C_0 - C_t}{C_0}\right) x100 \tag{2.2}$$

where q_t is the amount of phosphate adsorbed per unit mass of adsorbent (mg/g) at time t; C_o, C_t are the initial and final concentration of phosphate at time t (mg/L) respectively, V is the volume of the solution contacted with the adsorbent (L), M is mass of the adsorbent (g) and (%) is percent removal at time t. For data accuracy and error minimization, all experiments were conducted in duplicate and the average values were used for data interpretation and analysis.

2.2.4 Effects of Particle Size

The effect of particle size on the adsorption of P was studied as follows: 200 mL of a 10 mg/L phosphate solution was mixed with g of adsorbent (adsorbent to solution ratio = 1:25) size in a series of 250 Erlenmeyer flasks. Well-caped flasks were then placed in a horizontal shaker operating at 200 rpm for 240 min. The samples were withdrawn at different time intervals and phosphate concentrations were measured as usual.

2.2.5 Effects of Temperature

The effect of temperature on the adsorption of P was measure in a separate experiment. A gram of adsorbent was added to the series of 100 mL flasks containing 25 mL phosphate solution with a concentration of 10 mg/L and stirred with a magnetic stirring plate at predetermined temperatures (20, 40 and 60 °C) for 2 h. Then, the suspension solution filtered and phosphate detection analysis has been commenced as used for adsorption study.

2.2.6 Adsorption Kinetics

In order to investigate the adsorption kinetics, pseudo-first order and pseudo-second-order linear kinetic models were applied for the estimation of rate constants (Ajmal et al., 2006). Pseudo-first-order expression was employed as in Equation (2.3):

$$\log(q_e - q_t) = \log(q_e) - \frac{K_1 t}{2.0303} \qquad (2.3)$$

Where K_1 is the first-order rate constant of adsorption (min^{-1}); q_e (mg/g) and, q_t (mg/g) are the amount of phosphate adsorbed at equilibrium and at time t respectively. The values of K_1 and q_e can be obtained from the slope and the intercept of a linear straight-line plot of log ($q_e - q_t$) versus t.

The pseudo second-order equation can be written as shown in Equation (2.4): (Saki et al., 2019)

$$\frac{dq_t}{dt} = K_2(q_e - q_t)^2 \qquad (2.4)$$

And integrating provided the linear pseudo-second order expression as:

$$\frac{t}{q_t} = \frac{1}{x} + \frac{1}{q_e}t$$

where q_e (mg/g) and q_t (mg/g) are the amount of phosphate adsorbed at equilibrium and time t respectively; $x = K_2 q_e^2$ and K_2 is the rate constant of the pseudo second-order model (g/mg$^-$min). The value of x and q_e can be obtained from the linear t/q_t vs. t plot.

2.2.7 Adsorption Isotherm

Various models can be employed to characterize the adsorption behavior of a given compound analyzing experimental data. Adsorption isotherms relate the adsorbed amount of phosphate to the equilibrium solution concentration at a constant temperature. These relations are also named 'quantity-intensity-relations'. Freundlich and Langmuir isotherms are the most frequently used models to analyze experimental observations (Peleka & Deliyanni, 2009). These two non- linear isotherm models (Equations (2.5) and (2.6)) were applied to obtain the adsorption isotherm constants.

Langmuir equation:

$$q_e = \frac{K_L q_{max} C_e}{1 + K_L C_e} \qquad (2.5)$$

Freundlich equation:

$$q_e = K_F {C_e}^{1/n} \qquad (2.6)$$

Where q_e (mg/g) is the specific amount of adsorbate (phosphate), and C_e (mg/L) is the adsorbate concentration in the liquid phase at equilibrium. The constants K_L (L/mg) and q_{max} (mg/g) of the Langmuir isotherm are indicative of adsorption energy and adsorption density respectively. K_F and n (dimensionless) are Freundlich constants and indicate the total adsorption capacity and intensity of adsorption respectively.

The Langmuir equation is also used to obtain R_L, the separation factor, from the following expression: $R_L = \frac{1}{1+K_L C_0}$ in which Co (mg/L) is the initial concentration of phosphate in the solution. If $0 < R_L < 1$ then a favorable adsorption situation can be assumed, while $R_L > 1$ indicates an unfavorable adsorption, and $R_L = 1$ and $R_L = 0$ indicate a linear and irreversible adsorption isotherm respectively (Alemayehu & Lennartz, 2009). The model equations were fitted to the experimental data using the Microsoft Excel solver function.

2.2.8 Statistical Analysis—Central Composite Design (CCD)

The effect of experimental conditions on the adsorption process can be evaluated by either analyzing one factor at a time (varying only one parameter and holding the other parameters constant) or by a multiple factor optimization (parallel processing of two and more parameters). The first method is tedious and often inappropriate whereas the latter one is simple, efficient and precise for testing the effect of various parameters simultaneously (Asaithambi et al., 2018). Here it was used a multivariate mathematical model approach the so-called Response Surface Method (RSM). The Central Composite Design (CCD) is one of the majors of RSM and it was used to evaluate the relation and the combined effect of the selected independent parameters such as contact time (A), initial concentration (B) and solution pH (C) on the response parameters such as % removal (Y1) and adsorption capacity-q (Y2). The experimental results were analyzed using the CCD method, which is a widely used statistical approach in a multi-parameter operation for optimization experiments (Asaithambi et al., 2018; Sadhukhan et al., 2016). For three factors, as in this case, the number of required experiments is assessed as follows: $N = 2^k + 2k + z = 2^3 + 2 \times 3 + 6 = 20$; where N is the number of necessary experiments, k the number of factors and z is the number of replicate values at the central point. Accordingly, 20 experiments with six replicates were conducted (Table A2.6 in supplementary data) for the specific method. After conducting the experiments, the coefficients of the polynomial of the mathematical model were calculated using the following quadratic equation (2.7) (Saadat et al., 2018).

$$Y = \beta_O + \sum_{i=1}^{k} \beta_i X_i + \sum_{i<j} \sum \beta_{ij} X_i X_j + \sum_{i=1}^{k} \beta_{ii} X_i^2 \qquad 2.7$$

Where Y is predicted responses (% removal of phosphate or/and removal capacity, q), XiXj are the coded values of independent variables (contact time-A, initial concentration-B and solution pH-C), is β_o constant coefficient β_i, β_{ii} and β_{ij} are the linear, quadratic and interaction coefficients respectively. The statistical significance of the obtained model was tested and analyzed by an analysis of variance (ANOVA) which was performed by the Design Expert software (Version 11.0, StatEase, USA).

2.3 Results and Discussion

2.3.1 Raw Material Characterization

The energy dispersive X-ray (EDX) and the scanning electron microscope (SEM) images and elemental spectra of the adsorbent were described both before and after adsorption respectively (Figure 2.1). The SEM images of the adsorbent revealed that the leftover coal has a spherical shape and heterogeneous cross-sectional surfaces (Figure 2.1a, b). The EDX analysis showed the elemental composition and spectral peaks of the adsorbent. Figure 2.1c, d revealed that the peak with contents of carbon(C), silica (Si), aluminum (Al), sulfur (S), calcium (Ca) and iron (Fe) all at K-alpha signals. As expected, the leftover coal contains high amounts of SiO_2, Al_2O_3 and organic materials. The *p* was observed after adsorption at the peak position of 1.98 keV as K-alpha signal (Figure 2.1d), from which it is conclude that leftover coal material is suitable for phosphate removal.

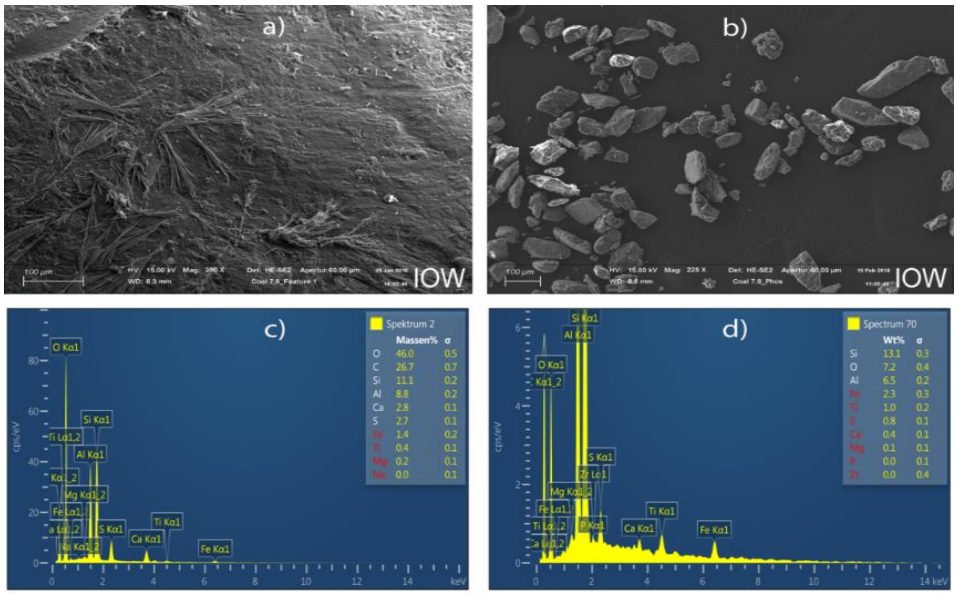

Figure 2. 1: Scanning electron microscope (SEM) images (a) before adsorption, (b) after adsorption; energy dispersive X-ray (EDX) elemental spectra (c) before adsorption and (d) after adsorption.

2.3.2 Effect of Contact Time and Adsorption Kinetics

The effect of contact time on phosphate removal by leftover coal is presented in Figure 2.2a. The phosphate capture on the surface of adsorbent was very rapid in the first 200 min, and equilibrium was attained after 720 min contact time. Increasing the contact time increased the uptake of

phosphate, indicating the high affinity of phosphate to bare surfaces and a fast filling of active sites due to boundary layer diffusion (Alemayehu & Lennartz, 2009; Nawar et al., 2015). It can be observed from Figure 2.2a that the adsorption process had a rapid and a slow component. The rapid adsorption (up to 200 min) was based on the availability of active sites and a high phosphate concentration in the solution at the early stages of the experiment. The following slow adsorption is due to intra-particle diffusion and an according phosphate mass transfer onto leftover coal particle. A similar finding has been reported in the literature (Du et al., 2017).

Commonly used two kinetic models, pseudo-first and pseudo-second-order models, were employed to fit the experimental data. Optimized model parameter values are presented in Table 2.1. The equilibrium capacity as obtained from the fitting procedure employing the pseudo second-order model (qe) very well represented the measured value. The pseudo second-order model best represents the experimental data (R^2 = 0.99; Figure 2.2b), which can be taken as an indicator that chemisorption was the dominant process (Pan et al., 2020; Witek-krowiak et al., 2011).

Table 2. 1: Adsorption kinetics constants

Initial Concentration (mg/L)	**Pseudo first-order**				**Pseudo second-order**			
	q_e, exp(mg/g)	q_e,cal (mg/g)	K_1 (Min^{-1})	R^2	q_e,exp (mg/g)	q_e,cal (mg/g)	K_2 (g/mg.min)	R^2
10	0.20283	0.11676	0.195	0.96	0.20283	0.20511	7.67	0.99

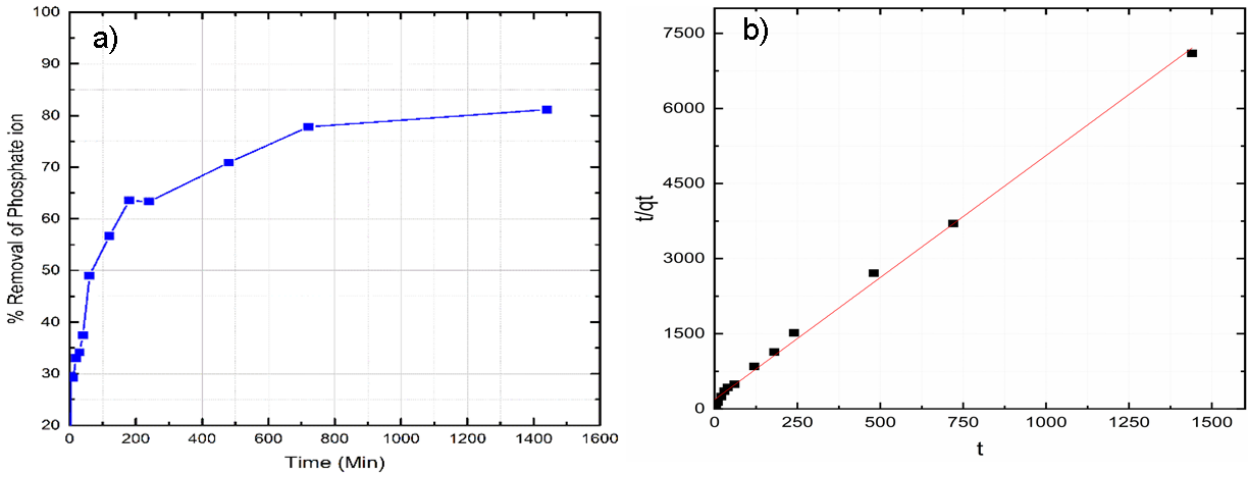

Figure 2. 2: Kinetic of phosphate adsorption process: (a) Effect of contact time on phosphate removal and (b) linear regression of t/q vs. time (pseudo second-order)

2.3.3 Effect of Initial pH

A pH zero point of charge (pHzpc) for leftover coal material was measured to be 4.6. It is known that adsorption of anions (i.e., phosphate-PO_4^{3}-) on the leftover coal at a pH lower than the pHzpc is elevated because of the high density of positive charges on the surface. On the other hand, adsorption at a pH higher than the pHzpc can be expected to be lower because of the repulsion of similar ions. It was reported in literature that pH is a critical factor that affects the adsorption of phosphate (Wu et al., 2017; Yadav et al., 2015). The effect of pH on phosphate adsorption onto leftover coal for this study is presented in Figure A2.2 in supplementary data. The percentage of phosphate removed from the aqueous solution decreased (from 86% to 68%) as the pH of the solution increased from 2 to 12 indicating that the adsorption of phosphate is likely to be based on physical interactions between the surfaces of the adsorbents and adsorbate (Benyoucef & Amrani, 2011). At the lower pH range adsorption increases at sites with a variable charge (e.g., –COOH, –NH_3) because of increasing protonation. At high pH values, the competition with OH ions increases, and phosphate adsorption decreases (Bui et al., 2018; Nawar et al., 2015). The results obtained here (Figure A2.2), however, revealed that the leftover coal material could adsorb phosphate over a wide pH range of 2–10. The maximum percent removal of phosphate (86%) was obtained at a lower pH = 2 and up to 80% removal can be maintained even up to a pH of 10. Adsorption at high pH values may be caused by bridging of cations, which are present at the surface of the adsorbent (Xiong et al., 2019). For pH greater than 10, the adsorption capacity decreases sharply because of the more negative charges on the surface of the adsorbent. Similar

reports confirm that phosphate removal is less efficient under alkaline conditions (Huang et al., 2014; Mallet et al., 2013).

2.3.4 Effect of Adsorbent Dose

The adsorbent dose is the ratio of the mass of adsorbent to solution volume and is one of the important factors in the removal process. The effect of adsorbent dose on the phosphate removal onto leftover coal was investigated in the range of 0.5–5 g and the results were presented in Figure A2.3. The percent of phosphate removal increased (from 58% to 96%) with the increase of the dose of leftover coal (from 0.5 g to 5 g). On the other side, the mass uptake per unit adsorbent (q, mg/g) was decreasing (from 2.9 mg/g to 0.5 mg/g) with increasing the dose of leftover coal from 0.5 g to 5 g, which can be related to the higher abundance of sorption sites. Similar observations have been reported by other investigators (Baral et al., 2006; Park & Jung, 2011; Rashidi et al., 2017).

2.3.5 Effect of Particle Size

The effect of particle size on the adsorption of phosphate was investigated with three different particle sizes. The particle sizes of the material were categorized as silt sand (less than 0.075 mm), fine sand (0.075 mm to 0.425 mm) and medium sand (0.425–2 mm). As can be seen from Figure 2.3, the percent of phosphate removed by the fine sand fraction was higher (94.5%) than that of the silt and medium sand of the adsorbent (91.8% and 92.1%) after 240 min reaction time. At an earlier stage of the experiment (after 90 min) differences were slightly more pronounced. The results showed that the particle size as investigated here has only minor effects on the adsorption capacity, which is only partially in agreement with earlier studies (Alemayehu & Lennartz, 2009). Based on the results from the particle size tests, all subsequent experiments were conducted with adsorbent material of the fine sand fraction (0.075 mm to 0.425 mm.

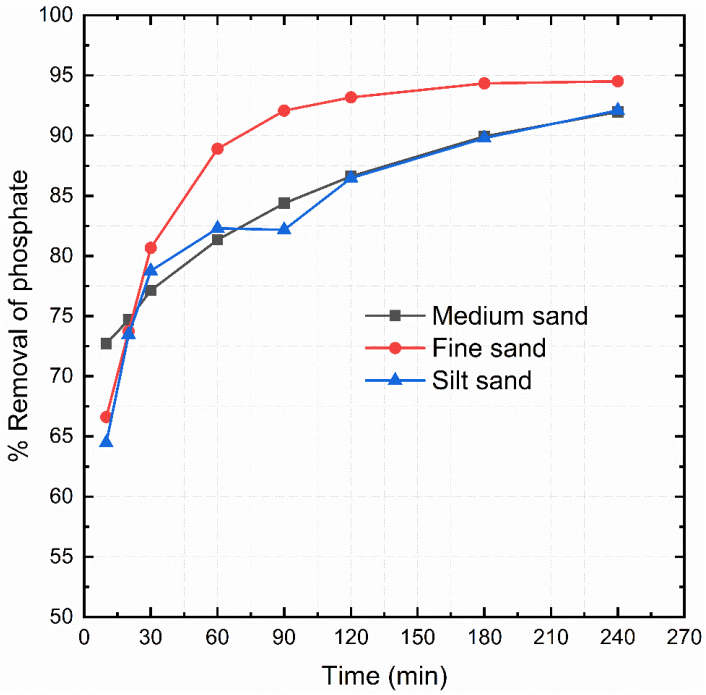

Figure 2. 3: Effect of particle size on removal of phosphate (temperature: 20 °C; Co: 10 mg/L; dose 40 g/L; contact time 240 min)

2.3.6 Effect of Initial Concentration

The percent removal of phosphate gradually decreased (from 93.4% to 55%) with increasing the initial concentration of phosphate (from 0.5 mg/L to 25 mg/L). It is likely that active adsorption sites become saturated at higher initial concentrations (Yadav et al., 2015). It has to be emphasized that the percent removal as presented here is based on concentrations (Equation (2.2)). If total amounts are considered, it can be observed that with increasing initial concentration the adsorbed amount (q, mg/g) is likewise increasing (0.011 mg/g to 0.344 mg/g; Figure A2.4). At higher concentrations, driving forces (diffusive gradient) are also higher and barriers of mass transfer between aqueous solution and solid interfaces are overcome (Lee et al., 2017). Although, the increased amount of phosphate removed on the surface of the adsorbent with increasing initial concentration is an indicator for the removal of highly contaminated water, the effects of other pollutants have to be considered otherwise the performance of the adsorbent material will be limited in real wastewater treatment and the surface of the leftover coal has to be modified for the better removal. Furthermore, credible pieces of evidence from scientific literature substantiate both beneficial and detrimental effects of coexisting anions in aqueous solution (Kim & Lee, 2012; Rashid et al., 2017; Saadat et al., 2018).

2.3.7 Adsorption Isotherm and Thermodynamics

Adsorption of phosphate onto leftover coal was described by both Freundlich and Langmuir isotherm models. Figure 2.4 and Table 2.2 summarizes the results. The Freundlich model assumes that adsorption occurs on a heterogeneous surface through multilayer adsorption, and the adsorbed amount increases with increasing equilibrium concentrations. In opposite, the Langmuir model assumes an asymptotic approach to monolayer surface coverage. From the obtained optimization procedure, it became evident that the Freundlich isotherm equation (R^2 = 0.99) described the system better than the Langmuir isotherm equation (R^2 = 0.76). The n-value of the Freundlich isotherm lies between 1 and 10, which is a good indicator for favorable adsorption (Pengthamkeerati et al., 2008). Furthermore, the value of 1/n, which was obtained from the slope of the linear plot of lnqe vs. lnCe of the Freundlich isotherm, was below unity implying that chemisorption is the governing process (Foo & Hameed, 2010). The separation factor, R_L as obtained from the Langmuir isotherm model was lower than unity, which likewise indicating to a favorable adsorption process (Baral et al., 2006; Kapur & Mondal, 2013; Yadav et al., 2015).

The temperature has a considerable effect on the efficiency of the adsorption process. Here, the influence of the temperature was tested by conducting batch experiments at 20 °C, 30 °C and 40 °C. It was found that, the percent removal of phosphate decreases with the increase of temperature from 20 °C to 40 °C, confirming the exothermic nature of the process (data not shown). An increase in temperature raises the thermal energy of the system which increases the mobility of phosphate ions fostering enhanced desorption. As a result, the overall adsorption is decreasing. Similar findings have been reported in previous research works (Baral et al., 2006; Kapur & Mondal, 2013; Yadav et al., 2015).

Table 2. 2: Freundlich and Langmuir isotherm constants

Adsorbent	Freundlich constants			Langmuir constants			
	K_F (L/mg)	n_F	R^2	K_L (L/mg)	q_{max} (mg/kg)	R^2	R_L
Coal leftover	0.112	1.67	0.901	1.315	38.01	0.7604	0.03- 0.60

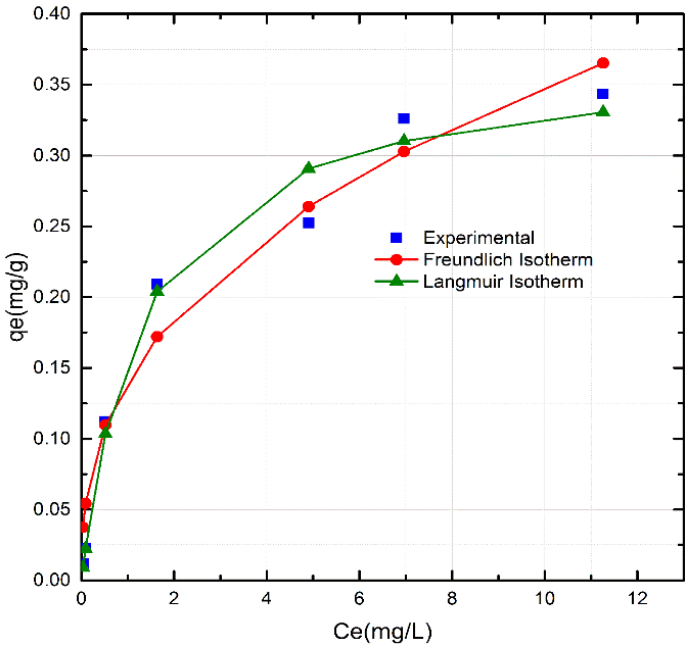

Figure 2. 4: The plot of Langmuir and Freundlich adsorption isotherm (Temperature: 20 °C; contact time 1440 min; dose 40 g/L; adsorbent size 0.075–0.425 mm)

2.3.8 Central Composite Design (CCD)

A three-factor and a three-level CCD method were employed in the present study to optimize and analyze the combined effects of parameters on responses such as % removal and removal capacity, q. The design summaries for both dependent and independent parameters with their corresponding constants were generated. Each of the independent variables were coded and set in the range of midpoint according to Asaithambi et al. (Asaithambi et al., 2018). The mean point for contact time, initial concentration, and solution pH was set by the software as 180

min, 15 mg/L, and 6 respectively; the coded low, coded high, minimum and maximum values for each parameter are summarized in Table A2.1 in the supplementary material.

The three parameters contact time (A), initial concentration (B) and solution pH (C) were selected for the optimization of two responses (percent removal -Y1 and adsorption capacity, q-Y2). Consequently, A, B, and C are selected by the software as independent variables whereas Y1 and Y2 are dependent variables as expressed in the second-order polynomial equations (Equations (2.8) and (2.9)). The equation in terms of coded factors can be used to make predictions about the responses for given levels of each factor (see Equation (2.7)).

$$Y_1(\%\ removal) = 71.03 + 1.02A - 6.04B - 0.2140C + 0.3400A * B + 0.3375A * C + 0.1150B * C - 1.14A^2 + 1.69B^2 + 0.3409C^2 \quad (2.8)$$

$$Y_2(q) = 0.1776 + 0.0025A - 0.0151B - 0.0005C + 0.0008AB + 0.0008AC + 0.0003BC - 0.0028A^2 + 0.0042B^2 + 0.0009C^2 \quad (2.9)$$

Equations (2.8) and (2.9) revealed how the combined variables affect the removal of phosphate from solution onto leftover coal material. The positive values in the equations indicated that the removal of phosphate rises by increasing the effect. The quadratic equation was found as the optimum model to interpret phosphate adsorption onto leftover coal because of the high determination coefficient (R^2 = 0.9987 for % removal and R^2 = 0.9986 for removal capacity) and low probability value (p-value <0.0001 both for % removal and removal capacity). A cubic model has higher values of R^2 and adjusted R^2 but was considered by the software as aliased and can, thus, not be used to interpret the experimental data because of an inadequate number of batch experiments (Saadat et al., 2018). Adequacy of the model tested and model summary of both % removal and removal capacity are summarized in Tables A2.2 and A2.3.

The capability and significance of the quadratic model and factors were analyzed by using analysis of variance (ANOVA). A combination of the Fisher test value (F-value) and probability value (p-value) can verify the signature of the model and the parameters used. F-values of greater than 4 and p-values of less than 0.05 indicate that the model is significant and can be used for accurate prediction of phosphate removal (Wang et al., 2007). In this case, A, B, C, AB, AC, A^2, B^2, C^2 are significant model terms. The F-value and p-value of BC (combined effect of initial concentration and solution pH) for % removal was 2.07 and 0.1804 respectively indicating that the model is not significant. The corresponding individual and combined results of each parameter for % removal and removal capacity, q is given in Tables A2.4 and A2.5 in the supplementary material.

The comparisons between experimental and predicted values are presented numerically in Table A2.6, graphically in Figure 2.5a, b. The plots of Figure 2.5 confirm the very good agreement between experimental values and model calculations.

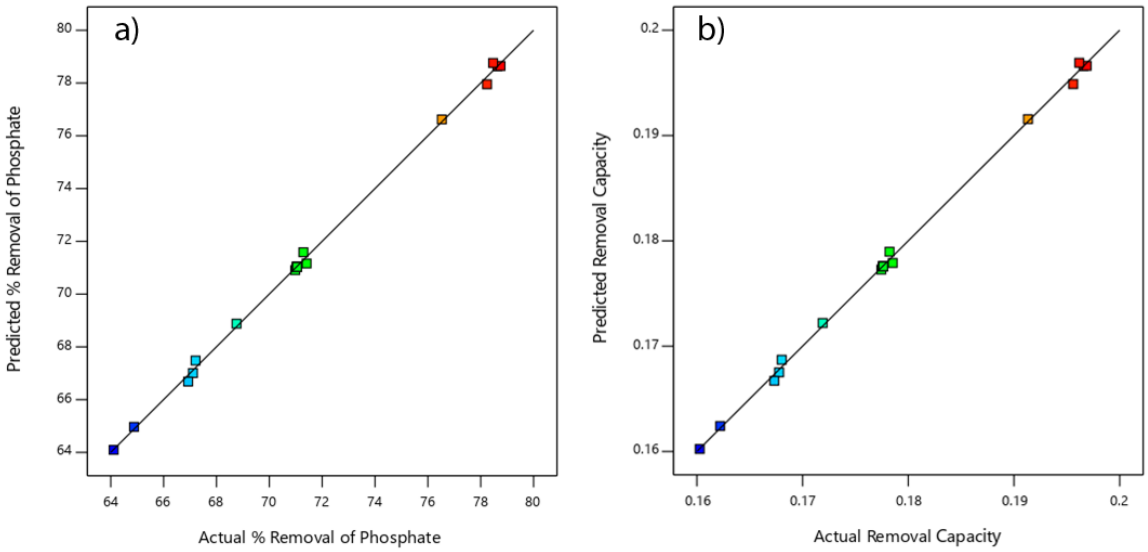

Figure 2. 5: The plot of predicted versus measured values for: (a) % removal and (b) removal capacity, q

Figure 2.6 elucidates the surface response of the combined effect of the tested experimental conditions on phosphate removal. It can be seen from Figure 2.6a that the percent removal of phosphate increases with increasing contact time from 120 min to 240 min at a minimum initial concentration of 5 mg/L. Similarly, Figure 2.6b, c shows the impact of initial concentration with solution pH and contact time with solution pH respectively. From Figure 2.6c, however, the impact of the combined effect of contact time and solution pH was not significant on the removal of the phosphate as compared to the impact of contact time and initial concentration.

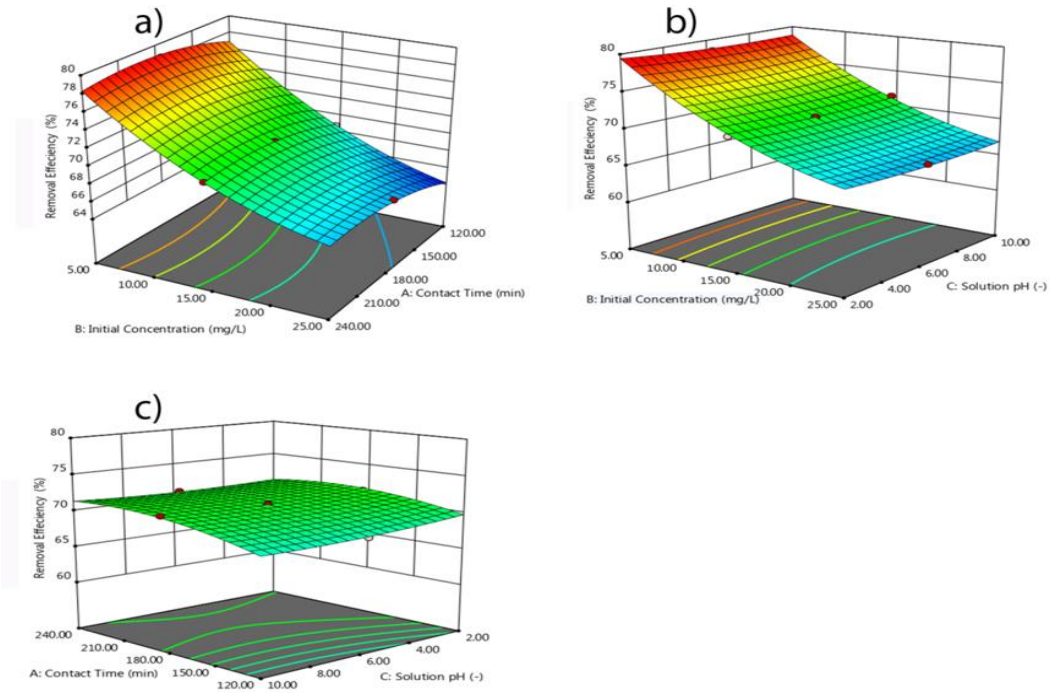

Figure 2. 6: The combined effect of (a) contact time and initial concentration, (b) contact time and pH, and (c) initial concentration and solution pH on % removal of phosphate

2.4 Conclusions

Credible evidence from scientific literature substantiates both beneficial and detrimental effects of coexisting anions in aqueous solution. However, this study focused on the effect of major design parameters on the adsorption of phosphate onto leftover coal without coexisting (competitive) anions. Accordingly, the following major conclusions can be drawn:

- When leftover coal is used for phosphate removal from aqueous solutions, design parameters such as initial phosphate concentration, initial solution pH, adsorbent dose, temperature, and contact time must be optimally selected to obtain the highest possible removal. Apparently, the adsorption of phosphate onto leftover coal increased markedly at pH value of 2, which is the actual pH value of most industrial effluents.

- The adsorption kinetics for phosphate removal could be well described by the pseudo-second-order equation with a correlation value of R^2 = 0.99 which revealed that, chemisorption was the dominant process.

- Observed temperature effects on phosphate adsorption reveal that the process is exothermic.

- The central composite design (CCD) was found to be an appropriate approach to optimize the variable affecting phosphate adsorption. The obtained quadratic regression model well depicted observed values of percent phosphate removal and phosphate removal capacity.

It is concluded that leftover coal could be employed as a low-cost adsorbent for the removal of phosphate ions from aqueous solutions. Future investigations shall be directed to phosphate removal from real wastewater that will give better insight into the effect of coexisting anions. The material should be tested in a flow-through set-up to drive practical solutions for local industries.

3. Adsorptive Removal of Phosphate from Aqueous Solutions Using Low-Cost Volcanic Rocks: Kinetics and Equilibrium Approaches (Paper 2)

Dereje Tadesse Mekonnen, Esayas Alemayehu and Bernd Lennartz

Materials/MDPI https://doi.org/10.3390/ma14051312

Abstract: The contamination of surface and groundwater with phosphate originating from industrial and household wastewater remains a serious environmental issue in low-income countries. Herein, phosphate removal from aqueous solutions was studied using low-cost volcanic rocks such as pumice (VPum) and scoria (VSco), obtained from the Ethiopian Great Rift Valley. Batch adsorption experiments were conducted using phosphate solutions with concentrations of 0.5 to 25 $mg \cdot L^{-1}$ to examine the adsorption kinetic as well as equilibrium conditions. The experimental adsorption data were tested by employing various equilibrium adsorption models, and the Freundlich and Dubinin-Radushkevich (D-R) isotherms best depicted the observations. The maximum phosphate adsorption capacities of VPum and VSco were calculated and found to be 294 $mg \cdot kg^{-1}$ and 169 $mg \cdot kg^{-1}$, respectively. A pseudo-second-order kinetic model best described the experimental data with a coefficient of correlation of $R^2 > 0.99$ for both VPum and VSco; however, VPum showed a slightly better selectivity for phosphate removal than VSco. The presence of competitive anions markedly reduced the removal efficiency of phosphate from the aqueous solution. The adsorptive removal of phosphate was affected by competitive anions in the order: $HCO_3^- > F^- > SO_4^{-2} > NO_3^- > Cl^-$ for VPum and $HCO_3^- > F^- > Cl^- > SO_4^{-2} > NO_3^-$ for VSco. The results indicate that the readily available volcanic rocks have a good adsorptive capacity for phosphate and shall be considered in future studies as test materials for phosphate removal from water in technical-scale experiments.

Keywords: adsorption kinetics; aqueous solution; eutrophication; isotherm models; pumice; scoria

3.1 Introduction

Phosphate, a molecule consisting of the elements phosphorus (P) and oxygen (Xiong et al., 2019b), is an essential macronutrient for all life (Acelas et al., 2014). With nitrogen and carbon, phosphorus is the primary source of productivity and is fundamental for freshwater ecosystems' sustainability (Jarvie et al., 2018). However, a high phosphate concentration above 0.1 $mg \cdot L^{-1}$ (Helmer &

Hespanhol, 1997) in water bodies has serious environmental repercussions, such as eutrophication, which is associated with massive algal growth, the excessive growth of microorganisms, and the depletion of dissolved oxygen (DO) in the water bodies, and, in turn, it harmfully effects life in the aquatic ecosystems (Asaoka & Yamamoto, 2010; Karageorgiou et al., 2007; Kim et al., 2015; Suresh et al., 2019; Yao et al., 2013). However, some researchers reported that a phosphate concentration as low as 0.05 $mg \cdot L^{-1}$ (Yadav et al., 2015b) or 0.02 $mg \cdot L^{-1}$ (Bacelo et al., 2020) in the water reservoir is sufficient to stimulate the growth of algae. Nowadays, the contamination of water bodies by pollutants like phosphorus has drawn attention globally. Industrialization, modern agriculture, and human activities are the primary sources that can pose a serious threat to freshwater ecosystems due to the pollutants released from these into the environment (Tao et al., 2020).

In many cases, pollutants from different point and non-point sources infiltrate at high concentrations into the nearby water bodies (Angello et al., 2020). Of the pollutants coming into water bodies, phosphate laden-water is the primary trouble of developing countries such as Ethiopia due to the formation of eutrophication in the surface water. The phosphate effluents from institutions, domestic activities, municipal activities, detergent-making industries, and agricultural-related activities are also the leading causes of eutrophication (Pengthamkeerati et al., 2008). Wastewater released from slaughtering houses, for example, contains about 25–200 $mg \cdot L^{-1}$ phosphate (Bacelo et al., 2020).

The elimination of phosphate from water can be achieved via many processes, such as biological process, chemical precipitation, and adsorption methods (Lalley et al., 2016; Tao et al., 2020). In comparison, biological processes and chemical precipitation are expensive and result in a large amount of waste sludge to dispose of, involving high operating costs (Choi et al., 2014; Han et al., 2017). Therefore, it is of great interest to develop reliable technologies that utilize viable adsorbents to remove excess phosphate from water. It has been reported that due to its ease of application, economic feasibility, and high efficiency among the mentioned methods, adsorption is the most efficient process for the removal of phosphate from water (Acelas et al., 2014; Saki et al., 2019).

Currently, a series of different adsorbents has been investigated for phosphate removal from synthesized aqueous water with or without surface modification. Some of these include zirconium

oxide nanoparticles (Su et al., 2013), exfoliated vermiculites (Huang et al., 2014), lanthanum hydroxide materials (Xie et al., 2014), bio-chars derived from crop straws (Jiang et al., 2015), rice husk ash (Mor et al., 2016); building waste (Yang et al., 2016), treated natural clinoptilolite (Mitrogiannis et al., 2017), modified wheat straw (Qiu et al., 2017), quaternary ammonium Chinese reed (Shang et al., 2017), zirconia-coated magnetite nanoparticles (Wang et al., 2017), corn stalks (Fan & Zhang, 2018), iron oxide waste (Shahid et al., 2019), and magnetic coal (George et al., 2019). However, many of these suffer from either poor regenerablity or high process costs or low adsorption capacity. In such cases, looking for the most low-cost, easily available, and easily accessible raw materials that can be used as adsorbents is a critical concern for developing countries such as Ethiopia.

Volcanic rocks are inorganic adsorbents that are available all over the world, as well as in Africa. Pumice (VPum) and scoria (VSco) are abundant volcanic rock materials found in many parts of the world (Asere et al., 2017). A vast amount of volcanic rocks are found in Ethiopia's Great Rift Valley, which covers about 30% of the area of the country (Alemayehu & Lennartz, 2009; Yasin et al., 2015). Due to their vascular structure, high contents of silica, alumina, iron oxides and alkaline earth metals, large surface areas, and environmental friendliness, VPum and VSco are given conspicuous roles for pollutants removal (i.e., phosphate ions) (Choi et al., 2014; Mboya et al., 2019). Previous studies have showed the adsorption efficiency of volcanic rocks (pumice and scoria) with heavy metals (Alemayehu et al., 2011; Alemu et al., 2018; Aregu et al., 2018; Kwon et al., 2010), fluoride (Geleta et al., 2021), and phosphorus (Zhang et al., 2014) in a single system. In Ethiopia, volcanic rocks are also applied to remove hazardous pollutants from tannery wastewater (Aregu et al., 2018), but there is little information on which raw volcanic rocks have been applied to remove phosphate from aqueous solutions. As such, the objectives of this study were (i) to investigate the recovery of phosphates from aqueous solution using volcanic rocks via classical slurry batch experiments, (ii) to determine the adsorption kinetics and adsorption isotherm models to compare the removal efficiency of the adsorbents (VPum and VSco), and (iii) to evaluate the impact of competitive/co-existing anions on the removal of phosphate.

3.2 Materials and Methods

3.2.1 Materials Preparation and Characterization

The volcanic rock materials, VPum and VSco, were obtained from the Great Rift Valley of Ethiopia. Before the experiments, the rock materials were washed several times using deionized water to remove dust, dirt, and adhering particles from the adsorbent's surface, and then dried for 24 h at 105 °C in the oven. The well-dried materials were ground to a powder form and sieved to the size of 0.075–0.425 mm. The well dried and ground materials were then coated with iron salts using iron (II) chloride tetrahydrate ($FeCl_2 \cdot 4H_2O$) to promote cations on the adsorbents' surface. Forty grams of the adsorbents were soaked with enough $FeCl_2 \cdot 4H_2O$ solution at a concentration of 0.01 M. The mixture was then sonicated at room temperature for 7 h using an ultrasonic mixer (BANDELIN SONOREX RK 16, Retsch GmbH, Haan, Germany). After sonication mixing, the decanted rock materials were heated at 90 °C for 18 h, then cooled and washed with deionized water several times until the suspension became clean, and then dried again at 105 °C in the oven for 24 h. The well-prepared adsorbent materials were labeled and stored in a desiccator until the next experiments resumed.

Proximate and ultimate analyses of the adsorbent materials (VPum and VSco) were performed according to the previous research (Mekonnen et al., 2020). The pH zero point charge (pHzpc) of adsorbent materials was measured according to Rao et al. (2012) using a solid addition method. The materials' organic matter and moisture content were measured according to previous study as well (Mekonnen et al., 2020), wherein the particle density and specific surface area (BET) of the rock materials were measured according to another previous study (Alemayehu & Lennartz, 2010). The organic matter, moisture content and pHzpc of the VPum were 4.95%, 0.85%, and 9.2, and those of the VSco were 0.21%, 0.45%, and 7.2, respectively. The specific surface area and particle density of the VPum were 3.5 $m^2 \cdot g^{-1}$ and 2.46 $g \cdot cm^{-3}$, and those of the VSco were 2.48 $m^2 \cdot g^{-1}$ and 2.98 $g \cdot cm^{-3}$, respectively. A scanning electron microscope equipped with an energy dispersive X-ray (SEM-EDX) was employed to analyze the adsorbents' surface morphology and the microstructure of the adsorbent materials. All the chemicals and reagents used in this study were of analytical grade unless otherwise specified. Table 3.1 (Alemayehu & Lennartz, 2009) shows that the chemical composition of raw VPum and VSco, measured by X-ray fluorescence (XRF) spectrometry, which was performed according to (Alemayehu & Lennartz, 2009). The greater the

presence metal ions such as Si and Fe, the more easily the materials attract phosphate ions by forming surface charges.

Table 3. 1: Chemical compositions of pumice (VPum) and scoria (VSco)

Chemical Compositions (wt. %)	SiO_2	Al_2O_3	Fe_2O_3	CaO	K_2O	Na_2O	MgO	TiO_2	Others
Vpum	68.6	8.9	4.9	1.8	5.5	4.1	0.2	0.3	5.7
Vsco	47.4	21.6	8.9	12.4	0.5	3.0	3.3	1.7	1.2

3.2.2 Batch Adsorption Studies

The equilibrium batch experiments were carried out to determine the removal capacities and the percentage removal of phosphate with the VPum and VSco. The procedures described in previous work (Mekonnen et al., 2020) were followed to prepare a working solution ranging from 0.5 to 25 $mg \cdot L^{-1}$, representing the minimum to typical phosphate concentration in water, by diluting a stock solution of potassium dihydrogen phosphate (KH_2PO_4). An initially known amount of each adsorbent was added to 10 $mg \cdot L^{-1}$ phosphate (1:5 solid to solution ratio) in 100 mL plastic flasks. The initial pH of each solution throughout the experiments was adjusted to 6 ± 0.5 and 5.0 ± 0.5 for VPum and VSco, respectively, at which levels monoanionic phosphate species exists. According to the repartition diagram of phosphate species, at the studied pH ranges (pH = 6.5 for VPum and pH = 5.5 for VSco), the phosphate species that predominantly exists could be $H_2PO_4^-$ (Pismenskaya et al., 2001).

The well-capped plastic flasks containing the mixtures of adsorbents and adsorbate were then placed on a horizontal mechanical shaker operating at 200 rpm and at room temperature. After 420 min of mixing, the mixtures were filtered through a 0.45 µm filter, and the concentration of phosphate in the filtrate was analyzed using a continuous flow analyzer (CFA) (AA3 from seal Analytical, GmbH, Norderstedt, Germany). Subsequently, the amount of adsorbed phosphate at equilibrium (q_e) and the percentage removal (A %) of phosphate from the aqueous solution were calculated using Equations (3.1) and (3.2), respectively:

$$q_e = \frac{(C_o - C_e)V}{M} \quad (3.1)$$

$$(A\%) = \left(1 - \frac{C_e}{C_o}\right) \times 100 \quad (3.2)$$

where qe is the amount of phosphate adsorbed (removal capacity) per unit mass of adsorbent at equilibrium; Co and Ce are the initial and final concentrations of phosphate at equilibrium ($mg \cdot L^{-1}$), respectively; V is the volume of the solution contacted with the adsorbent (L); M is mass of the adsorbent (g) and (A%) is percentage removal of phosphate at time t.

Similarly, phosphate's adsorption kinetics on the samples were evaluated by mixing 8 g of the VPum and VSco samples with 200 mL of solution at 10 $mg \cdot L^{-1}$ phosphate concentration in 250 mL plastic flasks. The mixtures were then shaken on the horizontal mechanical shaker, then the samples were withdrawn at each predetermined interval of time (5, 10, 20, 30, 40, 60, 90, 120, 180, 240, 300, and 420 min). At the end of each experiment, the mixture was immediately filtered using filter paper, and then phosphate analysis was carried out using CFA.

The effects of co-existing anions (nitrate (NO_3^-), sulfate (SO_4^{2-}), bicarbonate (HCO_3^-), chloride (Cl^-) and fluoride (F^-) from their respective salts of KNO_3, Na_2SO_4, $NaHCO_3$, NaCl and NaF, respectively) on the removal of phosphate were determined in a separate experiment. First, solutions were prepared from the respective salts at 0.1 M concentration using deionized water in a separate bottle. Then, 5 mL equal concentrations (0.1 M) of each anion were mixed with 20 mL of phosphate solution at 10 $mg \cdot L^{-1}$ concentration in a series of 100 mL Erlenmeyer plastic flasks. Then, 1 g of the adsorbents was added to a series of plastic flasks. The flasks were well capped and shaken on the horizontal shaker working at 200 rpm for 24 h at room temperature. The final suspension solution was collected and filtered, and then the phosphate concentration was measured with similar methods.

3.2.3 Adsorption Equilibrium Studies

To understand the quantity of adsorbates that are accommodated by the adsorbents' surface, adsorption equilibrium information is critical. The equilibrium of adsorption between solution and adsorbent is well described by different non-linear and linear forms of adsorption isotherms (Park & Jung, 2011). Langmuir, Freundlich, and Dubinin–Radushkevich (D-R) isotherms were employed to describe the equilibrium between the adsorbate and adsorbent for experimental data.

The Langmuir adsorption isotherm describes the formation of monolayer adsorption of the adsorbate on the surface of the adsorbent (Rangabhashiyam et al., 2014), and this can be expressed by Equations (3.3) and (3.4):

$$q_e = \frac{q_m K_L C_e}{1+K_L C_e} \text{ (non − linear form)} \quad (3.3)$$

$$\frac{C_e}{q_e} = \frac{1}{q_m K_L} + \frac{C_e}{q_m} \text{ (linear form)} \quad (3.4)$$

where q_e (mg·g^{-1}) is equilibrium adsorption capacity; C_e (mg·L^{-1}) is the equilibrium concentration of the adsorbate in the solution; q_m (mass of adsorbate per mass of adsorbent) is the maximum adsorption capacity of phosphate; K_L (L·mg^{-1}) is the Langmuir isotherm constant. The constants K_L and q_m can be calculated from the intercept and slope of the linear plot of C_e/q_e vs. C_e (Figure A3.1 in the supplementary data). The essential characteristics, feasibilities, and shapes of the Langmuir isotherm can be described by a dimensionless constant, the so-called separation factor, R_L (Equation (3.5)) (Naiya et al., 2009):

$$R_L = \frac{1}{1+K_L C_o} \quad (3.5)$$

where K_L and Co are Langmuir constant (L·mg^{-1}) and initial phosphate concentration (mg. L^{-1}) in the solution. The shape of the isotherm is determined by the values of the R_L; as $R_L = 0$ indicates irreversible adsorption, and $R_L = 1$ shows linear adsorption, where $R_L > 1$ and $0 < RL < 1$ indicate unfavorable and favorable adsorption, respectively, as indicated by (Alemayehu & Lennartz, 2009; Naiya et al., 2009).

The Freundlich isotherm involves heterogeneous adsorption or multi-layer adsorption (Padmavathy et al., 2016), and can be described by Equations (3.6) and (3.7):

$$q_e = K_F {C_e}^{1/n} \text{ (non − linear form)} \quad (3.6)$$

$$\ln q_e = \ln K_F + \frac{1}{n} \ln C_e \text{ (linear form)} \quad (3.7)$$

where q_e (mg·g^{-1}) is the equilibrium adsorption capacity; C_e (mg·L^{-1}) is the equilibrium concentration of the adsorbate in the solution; K_F, and n (unit-less) are the Freundlich isotherm constants related to sorption capacity and sorption energy, respectively. Freundlich isotherm's constants can be calculated from the slope and intercept of the linear plot of $\ln q_e$ vs. $\ln C_e$ (Figure

A3.2 in supplementary materials). The values of "n" indicate the type of adsorption isotherm; when the value of 1/n is greater than zero, which means $0 < 1/n < 1$, the adsorption is favorable and chemisorption occurs. When 1/n is greater than one, the adsorption is unfavorable, and irreversible adsorption occurs if 1/n is equal to unity (Al-ghouti & Da'ana, 2020).

The Dubinin-Radushkevich (D-R) isotherm is an empirical model that does not assume homogenous or constant sorption potential. It instead estimates the solute's mean free energy change when a mole of solute in the solution is transferred to the surface of the adsorbent (Foo & Hameed, 2010; Rao et al., 2012). The mean free energy describes the physical or chemical nature of the reaction for the adsorption. The D-R isotherm can therefore be expressed by Equation (3.8):

$$\ln q_e = \ln q_{max} - \beta\varepsilon^2 \qquad (3.8)$$

where q_e is the equilibrium adsorption capacity ($mol \cdot g^{-1}$), q_{max} is the maximum adsorption capacity ($mol \cdot g^{-1}$), β is the activity coefficient or adsorption constant depending on the mean free energy of adsorption, and ε is the Polanyi adsorption potential, which can be expressed by Equation (3.9):

$$\varepsilon = RT\ln\left(1 + \frac{1}{C_e}\right) \qquad (3.9)$$

where R is the universal gas constant ($kJ \cdot mol^{-1} \cdot K^{-1}$), T is the absolute temperature (K), and C_e is the equilibrium concentration of the adsorbate in the solution ($mol \cdot L^{-1}$). The q_{max} and β can be obtained from the linear plot of $\ln q_e$ vs. ε^2(Figure A3.3). The mean free energy of adsorption E ($kJ \cdot mol^{-1}$) can be obtained from the expression of Equation (3.10) (Hamayun et al., 2014):

$$E = \frac{1}{\sqrt{(2\beta)}} \qquad (3.10)$$

3.2.4 Adsorption Kinetics

To quantify the time-dependent adsorption process, adsorption kinetics were investigated using pseudo-first-order kinetics, pseudo-second-order kinetics, and intra-particle diffusion models.

Lagergren pseudo-first-order expression is given by Equation (3.11) (Rao et al., 2012):

$$\ln(q_e - q_t) = \ln(q_e) - K_1 t \qquad (3.11)$$

where K_1 is the first-order rate constant of adsorption (min^{-1}); q_e ($mg \cdot g^{-1}$) and q_t ($mg \cdot g^{-1}$) are the amount of phosphate adsorbed at equilibrium and at time t, respectively. The values of K_1 and q_e can be obtained from the slope and the intercept of a linear straight-line plot of $\ln(q_e-q_t)$ vs. t.

The pseudo-second-order expression can be described by Equations (3.12) and (3.13):

$$\frac{dq_t}{dt} = K_2(q_e - q_t)^2 \qquad (3.12)$$

which can be integrated via the linear expression as:

$$\frac{t}{q_t} = \frac{1}{h} + \frac{1}{q_e}t \qquad (3.13)$$

where q_e ($mg \cdot g^{-1}$) and q_t ($mg \cdot g^{-1}$) are the amount of phosphate adsorbed at equilibrium and time t, respectively; $h = K_2 qe^2$ and K_2 is the rate constant of the pseudo-second-order model ($g \cdot mg^{-1} \cdot min^{-1}$). The values of K_2 and q_e can be obtained, respectively, from the intercept and slope of the linear plot t/q_t vs. t.

The intra-particle diffusion equation can be expressed as shown in Equation (3.14) (Acelas et al., 2014):

$$q_t = K_{id} t^{0.5} + C \qquad (3.14)$$

where q_t is the amount of phosphate adsorbed at time t, K_{id} ($mg \cdot g^{-1} \cdot min^{-1/2}$) is the intra-particle diffusion rate constant obtained from the slope of the plot q_t vs. $t^{0.5}$, and C ($mg \cdot g^{-1}$) is the intercept of the plot, often referred to as the thickness of the boundary layer and obtained from the intercept of the plot (Chen et al., 2013).

3.3 Results and Discussions

3.3.1 Adsorbents Characterization

The scanning electron microscope (SEM) analysis revealed that the surface morphology of the VPum was rough and wrinkled, which potentially provides more adsorption sites for phosphates (Figure 3.1a) than VSco, where a relatively smooth and uniform surface structure was observed (Figure 3.1c). The pumice's porousness and cavities indicated that the pumice materials had a rougher surface compared to scoria, which implies that pumice has a better phosphate adsorption capacity than scoria. Figure 3.1b, d show the energy dispersive X-ray (EDX) image for the

adsorbent's elemental composition of VPum and VSco. The measured EDX image indicates that the oxides of Al, Si, Fe, and K were the main constituents of the adsorbent materials, while the rest of the elements, such as Mn and Pb, were detected at lower values (<0.1% weight).

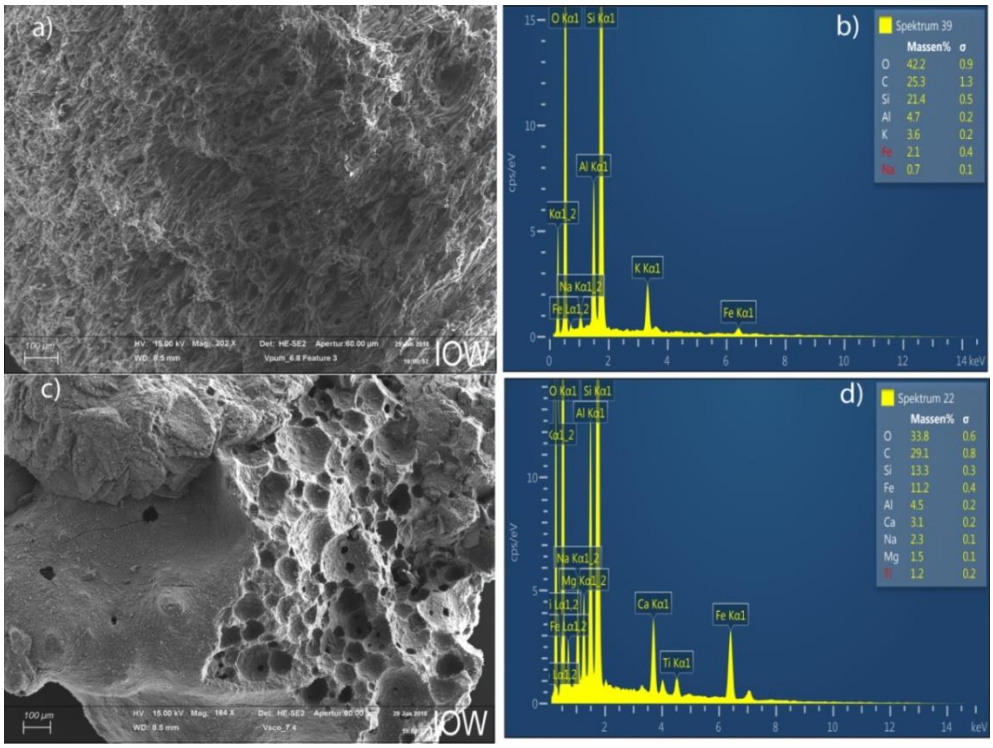

Figure 3. 1: Scanning electron microscope (SEM) and energy dispersive X-ray (EDX) patterns of Vpum (a,b) and Vsco (c,d), respectively

3.3.2 Effects of Contact Time

Designing an appropriate batch adsorption experiment is very important to get the rate at which the adsorption takes place, and the adsorption process' time dependence was described by varying the contact time between the adsorbates and the adsorbents' surface. Twelve contact points were examined to evaluate the effects of contact time on the abilities of VPum and VSco to remove phosphate at room temperature. The impact of contact time on the percent of removed phosphate is shown in Figure 3.2. The phosphate removal efficiencies of VPum and VSco were sharply increased for the first 240 min, from 0 to 81% for VPum and from 0 to 76% for VSco. The first fast increase in the removal efficiency was due to the significant validity of active free pore sites on the adsorbent's surface compared to the remaining adsorption time (Omari et al., 2019; Rout et al., 2015). As time goes on, the adsorbent's surface gets saturated with phosphate, and only a few phosphate removals occurred during the last 3h of equilibrium. Therefore, equilibrium was

achieved at the 420 min contact time. Similar materials were used to remove chromium from the aqueous solution, and adsorption equilibrium was attained at 540 min (Alemu et al., 2018). However, a fast equilibrium time was attained at 120 min for blended rock materials with chitosan, used to remove arsenic from aqueous solution (Asere et al., 2017). This indicates that the surface modification of the adsorbents provides a better adsorption time, as the contact time is crucial for calculating the process' optimum reaction time (Fan & Zhang, 2018).

It was also observed that the removal efficiency of VPum was slightly better than that of VSco, which was in agreement with the results for the adsorbents' surface morphology obtained from SEM. The more porous the surface is, the better the phosphate's adsorption onto the adsorbents' surfaces (Huang et al., 2016).

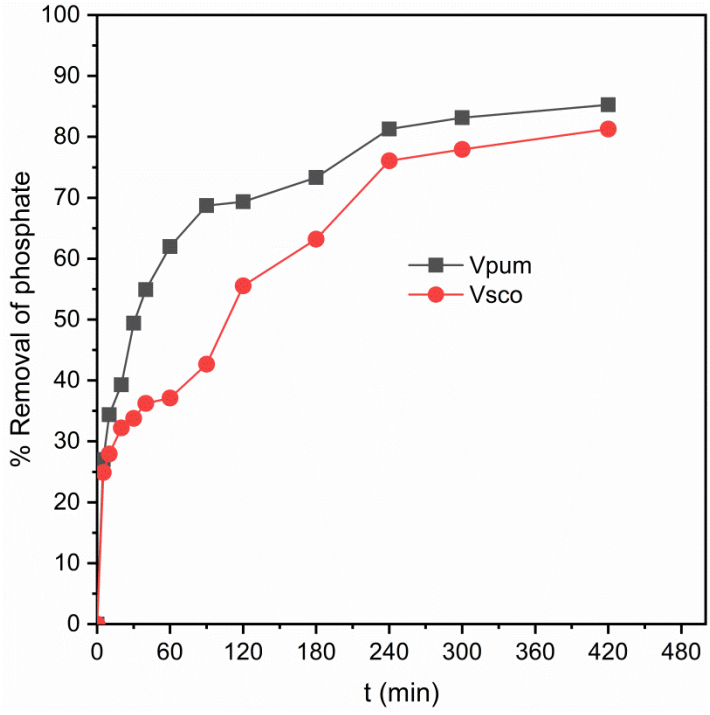

Figure 3. 2: Effect of contact time on the removal efficiency of phosphate

3.3.3 Adsorption Kinetics

Due to providing worthy information on the reaction pathways and adsorption mechanisms, adsorption kinetics analysis plays a vital role in the adsorption system (Vaghetti et al., 2008). The mass transfer and chemical reaction mechanisms of the adsorptive removal of phosphate onto VPum and VSco can be examined by various kinetic models, namely Lagergren pseudo-first-

order, pseudo-second-order, and Weber and Morris intra-particle diffusion kinetic models (Aljeboree et al., 2014; Lin et al., 2018). Therefore, their validity for use with the experimental adsorption data for phosphate onto VPum and VSco was investigated. The results obtained from the pseudo-second-order model exhibited higher correlation values ($R^2 > 0.99$) for both VPum and VSco than the pseudo-first-order model tested in this study. Moreover, the calculated adsorptive capacity values ($q_{e,\ cal}$) from the pseudo-second-order kinetic model were 228.22 $mg \cdot kg^{-1}$ and 216.84 $mg \cdot kg^{-1}$ for VPum and VSco, respectively. These values agreed well with the experimentally determined adsorptive capacity values (q_{exp}) of 238 $mg \cdot kg^{-1}$ and 234.75$mg \cdot kg^{-1}$ for VPum and VSco, respectively. Moreover, the pseudo-second-order linear plot (Figure 3.3) shows the good agreement of the experimental data with the calculated data for VPum and VSco. Nevertheless, the values of the calculated removal capacity and its linear plot (Figure A3.4) obtained from pseudo-first-order, compared to pseudo-second-order, for both VPum and VSco were not allied with the values of the removal capacity derived from the experimental values. This validates that the pseudo-first-order kinetic model does not adequately describe the adsorption process, whereas the adsorptive removal of phosphate by VPum and VSco followed the pseudo-second-order reaction (Ahn et al., 2009; Ozacar, 2003). The non-linear adsorption kinetics plots for pseudo-first-order, pseudo-second-order, and intra-particle diffusion are shown in Figure 3.4, which describes the nonlinear curve fitting of the adsorption kinetics and its corresponding constant parameters, and the calculated and experimental values of the adsorption kinetic models are summarized in Table 3.2.

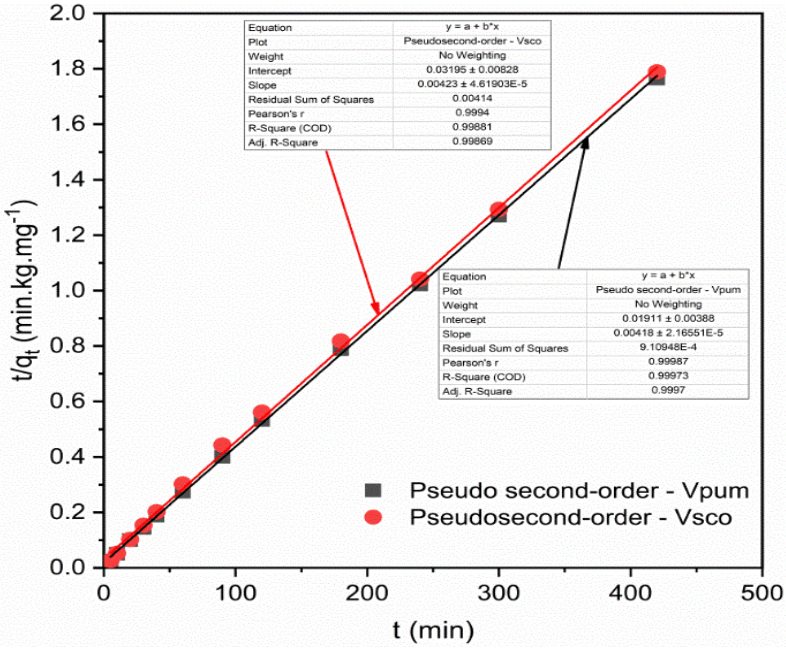

Figure 3. 3: Pseudo-second-order kinetic plot for VPum and VSco

Intra-particle diffusion is also responsive to the diffusion mechanism of the adsorbate in the solution. If the plots for the intra-particle diffusion q_t vs. $t^{0.5}$ of Equation (3.14) both for VPum and VSco are leaner and pass through the origin, then the intra-particle diffusion model is the sole rate-limiting step; otherwise, an adsorptive process other than intra-particle diffusion can occur (Ahn et al., 2009). According to the intra-particle diffusion model, three points can be valid: (i) if the plot of q_t vs. $t^{0.5}$ is linear, the intra-particle diffusion model will be involved in the rate-controlling step for the adsorption process; (ii) if this line passes through the origin, i.e., intercept = 0, then the intra-particle diffusion model is the sole rate-controlling step of the adsorption process, and (iii) if two or more slopes could occur, then there should be an indicator for the multi-step adsorption process (Pan et al., 2017). In this case, the linear plot of q_t vs. $t^{0.5}$ (Figure 3.5) did not pass through the origin, but was linear in some points, and two slopes were observed. Therefore, this validates that intra-particle diffusion was not the only rate-limiting step, and non-diffusive reaction also occurred between the phosphate ion and rock materials. This applicability of the intra-particle diffusion model for the present kinetic data is also in agreement with other studies (Pan et al., 2017; Saha et al., 2016).

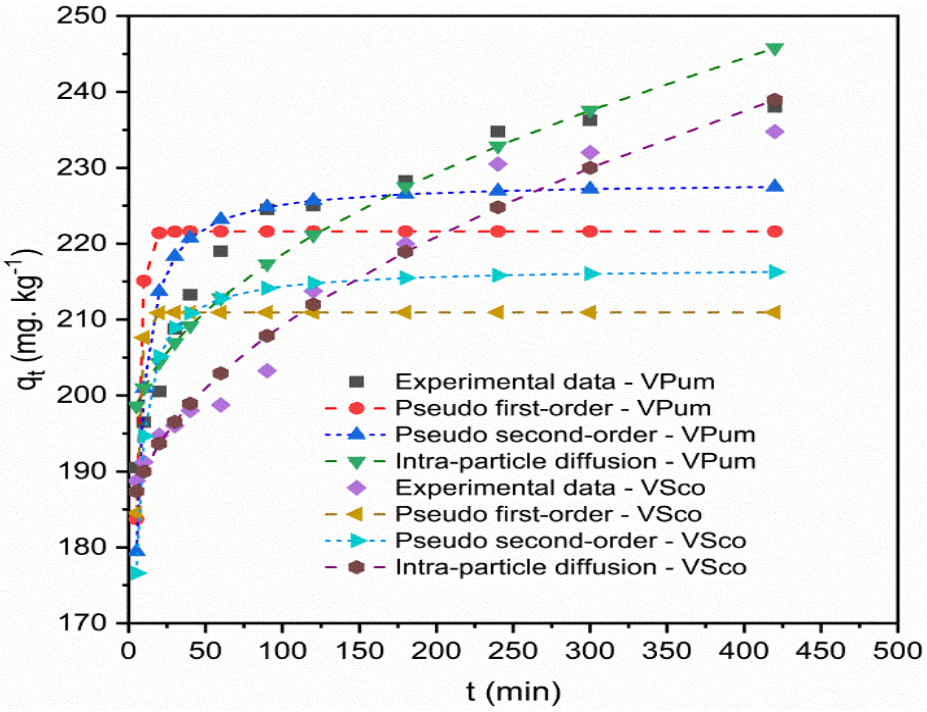

Figure 3. 4: Kinetics of phosphate adsorption on VPum and VSco, and data fitting for pseudo-first-order, pseudo-second-order, and intra-particle diffusion

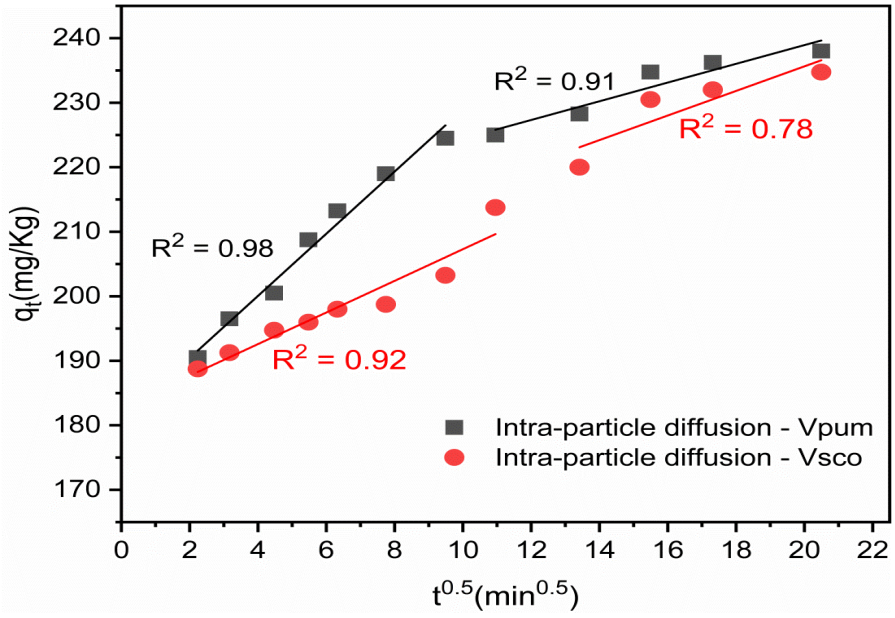

Figure 3. 5: Intra-particle diffusion plot for VPum and VSco with two different slopes

Table 3. 2: Calculated and experimental values of parameters for pseudo-first order, pseudo-second order, and the intra-particle diffusion kinetics model for phosphate adsorption onto volcanic rocks

Kinetic Model	Parameters	VPum	VSco
Experimental	qexp ($mg \cdot kg^{-1}$)	238.0	234.75
Pseudo-first-order	$q_{e,cal}$ ($mg \cdot kg^{-1}$)	221.60	210.94
	K_1 (min^{-1})	0.35	0.42
	R^2	0.97	0.98
Pseudo-second-order	$q_{e,cal}$ ($mg \cdot kg^{-1}$)	228.22	216.84
	K_2 (g. $mg^{-1}.min^{-1}$)	3.20	4.10
	R^2	0.999	0.999
Intra-particle diffusion	K_{1id} ($mg \cdot kg^{-1} \cdot min^{-1/2}$)	4.82	2.45
	K_{2id} ($mg \cdot kg^{-1} \cdot min^{-1/2}$)	1.45	1.90
	C_{1id} ($mg \cdot kg^{-1}$)	180.81	182.78
	C_{2id} ($mg \cdot kg^{-1}$)	209.92	197.55
	R_1^2	0.98	0.92
	R_2^2	0.91	0.78

3.3.4 Effects of Initial Concentration

The variation in phosphate removal by VPum and VSco as a function of the initial phosphate concentration is presented in Figure A3.5 in the supplementary material. It was noticed that the percent removal of phosphate decreased (from 93% to 43% and from 81% to 23%, for VPum and VSco, respectively) with an increase in initial phosphate concentration (from 0.5 to 25 $mg \cdot L^{-1}$). This is because the resistance to the up-taking of the adsorbate onto the adsorbents' surfaces is

higher, and the active site for adsorption gets saturated at higher concentrations (Yadav et al., 2015). In contrast, phosphate removal capacity, q_t, increased with increasing the initial phosphate concentration due to the higher driving forces provided by the higher initial concentrations, which were able to resist the mass transfer between the solid surface and aqueous solution (Lin et al., 2018), which enables the adsorbate to remain on the surface of the adsorbents. Furthermore, for the initial phosphate concentration in the range of 5 to 25 $mg \cdot L^{-1}$, the amount of phosphate adsorbed decreased in the order of VPum > VSco. This revealed that VPum has, relatively, a better removal capacity than VSco.

3.3.5 Adsorption Isotherm

The adsorption equilibrium data are represented with the correspondences of adsorption capacity, qe, and the adsorbate's concentration, Ce, at equilibrium. Figure 3.6 shows the isotherm plots and experimental data. As seen in Figure 3.6, the adsorption capacity qe increases with the increase in phosphate concentration. This is due to the increased mass transfer driving force with the increasing initial phosphate concentrations (Fan & Zhang, 2018). The constant values and coefficients of determination of the adsorption isotherms are described in Table 3.3. From the results obtained in Table 3.3, R_L values for the Langmuir and 1/n values for the Freundlich isotherms were less than unity, and this elucidates that the adsorption of phosphate onto VPum and VSco is favorable. Furthermore, the lower value of 1/n ($0 < 1/n < 1$) is also a good indicator that chemisorption was governing the adsorption process for VPum and VSco. Similar findings were reported in the literature (Al-ghouti & Da'ana, 2020; Foo & Hameed, 2010).

The adsorption behavior can be depicted as physical or chemical, depending on the value of the mean free energy (E) of the D-R isotherm model. When the mean free energy of adsorption is between 1 and 8 $kJ \cdot mol^{-1}$, the adsorption behavior can be depicted as physical adsorption. The force of attraction between the adsorbate and the adsorbent is feeble. Otherwise, it is represented as chemical adsorption if the value of the mean free energy of adsorption is greater than 8 $kJ \cdot mol^{-1}$. The chemical bond between the adsorbate and the adsorbent is very strong. From the results obtained in Table 3.3, the value of E for the D-R isotherm is between 1 and 8 $kJ \cdot mol^{-1}$ for both VPum and VSco, indicating that the adsorption process was also governed by physical adsorption due to Van der Waals forces (Lin et al., 2018; Naiya et al., 2009). Unlike the Langmuir and Freundlich isotherm models, a D-R isotherm model follows the pore-filling mechanisms with the

assumption of a multilayer character, which involves the Van der Waals force applied to the physical adsorption process. Still, from the adsorption kinetic values and Freundlich isotherm, the adsorption process followed chemisorption. The adsorption process' deviation confirmed phosphate adsorption onto VPum and VSco following the physisorption and chemisorption (Al-ghouti & Da'ana, 2020). The covalent forces of electron attraction due to metal ions exist on the adsorbent's surface, and surface attraction between the adsorbent and adsorbate is applied (Kudeyarova, 2010). A similar study was reported wherein both physisorption and chemisorption were applied to remove orange 16 onto hemp stalk activated carbon (Rehman et al., 2017).

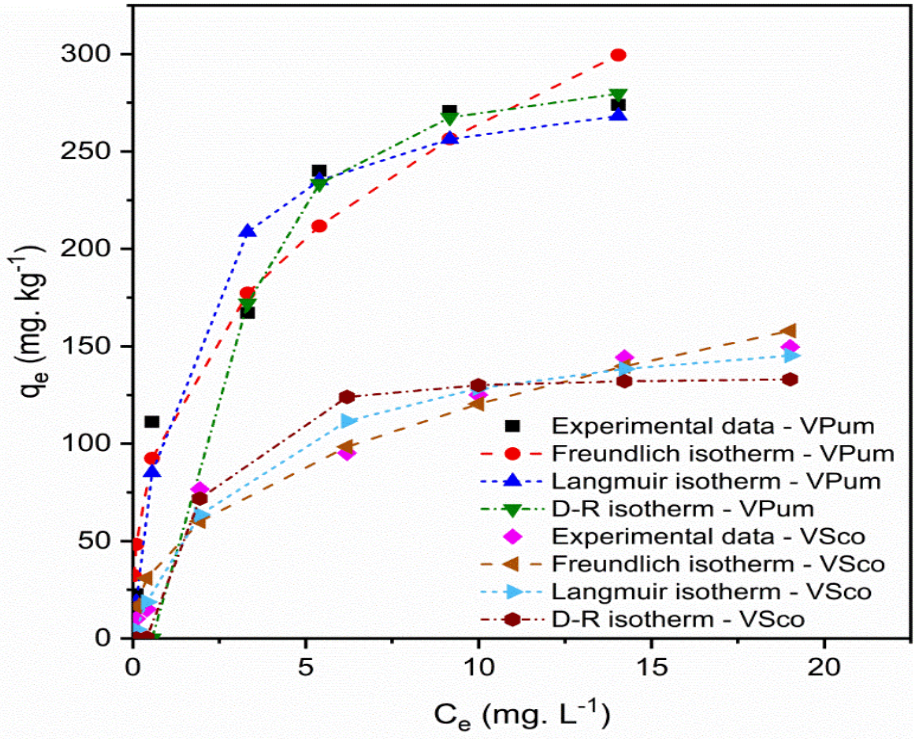

Figure 3. 6: Nonlinear phosphate adsorption isotherms for VPum and Vsco

Table 3. 3: Adsorption isotherm parameters for the adsorption of phosphate onto volcanic rocks

Isotherms	Parameters	Adsorbents	
		Pumice	**Scoria**
Langmuir isotherm	K_L ($L \cdot mg^{-1}$)	0.74	0.31
	q_m ($mg \cdot kg^{-1}$)	294.28	169.95
	R^2	0.73	0.81
	R_L	0.05–0.7	0.11–0.87
Freundlich isotherm	K_F $((mg \cdot kg^{-1})(mg \cdot L^{-1})1/n)^{-1}$	114.80	45.58
	n	2.76	2.37
	R^2	0.89	0.92
Dubinin-Radushkevich isotherm	q_{max} ($mg \cdot kg^{-1}$)	289.81	134.32
	E ($kJ \cdot mol^{-1}$)	3.31	5.44
	B	0.045	0.017
	R^2	0.80	0.69

3.3.6 Effects of Competitive Anions

Real wastewater commonly contains different anions, which exist in various forms of concentration (Boukemara & Boukhalfa, 2012; Kim & Lee, 2012). Phosphate adsorption onto VPum and VSco was independently studied in competing anions: nitrate (NO_3), sulfate (SO_4^{2-}), chloride (Cl^-), fluoride (F^-) and bicarbonate (HCO_3). The effects of competitive anions on phosphate removal onto the surface of the adsorbent materials showed that the phosphate removal efficiency of VPum and VSco with the absence of competitive anions was 85% and 79%, respectively (Figure 3.7). The reductions in phosphate removal efficiency were observed after

adding the competitive anions. When 0.1 M of bicarbonate ion was introduced to the phosphate solution, the removal efficiency was reduced by 14.1% for VPum and 11.4% for VSco. The addition of the bicarbonate ion may make the overall solution of phosphate alkaline, by raising the pH (from 6.5 to 9.6 and from 5.5 to 7.8, for VPum and VSco, respectively), which could be the reason for the decrease in phosphate's removal efficiency. In this case, an anion exchange reaction occurs between the phosphate ions and metal oxide, which favorably competes with hydroxide ions. The affinity of phosphate ions to the surface of the adsorbents becomes lower, and the adsorption efficiency is decreased. Similar findings were also reported in other studies (Huang et al., 2014; Rashid et al., 2017). Similarly, a fluoride ion has shown a high impact on the removal of phosphate onto VPum and VSco materials, whereby the removal efficiency of phosphate reduced by 13% and 7.6%, respectively. The noticeable reductions in phosphate removal efficiency by fluoride ion were likely due to the higher competition for fluoride ions binding to the adsorbents' surface than for phosphate ions (Li et al., 2016). From this result, it can be concluded that VPum and VSco as adsorbents can be applied for the simultaneous removal of phosphate and fluoride from water. However, no noticeable effect was observed due to chloride for VPum or nitrate for VSco materials. Similar studies reported that nitrate and chloride did not affect phosphate removal when bio-char from anaerobically digested sugar beet, silicate hybrid materials, and acid-coated magnetite nanoparticles was employed as the adsorbent, respectively (Rashid et al., 2017; Yao et al., 2011; Zhang et al., 2011). In contrast, the addition of nitrate into the aqueous solution greatly affected the removal efficiency of phosphate onto the modified sludge bio-char adsorbent (Saadat et al., 2018). These contradictions in the present study's results and previous studies might be attributable to different experimental conditions, such as anion concentration and other adsorbents' properties.

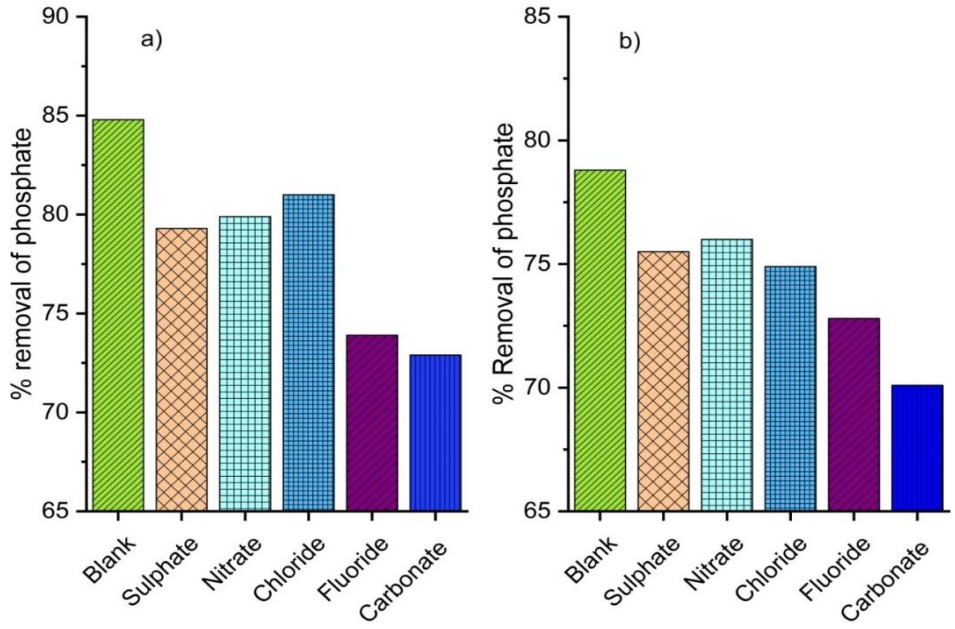

Figure 3. 7: Effects of competitive anions on phosphate removal: (a) pumice and (b) scoria

3.4 Conclusions

In the present study, cost-effective, environmentally friendly, and easily accessible volcanic rock materials (pumice and scoria) were used to recover phosphate from aqueous solution. The Freundlich and Dubinin-Radushkevich isotherms better described the adsorption process than the Langmuir isotherm model. The optimized parameter values for various adsorption kinetic models and adsorption isotherms advocate that the adsorption processes are mainly dominated by chemisorption and the strong attraction of covalent bonds. However, the value of mean free energy, as obtained from the Dubinin-Radushkevich isotherm, indicated that physisorption may likewise play an important role in the removal process due to Van der Waals forces. It was also observed that the removal of phosphate from the solution was dramatically affected by competitive anions. Thus, the simultaneous removal of pollutants has to be considered during water treatment. Overall, volcanic rocks (i.e., pumice and scoria) can be used as potential adsorbents to remove phosphate from water, but additional studies are required to further explore the potential of the rock material in a technical-scale (flow-through) set-up. In addition, several repetitions for the desorption and regeneration of the rock materials are highly recommended in further studies so as to increase the reusability of the materials.

4. Fixed-Bed Column Technique for the Removal of Phosphate from Water Using Leftover Coal (Paper 3)

Dereje Tadesse Mekonnen, Esayas Alemayehu, Bernd Lennartz

Materials/MDPI https://doi.org/10.3390/ma14195466

Abstract: The excessive discharge of phosphate from anthropogenic activities is a primary cause for the eutrophication of aquatic habitats. Several methodologies have been tested for the removal of phosphate from aqueous solutions, and adsorption in a flow-through reactor is an effective mechanism to reduce the nutrient loading of water. This research aimed to investigate the adsorption potential of leftover coal material to remove phosphate from a solution by using continuous flow fixed-bed column, and analyzes the obtained breakthrough curves. A series of column tests were performed to determine the phosphorus breakthrough characteristics by varying operational design parameters such as adsorbent bed height (5 to 8 cm), influent phosphate concentration (10–25 mg/L), and influent flow rate (1–2 mL/min). The amorphous and crystalline property of leftover coal material was studied using XRD technology. The FT-IR spectrum confirmed the interaction of adsorption sites with phosphate ions. Breakthrough time decreased with increasing flow rate and influent phosphate concentration, but increased with increasing adsorbent bed height. Breakthrough-curve analysis showed that phosphate adsorption onto the leftover coal material was most effective at a flow rate of 1 mL/min, influent phosphate concentration of 25 mg/L, and at a bed height of 8 cm. The maximal total phosphate adsorbed onto the coal material's surface was 243 mg/kg adsorbent. The Adams–Bohart model depicted the experimental breakthrough curve well, and overall performed better than the Thomas and Yoon–Nelson models did, with correlation values (R^2) ranging from 0.92 to 0.98. Lastly, leftover coal could be used in the purification of phosphorus-laden water, and the Adams–Bohart model can be employed to design filter units at a technical scale. leftover coal.

Keywords: Breakthrough Curve; Fixed-bed Column; Bed Height; Adsorption; eutrophication

4.1 Introduction

Increasing concern about the effect of phosphate released from different natural and human activities has resulted in more stringent environmental policies in recent years. Phosphate is one of the main nutrients for plants and aquatic lives, and is, in turn, primarily responsible for the eutrophication of water (Ajmal et al., 2018; Biswas et al., 2008; Hamzah et al., 2018; Khan, et al., 2013; Nagoya et al., 2019; Sellner et al., 2019). The eutrophication of water bodies due to phosphate discharges is a challenging issue for industrialized regions (Lin et al., 2015; Shahid et al., 2019). Domestic activities, detergent-making industries, and mining companies are the primary sources for phosphate discharged to water bodies. The uncontrolled use of fertilizers also releases phosphate and affects nearby water streams due to the runoff from agricultural activities (Hu et al., 2020; Ramirez et al., 2018). Water pollution by phosphate is tremendously increasing, and demand for the removal of excess phosphate from water bodies is thereby also increasing (Zhang et al., 2011).

There are numerous methods to remove phosphate from water, including chemical precipitation, biological treatment, physical process, coagulation, and adsorption (Đuričić et al., 2016; Qiu & Duan, 2019; Wang et al., 2018; Ye et al., 2019). Nevertheless, most of them, with the exception of adsorption, show drawbacks due to the high sludge production, the complexity of the process, and high operational costs compared with adsorption methods (Bezza & Chirwa, 2021; Castro et al., 2021). Adsorption has received immense interest due to its high removal efficiency, simple operation, better cost effectiveness, less or no sludge production, and invulnerability to coexisting pollutants (Jung et al., 2017; Rout et al., 2014; Woumfo et al., 2015). The application of low-cost and locally available materials for phosphate removal was widely investigated during this decade, such as with modified biochar (Jung et al., 2017), steel slag (Meyer et al., 2012), volcanic rock (Mekonnen et al., 2021), alkaline Tunisian soil (Beji et al., 2018), chitosan composite (Cui et al., 2019), alum sludge (Yang et al., 2006), and furnace slags (Xue et al., 2009).

Numerous studies were applied as adsorption methods and to remove phosphate from water by using batch experiments with different low-cost adsorbents (Cui et al., 2019; Huang et al., 2018; William et al., 2019; Zhang et al., 2019). At the industrial scheme, however, it was difficult to remove phosphate from a large amount of a water solution at the industrial level using batch adsorption (Ahn, et al., 2017), so continuous-flow fixed-bed column adsorption is versatile in the

removal of phosphate from large amounts of a water solution using low-cost adsorbents (Đuričić, et al., 2016).

In the present study, phosphate removal potential was examined in a fixed-bed column by using leftover coal material. The same authors verified the application of leftover-coal (Mekonnen et al., 2020) and volcanic-rock (Mekonnen et al., 2021) material as potential adsorbents for the recovery of phosphate from an aqueous solution through classical slurry batch experiments. However, batch-adsorption data are inconvenient for large-scale volumes due to the overestimation of sorption capacities (Negrea et al., 2020). In order to obtain convincing results, fixed-bed column adsorption is more realistic and popular in water treatment plants due to its continuous, high-yield, easy, and economical operation, and the ability to be scaled up from the laboratory scale (Nuryadin & Imai, 2021). Furthermore, few or no studies have reported on the phosphate adsorption capacity of leftover coal via continuous-flow fixed-bed column methods. Therefore, the main objective of this study is to: (i) investigate the application of fixed-bed column for the removal of phosphate using leftover coal material, (ii) study the effects of operational parameters on removal capacity by using breakthrough-curve analysis, and (iii) correlate experimental data with theoretical breakthrough-curve models to predict overall adsorption behaviors.

4.2 Materials and methods

4.2.1 Adsorbent Preparation and Characterization

The coal material was obtained from Yayu coal mining, as presented in the previous study (Mekonnen et al., 2020). Prior to the experiments, the coal material was washed several times using deionized water to remove dust, dirt, and adhering particles from the surface of the adsorbent, and then dried for 24 h at 105 °C in an oven dryer. The well-dried materials were ground into a powder form. The ground powder was sieved to the size of 0.075–0.425 mm. The well-prepared adsorbent materials were labeled and stored in desiccator until the following experiments.

Proximate and ultimate analyses of the adsorbent material were performed according to the previous research (Mekonnen et al., 2020). The pH zero point charge (pHzpc) of the adsorbent material was measured according to Rao et al. (2012) by using the solid-addition method. The organic matter, moisture content, and pHzpc of the material were measured to be 28.5%, 0.93%, and 4.6, respectively.

The functional groups of the adsorbent material were recorded using an FTIR machine (PerkinElmer, FT-IR spectrometer—Spectrum two) in the mid infrared region of 450–5000 cm^{-1} with a spectral resolution of 2 cm^{-1}. First, the pellet was prepared from dried sample materials by the proper mixing of potassium bromide (KBr) with a 1:9 adsorbent-to-KBr ratio (Jiang et al., 2018) and ground to a very fine size. The well-mixed material was pelletized using a pressure corporation machine, and the pellets were then measured accordingly (Alemu et al., 2018); the Fourier transform infrared (FT-IR) of the adsorbent material is shown in Figure 4.1.

X-ray diffraction (XRD) analysis was performed to observe the crystal structure and mineral composition of the adsorbents. The XRD patterns of the leftover coal were recorded using an XRD apparatus (XRD-7000, SHIMADZU Corporation, Japan). Before XRD analysis, the leftover coal material was washed, dried in an oven to the appropriate temperature, and milled and sifted through a 75-micrometer sieve to obtain uniform and homogeneous particles. Then, XRD analysis was recorded with CuKα as the source radiation at wave length of 1.4 nm, at 40 kV and 30 mA (Figure 4.2). All employed chemicals and reagents in this study were of analytical grade unless otherwise specified.

4.2.2 Phosphate Adsorption in a Fixed Bed Column

The fixed-bed column adsorption experiments were conducted using a Pyrex glass column of 130 mm height and 26 mm diameter. The column was packed with a known amount of adsorbent material (leftover coal) to achieve the intended bed heights (5 to 8 cm), and then caped at the top and at the bottom with glass wool to avoid bed height changes due to the loss of some adsorbents and to prevent adsorbent wash out. Artificial phosphate-laden wastewater was synthesized by previously diluting phosphate stock solution with a concentration of 1000 mg/L to the working solution at concentrations of 10 to 25 mg/L using distilled water, and the pH of each working solution was adjusted to 3.5 using HCl and NaOH by pH meter according to the previous works (Mekonnen et al., 2020). Depending on the pH of the working solution, phosphorus can be present in the solution in the form of H_3PO_4, $H_2PO_4^-$, HPO_4^{2-}, and PO_4^{-3}. At the working pH of 3.5, dihydrophosphate ion ($H_2PO_4^-$) species was dominating, which can be seen from the repartition or speciation diagram of phosphate ion (Kilpimaa et al., 2014).

Prior to the experiments, the filled and packed column was flushed upward by deionized water until steady flow conditions were established (Lee et al., 2015). The working solution then pumped up through the column with different flow rates (1 to 2 mL/min) using a peristaltic pump (MS-

REGLO, Labortechnik-Analytic, Zurich, Switzerland). In order to obtain the breakthrough curves, the effluent was collected at a predetermined interval of time. Lastly, equilibrium phosphate concentration was measured by continuous flow analyzer (AA3 from Seal analytical GmbH, Norderstedt, Germany).

4.2.3 Theory and Column Data Evaluation

The obtained data from the fixed-bed column studies were used to estimate the breakthrough curve by plotting the Ct/Co (the ratio of effluent phosphate concentration at time t to influent phosphate concentration) vs time. The breakthrough curve, therefore, could be calculated at breakthrough time (t_b) at which the Ct/Co = 10% and exhaustion time (t_e) at which Ct/Co = 90%, defined as Ct/Co = 0.1 and Ct/Co = 0.9, respectively. The breakthrough curve and its shape are the main characteristics that are used to investigate the dynamic response of the adsorption system (Alalwan et al., 2018). For a desired initial phosphate concentration and flow rate, the total amount of phosphate retained by the column, q_{total} (mg) could be calculated from the area under the breakthrough curve (Equation (4.1)), while the mass of phosphate adsorbed per mass of adsorbent at equilibrium (qe (mg/g)) was calculated from Equation (4.2) (Lalley et al., 2016).

$$q_{total} = \frac{QC_o}{1000}\int_{t=0}^{t=total}(1-\frac{C_t}{C_o})dt \tag{4.1}$$

$$q_e = \frac{q_{total}}{m} \tag{4.2}$$

where Q is the volumetric flow rate (mL/min), and m is mass of adsorbent packed within the column (g).

The mass transfer zone (MTZ) is defined as the active region of the coal material where the adsorption of phosphate takes place and can be defined as Equation (4.3) (Husein et al., 2017; Vieira et al., 2019).

$$MTZ = H_b\left(\frac{t_e - t_b}{t_e}\right) \tag{4.3}$$

where H_b is total bed height (cm), and tb and t_e are the breakthrough time and exhaustion time (min), respectively, which can be obtained from the area under the curves (Equations (4.4) and (4.5)) (Geleta et al., 2021; Golie & Upadhyayula, 2016; Yagub et al., 2015).

$$t_b = \int_0^{t_b} (1 - \frac{C_t}{C_o})\, dt \tag{4.4}$$

$$t_e = \int_0^{t_{total}} (1 - \frac{C_t}{C_o}) dt \tag{4.5}$$

Empty bed contact time (EBCT) is the time of contact between the water phase and the adsorbent (Equation (4.6)), and it measures critical depth and contact time for the adsorbent (Beji et al., 2018).

$$EBCT = \frac{V_b}{Q} \tag{4.6}$$

where V_b is adsorbent bed volume (mL), which can be described as ($V_b = \pi r^2 H_b$, H_b is the corresponding bed height in cm, r is the inner radius of the bed column tube), and Q is volumetric flow rate (mL/min). The total amount of phosphate (P_{total}, mg) entering the bed can be used to determine the removal efficiency of the column, and can be calculated according to Equation (4.7) (Hu et al., 2020; Jiang et al., 2018; Nunes et al., 2020).

$$P_{total} = \frac{Q C_o t_{total}}{1000} \tag{4.7}$$

where t_{total} (min) is the operation time for the saturation of the adsorbate. Effluent volume Ve (mL) can also be calculated from the product of flow rate and total time, where influent volume V_i is obtained from the product of flow rate and break though time (Tamez et al., 2009; Woumfo et al., 2015).

4.2.4 Theoretical Breakthrough Curve Models

Several theoretical adsorption models have been used to predict the dynamic adsorption behavior of the leftover coal in a fixed-bed column. Therefore, in this work, three of most commonly used mathematical models, the Thomas, Adams–Bohart, and Yoon–Nelson models, were applied.

Thomas model: It is the most widely used theoretical model to evaluate column performance and predict concentration–time profile of the whole breakthrough curve. The model assumes that adsorption is limited by the mass transfer at the interface rather than chemical interactions of the molecules; experimental data obey the Langmuir isotherm and the second-order reversible kinetic

model (Jung et al., 2017; Ramirez et al., 2018). The linear form of the Thomas model can be expressed using Equation (4.8).

$$\ln\left(\frac{C_o}{C_t} - 1\right) = \frac{K_{th} q_{Th} m}{Q} - K_{Th} C_o t \qquad (4.8)$$

where Co and Ct are influent and effluent phosphate concentration (mg/L), respectively, K_{Th} (mL/min.mg) is the Thomas rate constant, q_{Th} (mg/g) is predicted adsorption bed capacity, m (g) mass of adsorbent packed within the column, and Q (mL/min) is flow rate. From the plot of $\ln\left(\frac{C_o}{C_t} - 1\right)$ vs t, the values of K_{Th} and q_{Th} can be determined using the slope and intercept, respectively.

Adams–Bohart model: The bed depth service time (BDST) is the other linearized form of Adams–Bohart (A–B) model expression, commonly applied to illustrate the relationship between service time and bed depth at fixed-bed column study (Foo et al., 2013; Li et al., 2013). The A–B model generally predicts a linear relationship between bed height and the time required to reach breakthrough time (Chu, 2020). The linear form of A–B model can be expressed by Equation (4.9) (Han et al., 2008; Woumfo et al., 2015).

$$ln\left(\frac{C_t}{C_o}\right) = K_{AB} C_o t - K_{AB} N_o \left(\frac{H_b}{U}\right) \qquad (4.9)$$

where K_{AB} (L/mg min) is the Adams–Bohart rate constant, No (mg/L) is saturation concentration in column (adsorption capacity per unit volume), H_b (cm) is the column bed height, and U (cm/min) is linear velocity and is calculated by dividing Q (mL/min) by the cross sectional area (cm^2) of the bed ($U = \frac{Q}{A}$). This model is more appropriate for describing the initial parts of the adsorption breakthrough curve at which Ct/Co = 0–0.5 (Husein et al., 2017; Ramirez et al., 2018). The values of K_{AB} and No are determined from the linear plot of $\ln\left(\frac{C_t}{C_o}\right)$ vs t, which are equivalent to the slope and intercept of the linear plot, respectively (Chu, 2020).

Yoon–Nelson Model: This theoretical model is based on the assumption that the rate of adsorption for each adsorbate is proportion to the rate of decrease in adsorption. The model does not require explicitly elaborated information about the characteristics of adsorbate and its type (Aksu & Gönen, 2004). It rather predicts 50% of the breakthrough time and simulate the column data

obtained from single adsorbate system (Ye et al., 2019). The linear form of the model can be expressed by Equation (4.10) (Li et al., 2013).

$$\ln\left(\frac{C_t}{C_o - C_t}\right) = K_{YN}t - \tau K_{YN} \quad (4.10)$$

where K_{YN} (min−1) is the Yoon–Nelson rate constant, τ (min) is the required time for 50% of the phosphate breakthrough and t (min) is the running time. The values of K_{YN} and τ can be obtained from the linear plot of $\ln\left(\frac{C_t}{C_o - C_t}\right)$ vs t using the slope and intercept respectively.

4.3 Results and discussions

4.3.1 Adsorbent characterization

The FT-IR spectrum of the adsorbent material (leftover coal) at wavelengths ranging from 5000 to 450 cm^{-1} is shown in Figure 4.1. Five major bands were identified for the FT-IR spectrum of the coal material, from which a strong and broad band was formed due the stretching vibration of–OH functional groups at the wave number of 3694.15 cm^{-1}; the band around 1631.96 cm^{-1} indicated the bending vibration of –NH in NH_2 for the FT-IR spectrum of coal materials (Huang et al., 2020; Li & Bai, 2005). The band obtained at the wave number of 2931.82 cm^{-1} indicated stretching vibrations of C–H (Liu et al., 2020; Omari et al., 2019). The peak observed in FT-IR spectrum band at 1358.20 cm^{-1} for coal material is characteristic of the SiO_4^{-2} group, and is caused by the symmetric stretching vibration of Si–O–Si and the stretching vibration of –CO in –COH (Huang et al., 2020; Li & Bai, 2005; Li et al., 2010). The small peaks shown at the bands of 537.92 and 471.98 cm^{-1} in the FT-IR spectrum of the leftover coal material belong to the bending vibration of Si–O–Si bonds (Geleta et al., 2021; Pirsaheb et al., 2018). As shown in Figure 4.1b, after column adsorption, some weak bands occurred at the band wavelengths of 537 and 471 cm^{-1}. This shows the adsorption of phosphate onto the surface of the adsorbent (Nunes et al., 2020; Xie et al., 2014).

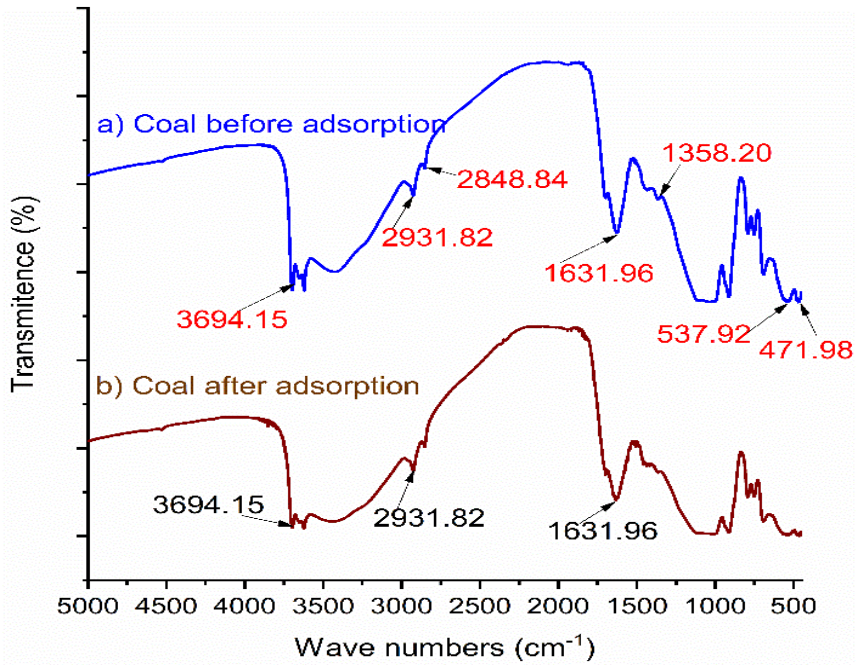

Figure 4. 1: FT-IR results for leftover coal material (a) before and (b) after adsorption

The XRD pattern of the leftover coal material before and after column adsorption is presented in Figure 4.2. A diffraction peak at 2θ = 12.6 degree is associated with kaolinite ($Al_2O_32SiO_2{\cdot}2H_2O$), and the typical peak obtained at 2θ = 25.4 degrees was induced by quartz (SiO_2). The small peak at 2θ = 35 degrees belongs to goethite, consisting of iron (III) oxide–hydroxide (Kajjumba et al., 2019; Yuan et al., 2016). Data for coal material obtained from XRD patters revealed the dominance of Si in coal material, which agrees with obtained SEM/EDX data from previous work (Mekonnen et al., 2020). The crystalline size of the XRD pattern of the coal material can be calculated from the Scherer equation as presented in Equation (4.11).

$$D = \frac{Kh}{\beta cos\,\theta} \qquad (4.11)$$

where D is the average crystalline size (nm), K crystal shape factor or Scherer constant (0.68 to 2.08 and 0.94 for spherical crystallites with cubic symmetry) (Langford & Wilson, 1978), λ is X-ray wavelength of radiation which is for Cukα = 1.4 Å, β peak breadth or line broadening at full width at half maximum (FWHM) in radian, and θ is equal to ½ of the 2θ position of the peak. The crystalline of the leftover coal material was 6.2 nm. However, the XRD peaks of the coal material showed amorphous rather than crystalline surface; the more amorphous the surface was, the higher the adsorption capacity (Kajjumba et al., 2019; Yang et al., 2018).

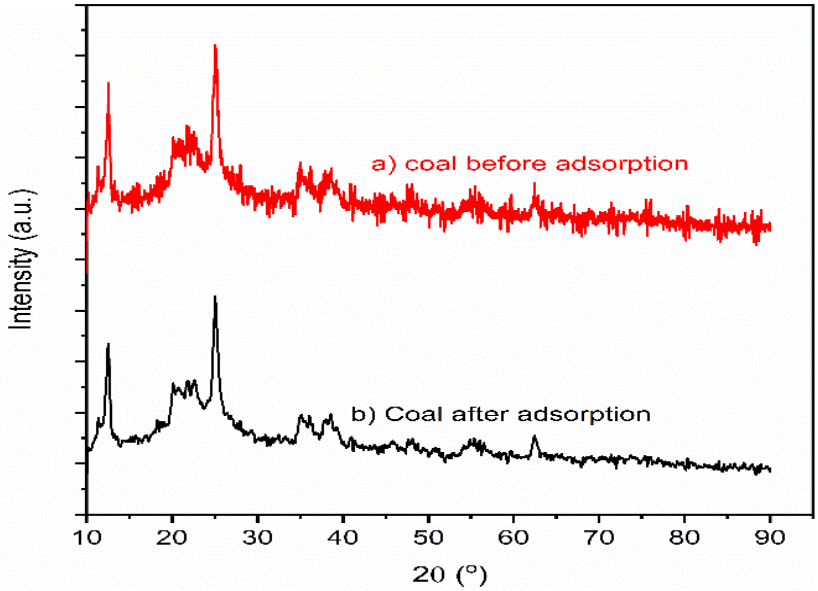

Figure 4. 2: XRD pattern of leftover coal material (a) before and (b) after adsorption

4.3.2 Effects of operational parameters

4.3.2.1 Effects of Adsorbent Bed Height

The effect of bed heights on the breakthrough curves of column adsorption were studied using bed heights of 5, 6, and 8 cm with a constant influent phosphate concentration of 10 mg/L and at a fixed flow rate of 1 mL/min. Figure 4.3 shows the related breakthrough curves with different bed heights. The removal efficiency of the phosphate was proportional to the proposed bed height. In all cases, breakthrough times were extended from 190 to 235 min, and then to 348 min, with increasing bed height from 5 to 8 cm. Subsequently, the influent volume of phosphate solution treated at the breakthrough time (V_i) and at exhaustion time (V_e) increased from 190 to 348 mL and from 273 to 381 mL, respectively, for longer bed heights as compared with for the shorter one (Table 4.1). This indicates that the shorter beds saturated faster than the longer one did because the longer bed heights need longer to become saturated (Rout et al., 2014). The increase in Vi and Ve was probably due to the high contact time between phosphate ions and adsorbent (Woumfo et al., 2015). Furthermore, the longer bed height (8 cm) used in this study had higher phosphate adsorption capacity (190.7 mg/kg) than that of 6 cm (178 mg/kg) and 5 cm (163 mg/kg) bed height. Therefore, the longer the bed height was, the longer the time taken was to reach complete exhaustion time due to broadened mass transfer zone for phosphate adsorption (Li et al., 2013; Tamez et al., 2009).

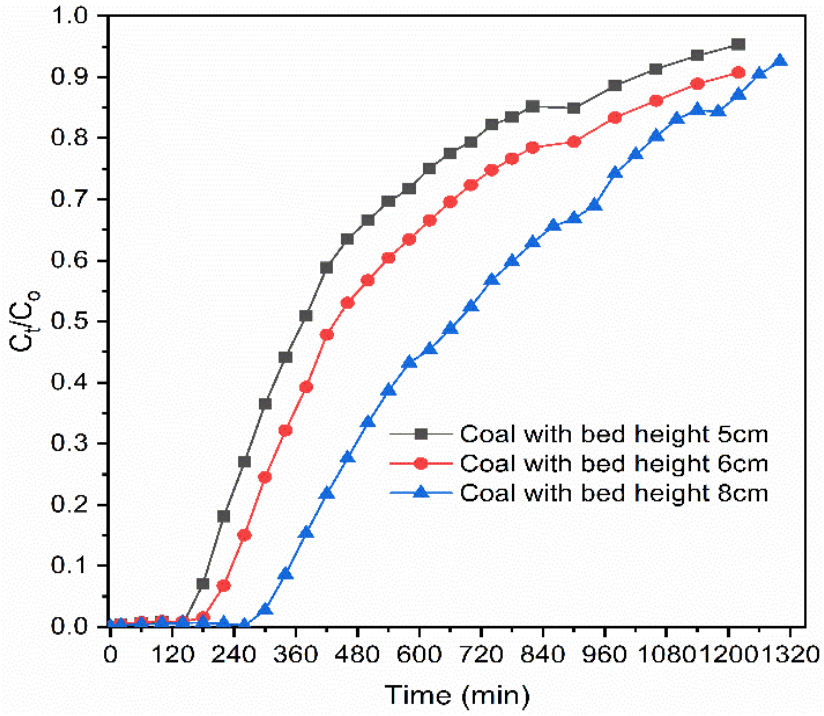

Figure 4. 3: Effects of adsorbent bed height

4.3.2.2 Effects of Influent Concentration

The effect of initial phosphate concentration on the performance of the column was studied by varying the inlet concentration from 10 to 25 mg/L while the same adsorbent bed height of 8 cm and flow rate of 1 mL/min were used. Figure 4.4 shows that a very fast breakthrough time occurred at the inlet concentration of 25 mg/L. At a higher influent concentration of the phosphate, the quick fill of the binding sites of the adsorbent material was observed (Chowdhury et al., 2013; Husein et al., 2017). As the influent phosphate concentration increased from 10 to 25 mg/L, exhaustion time also decreased from 348 to 144 min. The lower phosphate concentration caused the slower diffusion of the phosphate than that of the higher concentration onto the surface of the coal material due to the lower mass transfer coefficient, and contributed to the longer breakthrough time and exhaustion time (Husein et al., 2017; Rout et al., 2014). Equally, the higher the influent concentration was, the higher the concentration gradient and the lower the mass resistance were with shorter breakthrough time and exhaustion time. Similar tendencies were reported by (Nguyen et al., 2015) in the case of removing phosphate from an aqueous solution using zirconium-loaded okara. Nevertheless, the increase in influent concentration increased the phosphate removal capacity (from 190 to 243 mg/kg), but the total influent volume (Vi) of the treated solution was

decreased from 348 to 144 mL. Utilizing the lower influent phosphate concentration is preferable to a higher concentration when the treatment of a larger volume is prioritized. Calculated parameters for different concentrations are presented in Table 4.1.

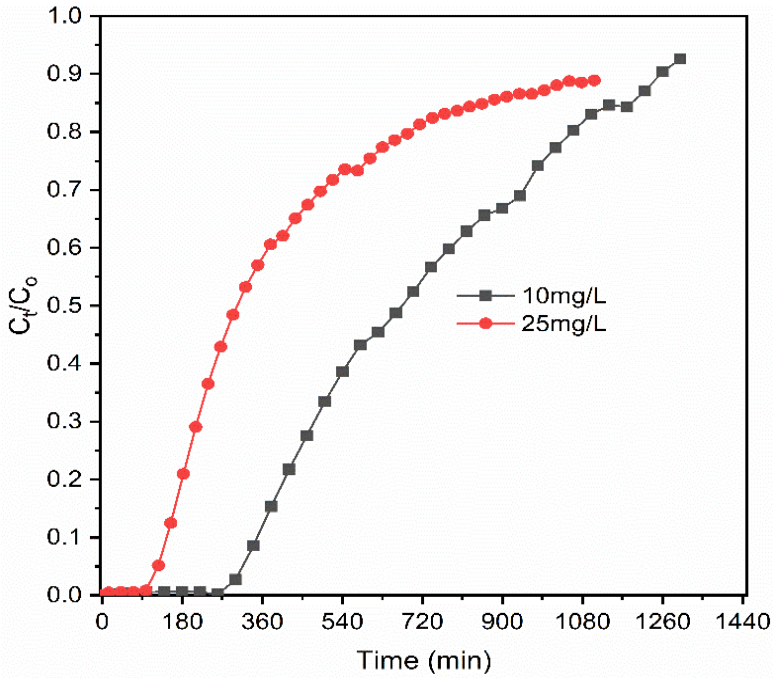

Figure 4. 4: Effects of influents concentrations on phosphate behavior

4.3.2.3 Effects of influent flow rate

The breakthrough curves at different flow rates (1 and 2 mL/min) using influent phosphate concentration of 10 mg/L and adsorbent bed height of 8 cm are presented in Figure 4.5. The breakthrough time and exhaustion time of the adsorbent material appeared significantly faster, which was related to the mass transfer process when the used flow rates were increased from 1 to 2 mL/min. In this case, the breakthrough time decreased from 348 to 187 min, and exhaustion time decreased from 381 to 313 min for the increase in flow rate from 1 to 2 mL/min. Another study reported a very fast breakthrough time (<40 min) for the removal of phosphate from a solution using andosol bagasse mixtures at the influent solution flow rate of 4 mL/min in 1.8 cm bed height (Woumfo et al., 2015). According to Chittoo and Sutherland (Chittoo & Sutherland, 2020), increasing the flow rate may reduce the resident time of the adsorbate to diffuse into the pores of the adsorbent materials; thus, the adsorbates predominately interact with surface functional groups.

At lower flow rates, adsorbates have enough time to interact with the surface of the adsorbents, and additional external mass transfer and intraparticle diffusion are thus enhanced (Zheng et al., 2019), where, at the higher flow rate, the adsorbate solution leaves the column before reaching the equilibrium point (Babu & Gupta, 2005). The adsorption parameters for varying bed depths, concentrations, and flow rates are presented in Table 4.1.

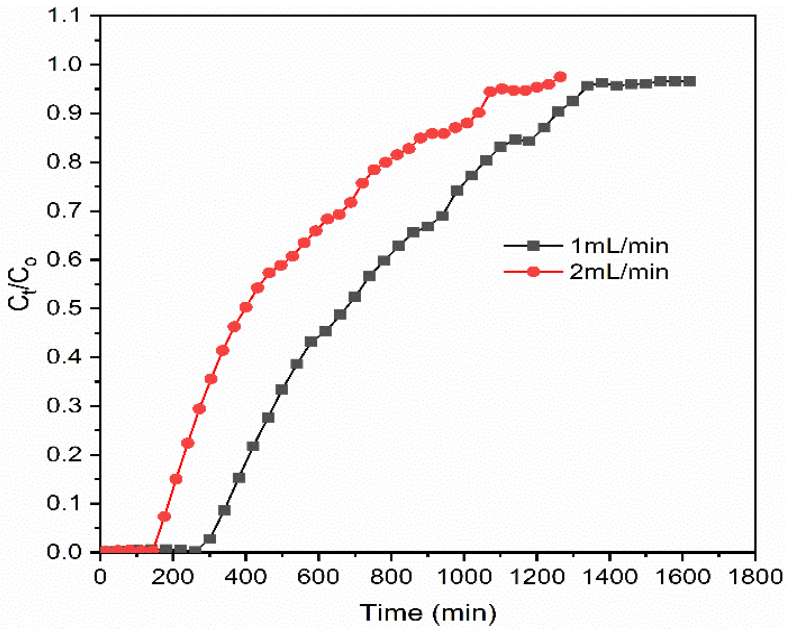

Figure 4. 5: Effects of influent flow rate on phosphate breakthrough

Table 4. 1: Obtained parameters from breakthrough curves for phosphate adsorption onto leftover coal material with different bed heights, initial phosphate concentrations, and flow rates

C_o(mg/L)	H_b(cm)	Q(mL/min)	V_i(mL)	t_b(min)	t_e (min)	EBCT (min)	MTZ (cm)	q_{total} (mg)	q_e (mg/kg)	V_e (mL)
10	8	1	348.39	348.39	381.37	607.79	5.78	5.72	190.7	381.37
10	8	2	374.06	187.03	313.39	303.89	6.56	6.27	208.9	626.78
10	5	1	190.68	190.68	273.21	257.33	3.96	4.1	163.9	273.21
10	6	1	235.73	235.73	297	357.81	4.59	4.46	178.2	297
10	8	1	348.39	348.39	381.37	607.79	5.78	5.72	190.7	381.37
10	8	1	348.39	348.39	381.37	607.79	5.78	5.72	190.7	381.37
25	8	1	144.45	144.45	291.92	607.79	6.96	7.3	243.2	291.79

V_i = influent volume; V_e = exhaustion/effluent volume.

Table 4. 2: Parameters for Thomas, Adam-Bohart, and Yoon-Nelson models at different parameters

Exp. Parameters	Co (mg/L)	Hb (cm)	Q (mL/min)	Thomas			Adams-Bohart			Yoon-Nelson		
				$K_{Th}x10^2$ (mL/min.mg)	q_{Th} (mg/g)	R^2	$K_{AB}x10^3$ (L/mg min)	N_0x10^3 (mg/L)	R^2	K_{YN} (min^{-1})	τ (min)	R^2
Q (mL/min)	10	8	1	2.83	0.215	0.87	0.188	1.69	0.98	2.831	6.453	0.9
	10	8	2	2.61	0.203	0.92	0.172	3.217	0.92	2.613	6.079	0.92
Hb (cm)	10	5	1	1.67	0.328	0.84	0.151	2.602	0.96	2.608	5.985	0.92
	10	6	1	2.43	0.253	0.93	0.155	2.188	0.98	2.43	6.174	0.93
	10	8	1	2.83	0.215	0.87	0.188	1.69	0.98	2.831	6.453	0.9
Co (mg/L)	10	8	1	2.83	0.215	0.87	0.188	1.69	0.98	2.831	6.453	0.9
	25	8	1	2.12	0.197	0.94	0.143	1.578	0.92	2.121	5.908	0.94

4.3.3 Prediction of breakthrough curves using adsorption models

Predicting fixed-bed column parameters in continuous flow analysis is very important for both laboratory- and industrial-scale processes (Ye et al., 2019). The breakthrough curve is a plot of ratios of effluent to influent concentrations versus running time, and its prediction provides the mechanisms and generally any changes in the adsorption processes. In the present study, three theoretical models, namely, the Thomas, Adams–Bohart, and Yoon–Nelson models, were applied to determine the best model for predicting the dynamic behaviors of the models (Bohart & Adams, 1920; Thomas, 1944).

The Thomas model is frequently used to determine adsorption capacity of the adsorbent. The rate constant, adsorption capacity, and other parameters were obtained from the linear plot of Equation (4.8) and numerical values are presented in Table 4.2. Table 4.2 shows that K_{Th} values increased from 1.67×10^2 to 2.83×10^2 mL/min mg, while the values of q_{Th} decreased from 328 to 203 mg/kg with increasing adsorbent bed height from 5 to 8 cm. However, other researchers reported a decreasing value of K_{Th} and increase in q_{Th} with increasing bed depth (Husein et al., 2017; Woumfo et al., 2015). This is may have been due to the experimental measuring and applying different adsorbents. On the other hand, the values of K_{Th} decreased with increasing influent phosphate concentration and flow rate. These values can be illustrated with the driving force due to the increase in concentration gradients and flow rate as reported in other studies (Negrea et al., 2020; Woumfo et al., 2015). Regression values (R^2) from the Thomas model ranged from 0.84 to 0.94, which illustrated a worse fit than that of other models.

The calculated data for the Adams–Bohart model are presented in Table 4.2. K_{AB} values increased with increasing adsorbent bed height, but decreased with increasing influent phosphate concentration and flow rate. The values of No decreased with increasing bed height and influent phosphate concentration, but increased with increasing flow rate. The calculated and experimental data for the A–B model using initial phosphate concentration and adsorbent bed height are illustrated in Figures 4.6 and 4.7, where the R^2 values of A–B model ranged in between 0.92 to 0.98, which provided a better fit than that of the Thomas and Y–N models.

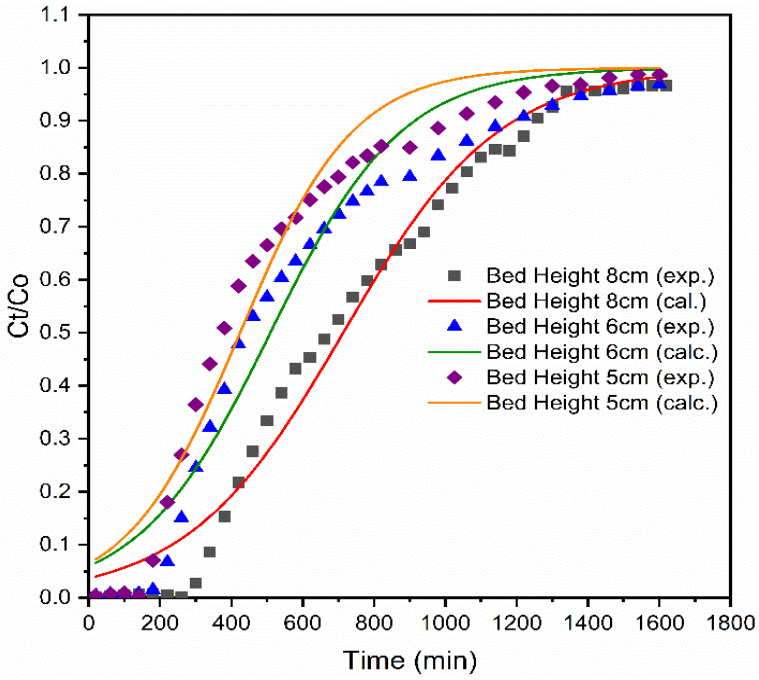

Figure 4. 6: Experimental and calculated breakthrough curve values for Adams-Bohart model at different values of adsorbent bed height

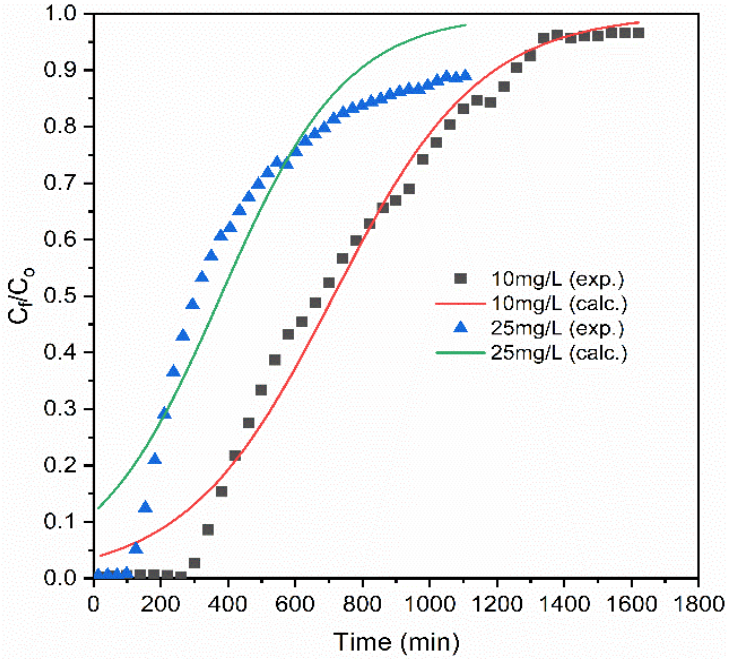

Figure 4.7: Experimental and calculated breakthrough curve values for Adams-Bohart model at different values of influent phosphate concentration

The Yoon-Nelson (N–Y) rate constant, K_{YN}, and time required for 50% breakthrough τ values at different operational parameters are presented in Table 4.2. The values of both K_{YN} and τ were decreased with increasing flow rate and influent phosphate concentration. The fitness of the N–Y model was evaluated using correlation values (R^2) ranging from 0.90 to 0.94. The Y–N model described the behavior of sorption of phosphate better than the Thomas model did under different experimental conditions. However, the Adams–Bohart model described the adsorption of the phosphate in the column better than the Thomas and Y–N models did at different operational conditions.

4.4 Conclusions

This study was conducted to test leftover coal as a material for the removal of phosphate from solutions by adsorption using continuous-flow fixed-bed column experiments. The adsorption performance and the breakthrough-curve characteristics of the column were influenced by influent phosphate concentration, adsorbent bed height, and the influent flow rate of the solution. The increase in bed height significantly improved the performance of the column by increasing the breakthrough and exhaustion times of the process, and increased the volume of water that could be treated. On the other hand, the increase in initial phosphate concentration and influent flow rate reduced the breakthrough and exhaustion times. This was due to the fast saturation of the surface of the adsorbent with phosphate ions and a lower resident time of the adsorbate. Adam–Bohart model fitted the experimental data well, and performed better than the Thomas and Yoon–Nelson adsorption models did. Overall, the results of this study suggest that phosphate removal using leftover coal material is a promising low-cost technology for the sustainable control of excess phosphate in water. However, additional testing of the adsorbent using surface modification and applying real sample water with competitive anions are required for final conclusions.

5. Synthesis

5.1 General Overview

As discussed in the previous chapters, phosphate is one of the most important nutrients for plants and animals and pollutes water bodies in excessive quantities where a well-organized and cost-effective removal is urgently needed. However, financial constraints, technical inefficiencies, and lack of commitment in Ethiopia have resulted in unsuccessful pollution management. As mentioned in the introduction section, excessive phosphate discharges from various sources into nearby aquatic ecosystems threaten mainly industrialized regions. Eutrophication of water bodies is one of the main consequences of this threat. Several studies have reported methods to remove phosphate from water in which advanced biological and chemical precipitation is the primary process. In addition, most water treatment methods are complex and inadequate. They use advanced water treatment techniques with high financial and resource constraints. In this context, adsorption is used in a variety of water treatment technologies, especially for phosphate removal techniques, due to its relatively low-cost, environmental friendliness, and easy accessibility.

Many adsorbents are used to remove phosphate from water and wastewater by adsorption (Bezza & Chirwa, 2021; Fu et al., 2018; Min et al., 2019; Shi et al., 2011; Zhang et al., 2011). Most of the adsorbents listed are often unsuitable for low-income countries such as Ethiopia due to their high cost. For example, the cost of commercial activated carbon is prohibitively expensive, and its regeneration after use is tedious (Kyzioł-Komosińska et al., 2014). The selection and application of low-cost and locally available materials as an adsorbent is currently receiving considerable attention (Husein et al., 2017). Coal leftover and volcanic rocks are abundant in Ethiopia (Alemayehu & Lennartz, 2010; Fantaw, 2019) and the use of these materials as adsorbents will benefit the country economically, environmentally, and technically.

Based on this, the main objective of this work is to develop locally and readily available leftover coal and volcanic rocks as adsorbents for the removal of phosphate from simulated phosphate containing water using batch and fixed-bed column adsorption technologies. Preparation and characterization of the adsorbent material was performed before and after adsorption. The effects of operating design parameters such as particle size, contact time, initial phosphate concentration, sorbent dosage, and solution pH were evaluated for specific adsorbents. The Response Surface Method analysis was used to determine an optimal removal capacity.

On the other hand, the effect of competing anions on phosphate removal was evaluated using a batch adsorption technique. The effects of three key operating parameters were investigated in continuous flow fixed bed experiments, such as influent flow rate, initial phosphate concentration, and adsorbent bed height. Finally, the removal capacity of the material was evaluated in a separate experiment to determine the removal efficiency of the adsorbent under various adsorption conditions as discussed in Chapters 2 to 4. Therefore, this chapter (Chapter 5) aims to provide an overview of the research and discuss the results of each specific objective.

5.2 Synthesis and general discussions

5.2.1 Batch adsorption experiments

The purpose of this sub-section is to discuss the relevant points of the previous discussions and to draw conclusion from previous chapters (chapter 2 and chapter 3).

5.2.1.1 Effects of contact time

Designing an appropriate batch adsorption experiment to determine the adsorption rate is very important, and separate kinetic experiments were performed to evaluate the effects of contact time on phosphate removal and to determine the optimum contact time. Phosphate removal on the adsorbent was very fast in the first 200 min for leftover coal (Mekonnen et al., 2020), and 300 min for both VPum and VSco (Mekonnen et al., 2021). The high initial rate of phosphate uptake may be attributed to the substantial free pore sites on the surface of the adsorbents in the initial phase (Omari et al., 2019). As the free pore sites are gradually occupied and filled up by the phosphate ions, the adsorption becomes lower and the kinetics slower due to intraparticle adsorption. Therefore, the equilibrium time was reached after 720 min for leftover coal and after 420 min for VPum and VSco. Hence, the optimum contact time was selected at the equilibrium time to achieve the maximum removal of phosphate ions from water with the adsorbents. However, in several studies the maximum removal was obtained at a lower contact time with modified adsorbents because the more modified the surface of the adsorbent the more porous the materials (Huang et al., 2026).

5.2.1.2 Effects of Particle size

In this study, kinetic experiments were performed to determine the effects of particle size of the adsorbent on the removal of phosphate ions from synthetic phosphate-containing water (Mekonnen et al., 2020). The results showed that the particle size of the adsorbent significantly

influenced the phosphate removal at the surface of the coal material. The maximum phosphate removal (94.5 %) was achieved with at fine sand particle size of 0.075 to 0.425 mm. Reducing the particle size from fine sand to the silty sand (>0.075 mm) resulted in a slight decrease in removal efficiency from 94.5 % to 91.8 %. The smaller the particle size, the larger is the surface area of the adsorbent. However, in this case, the higher removal efficiency was obtained with fine particle size, which is due to the fact that the surface area of the adsorbents is covered as the particle size increases. Therefore, all subsequent experiments were performed with fine sand particles size (0.075 -0.425mm).

5.2.1.3 Effects of solution pH

It is well known that the initial pH of a solution is important for adsorption experiments. This affects the degree of ionization, the speciation of phosphate ions, and the surface charge of the adsorbent. This is related to the competition of hydrogen ions (H^+) with phosphate ions for active sites on the adsorbent surface and the attraction of phosphate ions by H^+ ion in acidic environments. To obtain the effect of pH on phosphate removal using leftover coal material (chapter 2), separate series of experiments were performed which the pH of the solution was changed from 2 to 12. The results showed that the percentage of phosphate removed by the leftover coal material decreased from 86 to 68 % as the pH of the increased from 2 to 12. The pre-determined pH was adjusted depending on the pH_{zpc} value of the adsorbent. The calculated value of the pH_{zpc} of leftover coal was 4.6. In the lower pH ranges, the adsorption of phosphate on the leftover coal material increased due to the formation of cations on the surface of the coal material, and it decreased as the pH of the solution increased above pHzpc, when more OH^- was present to repel phosphate ions, thus decreasing the removal rate. Therefore, the optimal pH value (3.5) for adsorption of phosphate on leftover coal material was selected as slightly acidic. Since the pH ranges investigated were 6.5 for VPum and 5.5 for VSco (Mekonnen et al., 2021), the repartition diagram of phosphate indicated that the dominant phosphate species was between 80% and 100% for both VPum and VSco was (H_2PO_4-). However, the predominant phosphate species for leftover coal materials were dihydro phosphate ion ($H_2PO_4^-$) and tri-hydro phosphate ion ($H_3PO_4^-$) at the pH of 3.5.

5.2.1.4 Effects of initial concentration

It is known that the initial concentration of the phosphate solution affects the removal of phosphate on the adsorbent material (Yadav et al., 2015). In this study, the phosphate removal efficiency of leftover coal, VPum, and VSco decreased significantly from 93.4 to 55 %, from 93 to 43 %, and

from 81 to 23 % respectively where the initial phosphate concentration increased from 0.5 mg/L to 25 mg/L. This is because the surface of the adsorbent becomes more resistant to adsorbate uptake and the active sites for adsorption become saturated at high concentrations (Lin et al., 2018). However, the phosphate removal capacity per kg of adsorbent increases with higher initial phosphate concentrations due to the higher mass transfer driving force (Mekonnen et al., 2020; Mekonnen et al., 2021).

5.2.1.5 Effects of adsorbent dose

The effects of adsorbent dosage on phosphate removal onto leftover coal material were investigated in a separate batch experiment (Chapter 2). The more the adsorbent was included in the residue dose, the more efficient was the phosphate removal by the leftover coal material. However, the removal capacity per weight of adsorbent decreased from 2.9 mg/g to 0.5 mg/g as the adsorbent dose increased from 0.5 g to 5 g. This is due to the high frequency of sorption sites on the surface of the adsorbent. The studies of (Park and Jung, 2011; Rashidi et al., 2017) come to similar conclusions that the adsorbent dose is strongly correlated with the phosphate removal rates.

5.2.1.6 Adsorption kinetics

The adsorption rate plays a very important role in the adsorption process. Therefore, various adsorption kinetic models such as Lagergren pseudo-first-over, pseudo-second-order and intra-particle diffusion were applied to evaluate the sorption mechanisms of phosphate on leftover coal, and volcanic rock materials in batch experiments. The results of the study showed that the pseudo-second order equation best described the adsorption kinetics of phosphate with high correlation values of $R^2 > 0.99$ for all adsorbents used (Mekonnen et al., 2020; Mekonnen et al., 2021). Furthermore, the results obtained from the experimental outputs indicated that the intra-particle diffusion model was also responsive to the phosphate diffusion mechanism in solution (Aljeboree et al., 2014; Lin et al., 2018). As expected, the plot of qt vs $t^{0.5}$ was linear in some cases but crossed the origin resulting in two slopes and intercepts. This confirms that intra-particle diffusion is not the only rate-limiting step (Mekonnen et al., 2021).

5.2.1.7 Adsorption isotherms

Various isotherms such as Langmuir, Freundlich and Dubinin-Radushkevich (D-R) isotherm models have been applied to describe phosphate adsorption on adsorbent materials. The Freundlich isotherm assumes that adsorption occurs on heterogenous surface via multi-layer adsorption. The

value of 1/n obtained from the Freundlich isotherm is between 0 and 1 for all adsorbents, and it that can be concluded that the Freundlich isotherm describes the process well with a correlation value of $R^2 > 0.99$, which in turn shows that chemisorption governs the adsorption of phosphate on leftover coal and volcanic rocks. However, the D-R isotherm values obtained from the mathematical calculations ranged from 1 to 8 $kJ.mol^{-1}$ for VPum and VSco, indicating that phosphate adsorption on the volcanic rock was not only chemisorption but also physisorption (Mekonnen et al., 2021). Similar studies concluded that intraparticle diffusion was the indicator of the for the multistep adsorption process (Pan et al., 2017).

5.2.2 Fixed-Bed Column Experiments

This section summarizes the adsorption removal of phosphate on leftover coal materials using fixed-bed column (Chapter 4). The effects of selected design parameters such as bed height, influent flow rate, and initial influent concentration were discussed.

5.2.2.1 Effects of adsorbent bed height

The effect of adsorbent bed height on the column adsorption breakthrough curve was studied with bed heights of 5, 6, and 8cm, with constant influent flowrate and concentration set at the values of 1 mL/min and 10 mg/L respectively. The results showed that increasing the bed height from 5 cm to 8 cm increased the breakthrough time from 190 minute to 348 minutes. The volume of the threatened phosphate solution at the time of breakthrough (Vi) and the volume of solution at time of depletion (Ve) also increased with increasing adsorbent bed height (Vieira et al 2019). The more breakthrough time, the greater the volume of phosphate solution threatened. The higher the bed height, the longer phosphate ions have to move to have enough time to attach to the adsorbent surface when optimum flow rate and concentration were selected. Similar studies confirmed that increasing of the bed height increases the influent volume of the treated solution and also increases the contact time between the adsorbent and adsorbate (Husein et al., 2017).

5.2.2.2 Effects of influent concentration

The effect of initial phosphate concentration on the adsorption breakthrough curves was investigated by varying the initial influent concentration from 10 mg/L to 25 mg/L. At higher influent concentrations rapid filling of the adsorbent binding sites was observed, which was attributed to a higher affinity of the ions for the free surface. Therefore, the adsorption breakthrough curve decreased from 348 minutes to 144 minutes where the concentration increased

from 10 to 25 mg/L. However, the amount of phosphate removed per kg of adsorbent decreased with increasing feed concentration and flow rate (Chapter 4). This result is consistent with the phosphate adsorption determined in batch experiments at high concentrations. At the higher concentration, phosphate ions were able to fill all the vacant sites better than at the lower concentration. From the two experiments, i.e., batch and fixed-bed column experiments, it can be observed that the initial concentration of the adsorbent to be adsorbed has a direct effect on the removal efficiency of the adsorbent. Therefore, the ratio of adsorbent and adsorbate should be considered for better removal.

This leads to the following conclusions (but not limited to):

- The surface of the leftover coal material was used as an adsorbent at room temperature without surface modification, and a maximum removal capacity of 198 mg/kg was obtained at a contact time of 200min, an initial pH of 3.5, and an initial phosphate concentration of 5 mg/L using Response Surface Methods based on Central Composite Design methods. Similarly, a maximum removal of 294 and 169mg/kg was obtained for VPum and VSco, respectively for batch experiments. The Freundlich isotherm fitted the experimental data for both materials (Coal leftover and Rocks), however, D-R for volcanic rock indicates that physical sorption on the surface of the adsorbents also possible. This may indicate that the adsorption mechanism of phosphate on coal leftover and volcanic rocks is not limited to heterogeneous surface interaction but also surface homogeneity.
- The size of the adsorbent material strongly affects the phosphate adsorption capacity of the selected material, and the optimal removal was obtained with a size ranging from 0.075 mm to 0.425 mm for both leftover coal and volcanic rocks in batch and fixed-bed column experiments.
- The effects of contact time, initial phosphate concentration, adsorbent dosage, pH, and temperature were reported as factors for phosphate removal. The longer the contact time, the less the adsorption can be performed due to the saturation of the adsorbent surface. Increasing the concentration of the adsorbate also results in a decrease in the percent removal and an increase in the removal capacity. The higher the concentration of the adsorbate in the solution the more anions are occupied on the surface of the adsorbent materials and the higher the removal capacity. However, the percentage removal of the material decreases as the adsorbate concentration increases because the material becomes

saturated quickly. Therefore, the ratio of adsorbent to adsorbate should be chosen appropriately.

- In almost all cases, the adsorption data are well described by the Freundlich isotherm model, indicating the heterogeneity of phosphate sorption on the surface of the adsorbents. However, the D-R isotherm model in addition to the Freundlich isotherm best described the adsorption data for VPum and VSco. This means that the adsorption of phosphate on the surface of the adsorbents is not considered as heterogeneous adsorption only.
- XRD and FTIR characterization showed that the surface of the adsorbents was crystalline and amorphous, and many functional groups appeared on the surface, which uniquely describes the content of the materials.
- The effects of competing anions were studied under a variety of conditions, and fluoride ions were found to have very strong electron affinity as phosphate ions on the surface of adsorbents. However, when the final pH of the solution with competing anions was measured, it was observed that the pH of the solution with bicarbonate increased, and the phosphate removal decreased accordingly. This is probably due to the increase in OH^- ions on the surface of the adsorbent which repelled with the phosphate ions.
- Column experiments were conducted to investigate the effects of three operating paramet ers, i.e., adsorbent bed height, influent concentration and influent flow rate. Adsorption of phosphate in the column experiments was optimal at low flow rates, low influent concentrations, and high bed heights. This is due to the extended breakthrough time and exhaustion time. The longer the exhaustion time for the adsorbates and adsorbents, the longer they are in contact with each other.
- The adsorption models applied in the column experiments described the data with correlation values (R^2) greater than 80 %. However, the Adams-Bohart model fitted the adsorption data from the column experiments better than either of the Thomas and Yoon-Nelson models.

In conclusion, the different results from the different experiments indicate that the selected adsorbents have significant potential for phosphate removal. Therefore, the data obtained from the batch and continuous flow fixed bed experiments can be used as secondary data for the preliminary scale-up-flow analysis.

5.3 Recommendations for future work

The objective of this study is to investigate the adsorption process of phosphate on leftover coal and volcanic rock materials (VPum and VSco). The experiments presented in this study have shown that three adsorbents, such as coal leftover, VPum, and VSco have the potential to be used in wastewater treatment. Batch and fixed bed column experiments have yielded promising results in removing phosphate from simulated water using coal leftover and volcanic rocks. Although the original objectives were achieved in this study, there are some other aspects that were not within the scope of this study due to time constraints. Therefore, further investigation is required. Optimization and full utilization of adsorbents for phosphate removal in wastewater technologies can be exploited. Therefore, the following key issues are strongly recommended (but not limited to);

- In Chapter 2, the phosphate retention capacity of leftover coal was tested. This is the first time that such a material has been studied in more detail. The objective of this chapter is to (i) clarify the maximum adsorption potential and (ii) gain more insight into the impacts of operational processes on the removal of phosphate on leftover coal. This idea was pursued using an aqueous model solution rather than natural wastewater. Wastewater is not a well-defined compound, but varies greatly depending on the source. For instance, wastewater from the tanning industry is fundamentally different from wastewater from glass manufacturing (both industries are found in Africa and Ethiopia). Thus, the results of experimental studies with natural wastewater would depend on the type of wastewater and could hardly be used to reveal the underlying processes. Therefore, based on the parameters studied, the test for actual wastewater containing different anions should be investigated, and recycling/or regeneration of adsorbent material is strongly recommended for future work.
- Although the removal efficiency of the selected materials was reasonable, it is strongly recommended that the surface area of the absorbents be modified to achieve the optimum removal capacity and get the most out of the adsorbents.
- Continuous flow experiments in fixed bed were performed under various adsorption conditions with laboratory-synthesized water. Next, the recycling potential of P-laden leftover coal and rock materials should be thoroughly analyzed. The effects of different anions on the removal of phosphate on rock materials and phosphate containing industrial effluents are strongly recommended.

- Adsorbents have been tested for the remove of phosphate from synthetic water. But it is recommended to use these materials also for other cations to evaluate the simultaneous removal efficiency of the materials. Because successful application for hazardous cations/toxic contaminants will allow the adsorbents to be used in other wastewater practice as well.
- Small Pyrex laboratory tubes with an inner diameter of 2.6 cm and a height of 13 cm were used for the continuous flow fixed-bed experiments. These small diameters and heights are only used at low flow rates. However, for future work, it is strongly recommended to work at high flow rates and large scale.
- In this work, only a few adsorption models were applied to demonstrate the compatibility of experimental and theoretical results in both batch and column flow experiments. However, the application of other adsorption models such as Temkin, Clark, and Yan, is strongly recommended for a detailed description of the adsorption data.
- This study has demonstrated the feasibility of using leftover coal and volcanic rock materials as low-cost and readily available materials in water purification systems. However, pilot and large-scale studies are recommended to evaluate the practical application of the materials and to apply the findings to wastewater treatment plants.

References

Acelas, N. Y., Martin, B. D., López, D., & Jefferson, B. (2014). Selective removal of phosphate from wastewater using hydrated metal oxides dispersed within anionic exchange media. *Chemosphere*, *119*, 1353–1360.

Ademe, A. S. (2014). Source and Determinants of Water Pollution in Ethiopia: Distributed Lag Modeling Approach. *Intellectual Property Rights: Open Access*, *2*(2).

Adeogun, A. I., Idowu, M. A., Ofudje, A. E., Kareem, S. O., & Ahmed, S. A. (2013). Comparative biosorption of Mn(II) and Pb(II) ions on raw and oxalic acid modified maize husk: kinetic, thermodynamic and isothermal studies. *Applied Water Science*, *3*(1), 167-179.

Ahn, Kyung-Won Jung, Tae-Un Jeong, Brian Hyun Choi, Ho- Jeong Kang, and K.-H. (2017). Phosphate Adsorption from Aqueous Solution by Laminaria japonica-Derived Biochar-Calcium Alginate Beads in a Fixed-Bed Column: Experiments and Prediction of Breakthrou gh Curves. *Environmental Progress & Sustainable Energy*, *33*(3), 1-9.

Ahn, C. K., Park, D., Woo, S. H., & Park, J. M. (2009). Removal of cationic heavy metal from aqueous solution by activated carbon impregnated with anionic surfactants. *Journal of Hazardous Materials*, *164*, 1130–1136.

Ajmal, M., Ali, R., Rao, K., Ahmad, R., & Khan, M. A. (2006). Adsorption studies on Parthenium hysterophorous weed : Removal and recovery of Cd (II) from wastewater. *Journal of Hazardous Materials*, *B135*, 242–248.

Ajmal, Z., Muhmood, A., Usman, M., Kizito, S., Lu, J., Dong, R., & Wu, S. (2018). Phosphate removal from aqueous solution using iron oxides : adsorption , desorption and regeneration characteristics. *Journal of Colloid And Interface Science*, *525*, 145-155.

Aksu, Z., & Gönen, F. (2004). Biosorption of phenol by immobilized activated sludge in a continuous packed bed: Prediction of breakthrough curves. *Process Biochemistry*, *39*(5), 599–613.

Al-ghouti, M. A., & Da'ana, D. A. (2020). Guidelines for the use and interpretation of adsorption isotherm models: A review. *Journal of Hazardous Materials*, *393*.

Alalwan, H. A., Abbas, M. N., Abudi, Z. N., & Alminshid, A. H. (2018). Adsorption of thallium ion (Tl+3) from aqueous solutions by rice husk in a fixed-bed column: Experiment and prediction of breakthrough curves. *Environmental Technology and Innovation*, *12*, 1–13.

Alemayehu, E., & Lennartz, B. (2009). Virgin volcanic rocks : Kinetics and equilibrium studies for the adsorption of cadmium from water. *Journal of Hazardous Materials*, *169*, 395–401.

Alemayehu, E., & Lennartz, B. (2010). Adsorptive removal of nickel from water using volcanic rocks. *Applied Geochemistry*, *25*(10), 1596-1602.

Alemayehu, E., Thiele-bruhn, S., & Lennartz, B. (2011). Adsorption behaviour of Cr (VI) onto macro and micro-vesicular volcanic rocks from water. *Separation and Purification Technology*, *78*, 55–61.

Alemu, A., Lemma, B., Gabbiye, N., Tadele, M., & Teferi, M. (2018). Removal of chromium (VI) from aqueous solution using vesicular basalt : A potential low cost wastewater treatment system. *Heliyon*, *4*, 1–22.

Ali, R., Rao, K., Rehman, F., & Kashifuddin, M. (2012). Removal of Cr (VI) from electroplating wastewater using fruit peel of Leechi (Litchi chinensis). *Desalination and Water Treatment*, *49*(1–3), 136–146.

Aljeboree, A. M., Alshirifi, A. N., & Alkaim, A. F. (2014). Kinetics and equilibrium study for the adsorption of textile dyes on coconut shell activated carbon. *Arabian Journal of Chemistry*, *10*, S3381–S3393.

An, B., Lee, S., Kim, H. G., Zhao, D., Park, J. A., & Choi, J. W. (2019). Organic/inorganic hybrid adsorbent for efficient phosphate removal from a reservoir affected by algae bloom. *Journal of Industrial and Engineering Chemistry*, *69*, 211 -216.

Angello, Z. A., Behailu, B. M., & Tränckner, J. (2020). Integral Application of Chemical Mass Balance and Watershed Model to Estimate Point and Nonpoint Source Pollutant Loads in Data-Scarce Little Akaki. *Sustainability*, *12*(17).

Aregu, M. B., Asfaw, S. L., & Khan, M. M. (2018). Identification of two low - cost and locally available filter media (pumice and scoria) for removal of hazardous pollutants from tannery wastewater. *Environmental Systems Research*, *10*(7), 2–14.

Arshadi, M., Eskandarloo, H., Azizi, M., Abbaspourrad, A., Abdolmaleki, M. K., Eskandarloo, H., Azizi, M., & Abbaspourrad, A. (2018). Synthesis of Highly Monodispersed, Stable, and Spherical NZVI of 20 − 30 nm on Filter Paper for the Removal of Phosphate from Wastewater: Batch and Column Study. *ACS Sustainable Chemistry & Engineering*, *6*(9), 11662–11676.

Asaithambi, P., Beyene, D., Aziz, A. R. A., & Alemayehu, E. (2018). Removal of pollutants with determination of power consumption from landfill leachate wastewater using an electrocoagulation process: optimization using response surface methodology (RSM). *Applied Water Science*, *69*(8), 1–12.

Asaoka, S., & Yamamoto, T. (2010). Characteristics of phosphate adsorption onto granulated coal ash in seawater. *Marine Pollution Bulletin*, *60*, 1188-1192.

Asere, T. G., Mincke, S., Clercq, J. De, Verbeken, K., Tessema, D. A., Fufa, F., Stevens, C. V, & Laing, G. Du. (2017). Removal of Arsenic (V) from Aqueous Solutions Using Chitosan – Red Scoria and Chitosan – Pumice Blends. *International Journal of Environmental Research and Public Health*, *14*(8), 1–19.

Ashley, K., Cordell, D., & Mavinic, D. (2011). A brief history of phosphorus: From the philosopher's stone to nutrient recovery and reuse. *Chemosphere*, *84*(6), 737–746.

Awual, R., Jyo, A., Ihara, T., & Seko, N. (2011). Enhanced trace phosphate removal from water by zirconium (IV) loaded fibrous adsorbent. *Water Research*, *45*(15), 4592 4600.

Babu, B. V., & Gupta, S. (2005). Modeling And Simulation Of Fixed Bed Adsorption Column: Effect Of Velocity Variation. *I-Manager's Journal on Future Engineering and Technology*, *1*(1), 60–66.

Bacelo, H., Pintor, A. M. A., Santos, S. C. R., Boaventura, R. A. R., & Botelho, C. M. S. (2020). Performance and prospects of different adsorbents for phosphorus uptake and recovery from water. *Chemical Engineering Journal*, *381*, 1–18.

Baral, S. S., Das, S. N., & Rath, P. (2006). Hexavalent chromium removal from aqueous solution by adsorption on treated sawdust. *Biochemical Engineering Journal*, *31*, 216–222.

Beji, R., Hamdi, W., Kesraoui, A., & Seffen, M. (2018). Adsorption of phosphorus by alkaline

Tunisian soil in a fixed bed column. *Water Science and Technology*, *78*(4), 751–763.

Benyoucef, S., & Amrani, M. (2011). Adsorption of phosphate ions onto low cost Aleppo pine adsorbent. *Desalination*, *275*, 231–236.

Bezza, F. A., & Chirwa, E. M. N. (2021). Removal of phosphate from contaminated water using activated carbon supported nanoscale zero-valent iron (nZVI) particles. *Chemical Engineering Transactions*, *84*, 55–60.

Biswas, B. K., Inoue, K., Ghimire, K. N., Harada, H., Ohto, K., & Kawakita, H. (2008). Removal and recovery of phosphorus from water by means of adsorption onto orange waste gel loaded with zirconium. *Bioresource Technology*, *99*(18), 8685-8690.

Bohart, G. S., & Adams, E. Q. (1920). Some Aspects of the Behavior of Charcoal with Respect To Chlorine. *J. Chem. Soc.*, *42*, 523–544.

Bouamra, F., Drouiche, N., Abdi, N., Grib, H., Mameri, N., & Lounici, H. (2018). Removal of Phosphate from Wastewater by Adsorption on Marble Waste: Effect of Process Parameters and Kinetic Modeling. *International Journal of Environmental Research*, *12*(1), 13–27.

Boukemara, L., & Boukhalfa, C. (2012). Phosphate Removal from Aqueous Solution by Hydrous Iron Oxide Freshly Prepared Effects of pH , Iron Concentration and Competitive Ions. *Procedia Engineering*, *33*, 163–167.

Bui, T. H., Hong, S. P., & Yoon, J. (2018). Development of nanoscale zirconium molybdate embedded anion exchange resin for selective removal of phosphate. *Water Research*, *134*, 22–31.

Castro, D., Rosas-Laverde, N. M., Aldás, M. B., Almeida-Naranjo, C. E., Guerrero, V. H., & Pruna, A. I. (2021). Chemical modification of agro-industrial waste-based bioadsorbents for enhanced removal of zn(Ii) ions from aqueous solutions. *Materials*, *14*(9).

Chen, J., Cai, Y., Clark, M., & Yu, Y. (2013). Equilibrium and Kinetic Studies of Phosphate Removal from Solution onto a Hydrothermally Modified Oyster Shell Material. *PLOS ONE*, *8*(4), 1–10.

Cheng, P., Chen, D., Liu, H., Zou, X., Wu, Z., Xie, J., Qing, C., Kong, D., & Chen, T. (2018).

Synergetic effects of anhydrite and brucite-periclase materials on phosphate removal from aqueous solution. *Journal of Molecular Liquids*, *254*, 145-153.

Chittoo, B. S., & Sutherland, C. (2020). Column breakthrough studies for the removal and recovery of phosphate by lime-iron sludge: Modeling and optimization using artificial neural network and adaptive neuro-fuzzy inference system. *Chinese Journal of Chemical Engineering*, *28*(7), 1847–1859.

Choi, J., Ryu, J., Kwon, K., Song, M., Lee, S., Kim, S., & Lee, S. (2014). Adsorption of Ammonium Nitrogen and Phosphate onto Basanite and Evaluation of Toxicity. *Water Air and Soil Pollusion*, *125*.

Chowdhury, Z. Z., Zain, S. M., Rashid, A. K., Rafique, R. F., & Khalid, K. (2013). Breakthrough curve analysis for column dynamics sorption of Mn(II) ions from wastewater by using Mangostana garcinia peel-based granular-activated carbon. *Journal of Chemistry*, *2013*, 1–9.

Chu, K. H. (2020). Breakthrough curve analysis by simplistic models of fixed bed adsorption: In defense of the century-old Bohart-Adams model. *Chemical Engineering Journal*, *380*, 122513.

Cui, X., Li, H., Yao, Z., Shen, Y., He, Z., Yang, X., Ng, H. Y., & Wang, C. H. (2019). Removal of nitrate and phosphate by chitosan composited beads derived from crude oil refinery waste: Sorption and cost-benefit analysis. *Journal of Cleaner Production*, *207*, 846–856.

Gisi, S., Lofrano, G., Grassi, M., & Notarnicola, M. (2016). Characteristics and adsorption capacities of low-cost sorbents for wastewater treatment: A review. *Sustainable Materials and Technologies*, *9*, 10–40.

Ding, W., Bai, S., Mu, H., & Naren, G. (2017). Investigation of phosphate removal from aqueous solution by both coal gangues. *Water Science & Technology*, *76*(3–4), 785–792.

Du, X., Han, Q., Li, J., & Li, H. (2017). The behavior of phosphate adsorption and its reactions on the surfaces of Fe–Mn oxide adsorbent. *Journal of the Taiwan Institute of Chemical Engineers*, *76*, 167–175.

Đuričić, T.; Malinović, B.N.; Bijelić, D. (2016). The phosphate removal efficiency electrocoagulation wastewater using iron and aluminum electrodes. *Bullllettiin off Tthe*

Chemiistts and Technollogiistts off Bosniia and Herzegoviina, *47*, 33–38.

Eriksson, M., & Sigvant, J. (2019). *Causes and impact of surface water pollution in Addis Ababa , Ethiopia*.

Fan, C., & Zhang, Y. (2018). Adsorption isotherms , kinetics and thermodynamics of nitrate and phosphate in binary systems on a novel adsorbent derived from corn stalks. *Journal of Geochemical Exploration*, *188*, 95–100.

Fantaw, D. (2019). *The resource potential of Coal in Ethiopia-Report*. https://doi.org/10.13140/RG.2.2.28475.16166

Fernando, A., Monteiro, S., Pinto, F., & Mendes, B. (2009). *Production of biosorbents from waste olive cake and its adsorption characteristics for Zn2+ ion*. Sustainability.

Fiol, N., & Villaescusa, I. (2009). Determination of sorbent point zero charge: Usefulness in sorption studies. *Environmental Chemistry Letters*, *7*(1), 79-84.

Foo, K. Y., & Hameed, B. H. (2010). Insights into the modeling of adsorption isotherm systems. *Chemical Engineering Journal*, *156*(1), 2–10.

Foo, K. Y., Lee, L. K., & Hameed, B. H. (2013). Preparation of tamarind fruit seed activated carbon by microwave heating for the adsorptive treatment of landfill leachate: A laboratory column evaluation. *Bioresource Technology*, *133*, 599-605.

Fu, H., Yang, Y., Zhu, R., Liu, J., Usman, M., Chen, Q., & He, H. (2018). Superior adsorption of phosphate by ferrihydrite-coated and lanthanum-decorated magnetite. *Journal of Colloid and Interface Science*, *530*, 704–713.

Geleta, W. S., Alemayehu, E., & Lennartz, B. (2021). Volcanic rock materials for defluoridation Ofwater in fixed bed column systems. *Molecules*, *26*(4), 1 20.

George, W. K., Eren, Y., Ayd, S., Emik, S., Tuba, A., Osra, F., & Wasswa, J. (2019). A facile polymerisation of magnetic coal to enhanced phosphate removal from solution. *Journal of Environmental Management*, *247*, 356–362.

Ghaneian, M. T., Ghanizadeh, G., Alizadeh, M. T. H., Ehrampoush, M. H., & Said, F. M. (2014). Equilibrium and kinetics of phosphorous adsorption onto bone charcoal from aqueous

solution. *Environmental Technology (United Kingdom)*, *35*(7), 882-890.

Golie, W. M., & Upadhyayula, S. (2016). Continuous fixed-bed column study for the removal of nitrate from water using chitosan/alumina composite. *Journal of Water Process Engineering*, *12*, 58–65.

Gupta, V. K., Carrott, P. J. M., Ribeiro Carrott, M. M. L., & Suhas. (2009). Low-Cost adsorbents: Growing approach to wastewater treatment-a review. *Critical Reviews in Environmental Science and Technology*, *39*(10), 783–842.

Hamayun, M., Mahmood, T., Naeem, A., Muska, M., Din, S. U., & Waseem, M. (2014). Equilibrium and kinetics studies of arsenate adsorption by FePO 4. *Chemosphere*, *99*, 207–215.

Hamzah, S., Razali, N. A., Yatim, N. I., Alias, M., Ali, A., Zaini, N. S., & Abuhabib, A. A. M. (2018). Characterisation and performance of thermally treated rice husk as efficient adsorbent for phosphate removal. *Journal of Water Supply: Research and Technology - AQUA*, *67*(8), 766–778.

Han, C., Lalley, J., Iyanna, N., & Nadagouda, M. N. (2017). Removal of phosphate using calcium and magnesium-modified iron-based adsorbents. *Materials Chemistry and Physics*, *198*, 115–124.

Han, R., Ding, D., Xu, Y., Zou, W., Wang, Y., Li, Y., & Zou, L. (2008). Use of rice husk for the adsorption of congo red from aqueous solution in column mode. *Bioresource Technology*, *99*(8), 2938–2946.

Helmer, R., & Hespanhol, I. (1997). *Water Pollution Control - A Guide to the Use of Water Quality Management Principles*.

Hu, A., Ren, G., Che, J., Guo, Y., Ye, J., & Zhou, S. (2020). Phosphate recovery with granular acid-activated neutralized red mud: Fixed-bed column performance and breakthrough curve modelling. *Journal of Environmental Sciences (China)*, *90*, 78-86.

Huang, L., Fang, H., He, G., & Chen, M. (2016). Phosphorus adsorption on natural sediments with different pH incorporating surface morphology characterization. *Environmental Science and Pollution Research*, 18883–18891.

Huang, W. Y., Li, D., Liu, Z. Q., Tao, Q., Zhu, Y., Yang, J., & Zhang, Y. M. (2014). Kinetics, isotherm, thermodynamic, and adsorption mechanism studies of La(OH)3-modified exfoliat ed vermiculites as highly efficient phosphate adsorbents. *Chemical Engineering Journal*, *236*, 191–201.

Huang, Y., Lee, X., Grattieri, M., Yuan, M., Cai, R., Macazo, F. C., & Minteer, S. D. (2020). Modified biochar for phosphate adsorption in environmentally relevant conditions. *Chemical Engineering Journal*, *380*(June 2019), 122375.

Huang, Yimin, Lee, X., Grattieri, M., Macazo, F. C., Cai, R., & Minteer, S. D. (2018). A sustainable adsorbent for phosphate removal: modifying multi-walled carbon nanotubes with chitosan. *Journal of Materials Science*, *53*(17), 12641-12649.

Husein, D. Z., Al-Radadi, T., & Danish, E. Y. (2017). Adsorption of Phosphate Using Alginate-/Zirconium-Grafted Newspaper Pellets: Fixed-Bed Column Study and Application. *Arabian Journal for Science and Engineering*, *42*(4), 1399–1412.

Jarvie, H. P., Smith, D. R., Norton, L. R., Edwards, F. K., Bowes, M. J., King, S. M., Scarlett, P., Davies, S., Dils, R. M., & Bachiller-Jareno, N. (2018). Phosphorus and nitrogen limitation and impairment of headwater streams relative to rivers in Great Britain: A national perspective on eutrophication. *Science of the Total Environment*, *621*, 849-862.

Jiang, D., Chu, B., Amano, Y., & Machida, M. (2018). Removal and recovery of phosphate from water by Mg-laden biochar: Batch and column studies. *Colloids and Surfaces A: Physicoch emical and Engineering Aspects*, *558*, 429-437.

Jiang, J., Yuan, M., Xu, R., & Bish, D. L. (2015). Mobilization of phosphate in variable-charge soils amended with biochars derived from crop straws. *Soil & Tillage Research*, *146*, 139–147.

Jung, K. W., Jeong, T. U., Choi, J. W., Ahn, K. H., & Lee, S. H. (2017). Adsorption of phosphate from aqueous solution using electrochemically modified biochar calcium-alginate beads: Batch and fixed-bed column performance. *Bioresource Technology*, *244*, 23–32.

Kagalou, I., Papastergiadou, E., & Leonardos, I. (2008). Long term changes in the eutrophication process in a shallow Mediterranean lake ecosystem of W. Greece: Response after the

reduction of external load. *Journal of Environmental Management*, *87*, 497–506.

Kajjumba, G. W., Yıldırım, E., Aydın, S., Emik, S., Ağun, T., Osra, F., & Wasswa, J. (2019). A facile polymerisation of magnetic coal to enhanced phosphate removal from solution. *Journal of Environmental Management*, *247*(February), 356-362.

Kapur, M., & Mondal, M. K. (2013). Mass transfer and related phenomena for Cr (VI) adsorption from aqueous solutions onto Mangifera indica sawdust. *Chemical Engineering Journal*, *218*, 138–146.

Karageorgiou, K., Paschalis, M., & Anastassakis, G. N. (2007). Removal of phosphate species from solution by adsorption onto calcite used as natural adsorbent. *Journal of Hazardous Materials*, *139*(3), 447–452.

Khan, S., Ishaq, M., & Ahmad, I. (2013). Evaluation of coal as adsorbent for phosphate removal. *Arabian Journal of Geosciences*, *6*(4), 1113–1117.

Kilpimaa, S., Runtti, H., Kangas, T., Lassi, U., & Kuokkanen, T. (2014). Physical activation of carbon residue from biomass gasification: Novel sorbent for the removal of phosphates and nitrates from aqueous solution. *Journal of Industrial and Engineering Chemistry*, *21*, 1354–1364.

Kim, J. Y., Balathanigaimani, M. S., & Moon, H. (2015). Adsorptive Removal of Nitrate and Phosphate Using MCM-48, SBA-15, Chitosan, and Volcanic Pumice. *Water Air and Soil Pollusion*, *226*, 1–11.

Kim, S. H. D., & Lee, S. (2012). Effect of pH and Coexisting Anions on Removai of Phospiiate from Aqueous Soiutions by Inorganic-Based Mesostructures. *Water Environment Research*, *84*.

Kopp, O. C. (2021). *World distribution of coal*. Wikipedia. https://www.britannica.com/science/coal-fossil-fuel/World-distribution-of-coal (Accessed June 04, 2020)

Králik, M. (2014). Adsorption, chemisorption, and catalysis. *Chemical Papers*, *68*(12), 1625–1638.

Krishna, D., Kannan, P., Nesakumar, T., Immanuel, J., & Senthilkumar, A. (2017). Biochar from

green waste for phosphate removal with subsequent disposal. *Waste Management*, *68*, 752–759.

Kudeyarova, A. Y. (2010). Chemisorption of Phosphate Ions and Destruction of Organomineral Sorbents in Acid Soils. *Eurasian Soil Science*, *43*, 635-650.

Kumar, I. A., & Viswanathan, N. (2018). Development and Reuse of Amine-Grafted Chitosan Hybrid Beads in the Retention of Nitrate and Phosphate. *Journal of Chemical and Engineering Data*, *63*, 147–158.

Kumar, P. S. (2018). Phosphate recovery from wastewater via reversible adsorption. In *TU Delft University of Technology (Ph.D dissertation)*. https://doi.org/10.4233/uuid:f75d3713-8ef2-4f92-884f-06664b040f47

Kwon, J., Yun, S., Lee, J., Kim, S., & Young, H. (2010). Removal of divalent heavy metals (Cd , Cu , Pb , and Zn) and arsenic (III) from aqueous solutions using scoria : Kinetics and equilibria of sorption. *Journal of Hazardous Materials*, *174*, 307-313.

Kyzioł-Komosińska, J., Rosik-Dulewska, C., Dzieniszewska, A., Pająk, M., & Krzyzewska, I. (2014). Removal of Cr(III) ions from water and wastewater by sorption onto peats and clays occurring in an overburden of lignite beds in central Poland. *Environment Protection Engineering*, *40*(1), 5–22.

Lalley, J., Han, C., Li, X., Dionysiou, D. D., & Nadagouda, M. N. (2016). Phosphate adsorption using modified iron oxide-based sorbents in lake water: Kinetics, equilibrium, and column tests. *Chemical Engineering Journal*, *284*, 1386-1396.

Lam, N. H., Ma, H. T., Bashir, M. J. K., Eppe, G., & Nguyen, T. T. (2020). Removal of phosphate from wastewater using coal slag. *International Journal of Environmental Analytical Chemistry*, 1–11.

Langford, J. I., & Wilson, A. J. C. (1978). Scherrer after sixty years: A survey and some new results in the determination of crystallite size. *Journal of Applied Crystallography*, *11*(2), 102–113.

Largitte, L., & Pasquier, R. (2016). A review of the kinetics adsorption models and their application to the adsorption of lead by an activated carbon. *Chemical Engineering Research*

and Design, *109*, 495–504.

Le Bas, M. J., & Streckeisen, A. L. (1991). The IUGS systematics of igneous rocks. *Journal of the Geological Society*, *148*(5), 825–833.

Lee, C. G., Kim, J. H., Kang, J. K., Kim, S. B., Park, S. J., Lee, S. H., & Choi, J. W. (2015). Comparative analysis of fixed-bed sorption models using phosphate breakthrough curves in slag filter media. *Desalination and Water Treatment*, *55*(7), 1-11.

Lee, C., Jung, J., Pawar, R. R., Kim, M., Lalhmunsiama, & Lee, S. M. (2017). Arsenate and phosphate removal from water using Fe-sericite composite beads in batch and fixed-bed systems. *Journal of Industrial and Engineering Chemistry*, *47*, 375-383.

Lemraski, E. G., & Sharafinia, S. (2016). Kinetics, equilibrium and thermodynamics studies of Pb2+ adsorption onto new activated carbon prepared from Persian mesquite grain. *Journal of Molecular Liquids*, *219*, 482–492.

Li, N., & Bai, R. (2005). A novel amine-shielded surface cross-linking of chitosan hydrogel beads for enhanced metal adsorption performance. *Industrial and Engineering Chemistry Research*, *44*(17), 6692–6700.

Li, N., Ren, J., Zhao, L., & Wang, Z. L. (2013). Fixed bed adsorption study on phosphate removal using nanosized FeOOH-modified anion resin. *Journal of Nanomaterials*, *2013*, 1–6.

Li, R., Wang, J. J., Zhou, B., Kumar, M., Ali, A., Zhang, Z., Gaston, L. A., Hussain, A., & Mahar, A. (2016). Enhancing phosphate adsorption by Mg / Al layered double hydroxide functionalized biochar with different Mg / Al ratios. *Science of the Total Environment*, *559*, 121–129.

Li, X., Weihu, Y., Zou, Q., & Zuo, Y. (2010). Investigation on microstructure, composition, and cytocompatibility of natural pumice for potential biomedical application. *Tissue Engineering - Part C: Methods*, *16*(3), 427–434.

Lin, J., Jiang, B., & Zhan, Y. (2018). Effect of pre-treatment of bentonite with sodium and calcium ions on phosphate adsorption onto zirconium-modi fi ed bentonite. *Journal of Environmental Management*, *217*, 183–195.

Lin, K. Y. A., Chen, S. Y., & Jochems, A. P. (2015). Zirconium-based metal organic frameworks: Highly selective adsorbents for removal of phosphate from water and urine. *Materials Chemistry and Physics*, *160*, 168–176.

Liu, D., Zhu, H., Wu, K., Wang, F., Zhao, X., & Liao, Q. (2020). Understanding the effect of particle size of waste concrete powder on phosphorus removal efficiency. *Construction and Building Materials*, *236*, 117526.

Lyngsie, G., Katika, K., Fabricius, I. L., Hansen, H. C. B., & Borggaard, O. K. (2019). Phosphate removal by iron oxide-coated diatomite: Laboratory test of a new method for cleaning drainage water. *Chemosphere*, *222*, 884-890.

Mallet, M., Barthélémy, K., Ruby, C., Renard, A., & Naille, S. (2013). Investigation of phosphate adsorption onto ferrihydrite by X-ray Photoelectron Spectroscopy. *Journal of Colloid and Interface Science*, *407*, 95–101.

Manville, V., White, J. D. L., Houghton, B. F., & Wilson, C. J. N. (1998). The saturation behaviour of pumice and some sedimentological implications. *Sedimentary Geology*, *119*, 5–16.

Matsubara, M. E. (2018). Evaluation of the Use of Fly Ash as a Low Cost Technology for Phosphorus Removal in Wastewater Treatment. *An Interdisciplinary Journal of Applied Science*, *13*(3).

Matsuo, T. Hanaki, S. Takizawa, & H. Satoh. (2001). *Advances in water and Wastewater Treatment Technology*..

Mboya, H. A., King'ondu, C. K., Njau, K. N., & Mrema, A. L. (2017). Measurement of Pozzolanic Activity Index of Scoria, Pumice, and Rice Husk Ash as Potential Supplementary Cementitious Materials for Portland Cement. *Advances in Civil Engineering*, *2017*, 1–14.

Mboya, H. A., Njau, K. N., Mrema, A. L., & King, C. K. (2019). Influence of scoria and pumice on key performance indicators of Portland cement concrete. *Construction and Building Materials*, *197*, 444–453.

Mehrabi, N., Soleimani, M., Sharififard, H., & Yeganeh, M. M. (2016). Optimization of phosphate removal from drinking water with activated carbon using response surface methodology (RSM). *Desalination and WaterTreatment Treatment*, *57*(33), 15613-15618.

Mekonnen, D. T., Alemayehu, E., & Lennartz, B. (2020). Removal of Phosphate Ions from Aqueous Solutions by Adsorption onto Leftover Coal. *Water*, *12*(5), 1-15.

Mekonnen, D. T., Alemayehu, E., & Lennartz, B. (2021). Adsorptive removal of phosphate from aqueous solutions using low-cost volcanic rocks: Kinetics and equilibrium approaches. *Materials*, *14*(5).

Meyer, D., Chazarenc, F., Andre, Y., Barca, C., Ge, C., Nantes, M. De, Kastler, A., & Universite, L. U. (2012). Phosphate removal from synthetic and real wastewater using steel slags produced in Europe. *Water Research*, *26*(7), 2376-2384.

Mhemeed, A. H. (2018). A General Overview on the Adsorption. *Indian Journal of Natural Science*, *9*(51), 16127–16131.

Min, X., Wu, X., Shao, P., Ren, Z., Ding, L., & Luo, X. (2019). Ultra-high capacity of lanthanum-doped UiO-66 for phosphate capture: Unusual doping of lanthanum by the reduction of coordination number. *Chemical Engineering Journal*, *358*(October 2018), 321–330.

Mitchell, S. M., & Ullman, J. L. (2016). Removal of Phosphorus, BOD, and Pharmaceuticals by Rapid Rate Sand Filtration and Ultrafiltration Systems. *Journal of Environmental Engineering*, *142*(11), 06016006.

Mitrogiannis, D., Psychoyou, M., Baziotis, I., Vassilis, J., Koukouzas, N., Tsoukalas, N., & Palles, D. (2017). Removal of phosphate from aqueous solutions by adsorption onto Ca(OH)2 treated natural clinoptilolite. *Chemical Engineering Journal*, *320*, 510-522.

Mor, S., Chhoden, K., & Khaiwal, R. (2016). Application of Agro-waste Rice Husk Ash for the Removal of Phosphate from the Wastewater. *Journal of Cleaner Production*, *129*, 673–680.

Nageeb, M. (2013). Adsorption Technique for the Removal of Organic Pollutants from Water and Wastewater. In *IntechOpen*.

Nagoya, S., Nakamichi, S., & Kawase, Y. (2019). Mechanisms of phosphate removal from aqueous solution by zero-valent iron: A novel kinetic model for electrostatic adsorption, surface complexation and precipitation of phosphate under oxic conditions. *Separation and Purification Technology*, *218*, 120–129.

Naiya, T. K., Kumar, A., Mandal, S., & Kumar, S. (2009). The sorption of lead (II) ions on rice husk ash. *Journal of Hazardous Materials*, *163*, 1254-1264.

Nawar, N., Ahmad, M. E., Said, W. M. El, & Moalla, S. M. N. (2015). Adsorptive Removal of Phosphorous from Wastewater Using Drinking Water Treatment-Alum Sludge (DWT-AS) as Low Cost Adsorbent. *American Journal of Chemistry and Application*, *2*(6), 79–85.

Negrea, A., Mihailescu, M., Mosoarca, G., Ciopec, M., Duteanu, N., Negrea, P., & Minzatu, V. (2020). Estimation on fixed-bed column parameters of breakthrough behaviors for gold recovery by adsorption onto modified/functionalized amberlite xad7. *International Journal of Environmental Research and Public Health*, *17*(18), 1-14.

Newcombe, R. L., Rule, R. A., Hart, B. K., & Möller, G. (2008). Phosphorus Removal from Municipal Wastewater by Hydrous Ferric Oxide Reactive Filtration and Coupled Chemically Enhanced Secondary Treatment: Part I-Performance. *Water Environment Research*, *80*(3), 238–247.

Nguyen, T. A. H., Ngo, H. H., Guo, W. S., Pham, T. Q., Li, F. M., Nguyen, & Bui, X. T. (2015). Adsorption of phosphate from aqueous solutions and sewage using zirconium loaded okara (ZLO): Fixed-bed column study. *Science of the Total Environment*, *523*, 40–49.

Nunes, K. G. P., Batistel, N. R., Barbosa, D., Rosa, I. R., Davila, I. V. J., & Féris, L. A. (2020). Adsorption of hexavalent chromium on a coal beneficiation tailing material in batch and fixed-bed column. *Acta Brasiliensis*, *4*(2), 121–127.

Nuryadin, A., & Imai, T. (2021). Application of Amorphous Zirconium (hydr)oxide/MgFe Layered Double Hydroxides Composite in Fixed-bed Column for Phosphate Removal from Water. *Global Journal of Environmental Science and Management*, *7*(4), 485–502.

Omari, H., Dehbi, A., Lammini, A., & Abdallaoui, A. (2019). Study of the Phosphorus Adsorption on the Sediments. *Journal of Chemistry*, 1–10.

Ozacar, M. (2003). Equilibrium and Kinetic Modelling of Adsorption of Phosphorus on Calcined Alunite. *Adsorption*, *9*, 125–132.

Padmavathy, K. S., Madhu, G., & Haseena, P. V. (2016). A study on effects of pH , adsorbent dosage , time , initial concentration and adsorption isotherm study for the removal of

hexavalent chromium (Cr (VI)) from wastewater by magnetite nanoparticles. *Procedia Technology*, *24*, 585–594.

Pan, J., Gao, B., Song, W., Xu, X., & Yue, Q. (2020). Modified biogas residues as an eco-friendly and easily-recoverable biosorbent for nitrate and phosphate removals from surface water. *Journal of Hazardous Materials*, *382*, 1–11.

Pan, M., Lin, X., Xie, J., & Huang, X. (2017). Kinetic , equilibrium and thermodynamic studies for modi fi ed palygorskite nano-composites. *RSC Advances*, *8*, 4492–4500.

Park, J. H., & Jung, D. Il. (2011). Removal of total phosphorus (TP) from municipal wastewater using loess. *Desalination*, *269*, 104–110.

Peleka, E. N., & Deliyanni, E. A. (2009). Adsorptive removal of phosphates from aqueous solutions. *Desalination*, *245*(1–3), 357–371.

Peng, L., Dai, H., Wu, Y., Peng, Y., & Lu, X. (2018). A comprehensive review of phosphorus recovery from wastewater by crystallization processes. *Chemosphere*, *197*, 768–781.

Pengthamkeerati, P., Satapanajaru, T., & Chularuengoaksorn, P. (2008). Chemical modification of coal fly ash for the removal of phosphate from aqueous solution. *Fuel*, *87*(12), 2469–2476.

Penn, C. J., & Bowen, J. M. (2018). *Design and Construction of Phosphorus Removal Structures for Improving Water Quality*. Springer. http://link.springer.com/10.1007/978-3-319-58658-8

Pirsaheb, M., Mohammadi, H., Sharafi, K., & Asadi, A. (2018). Fluoride and nitrate adsorption from water by Fe(III)-doped scoria: optimizing using response surface modeling, kinetic and equilibrium study. *Water Science and Technology: Water Supply*, *18*(3), 1117–1132.

Pismenskaya, N., Laktionov, E., Nikonenko, V., El Attar, A., Auclair, B., & Pourcelly, G. (2001). Dependence of composition of anion-exchange membranes and their electrical conductivity on concentration of sodium salts of carbonic and phosphoric acids. *Journal of Membrane Science*, *181*(2), 185–197.

Qiu, B., & Duan, F. (2019). Synthesis of industrial solid wastes/biochar composites and their use for adsorption of phosphate: From surface properties to sorption mechanism. *Colloids and Surfaces A: Physicochemical and Engineering Aspects*, *571*, 86-93.

Qiu, H., Liang, C., Yu, J., Zhang, Q., Song, M., & Chen, F. (2017). Preferable phosphate sequestration by nano-La (III) (hydr) oxides modified wheat straw with excellent properties in regeneration. *Chemical Engineering Journal*, *315*, 345-354.

Ramirez, A., Giraldo, S., García-Nunez, J., Flórez, E., & Acelas, N. (2018). Phosphate removal from water using a hybrid material in a fixed-bed column. *Journal of Water Process Engineering*, *26*, 131–137.

Rangabhashiyam, S., Anu, N., Nandagopal, M. S. G., & Selvaraju, N. (2014). Relevance of isotherm models in biosorption of pollutants by agricultural byproducts. *Journal of Environmental Chemical Engineering*, *2*, 398-414.

Rao, R. A. K., Rehman, F., & Kashifuddin, M. (2012). Removal of Cr(VI) from electroplating wastewater using fruit peel of Leechi (Litchi chinensis). *Desalination and Water Treatment*, *49*(1–3), 136–146.

Rashid, M., Price, N. T., Angel, M., Pinilla, G., & Shea, K. E. O. (2017). Effective removal of phosphate from aqueous solution using humic acid coated magnetite nanoparticles. *Water Research*, *123*, 353–360.

Rashidi Nodeh, H., Sereshti, H., Zamiri Afsharian, E., & Nouri, N. (2017). Enhanced removal of phosphate and nitrate ions from aqueous media using nanosized lanthanum hydrous doped on magnetic graphene nanocomposite. *Journal of Environmental Management*, *197*, 265–274.

Regassa, M., Melak, F., Birke, W., & Alemayehu, E. (2016). Defluoridation of Water Using Natural and Activated Coal. *International Advanced Research Journal in Science, Engineering and Technology*, *3*(1), 1–7.

Rehman, S., Tariq, M., Shah, J. A., Ahmad, R., Shahzad, M., Abbasi, M., Ullah, A., Ismail, B., & Bilal, M. (2017). Simultaneous physisorption and chemisorption of reactive Orange 16 onto hemp stalks activated carbon: proof from isotherm modeling. *Biointerface Research in Applied Chemistry*, *7*(2), 2021–2029.

Rout, Prangya R., Dash, R. R., & Bhunia, P. (2014). Modelling and packed bed column studies on adsorptive removal of phosphate from aqueous solutions by a mixture of ground burnt patties and red soil. *Advances in Environmental Research*, *3*(3), 231-251.

Rout, Prangya Ranjan, Bhunia, P., & Dash, R. R. (2015). A mechanistic approach to evaluate the effectiveness of red soil as a natural adsorbent for phosphate removal from wastewater. *Desalination and Water Treatment*, *54*, 358-373.

Saadat, S., Raei, E., & Talebbeydokhti, N. (2018). Enhanced removal of phosphate from aqueous solutions using a modi fi ed sludge derived biochar : Comparative study of various modifying cations and RSM based optimization of pyrolysis parameters. *Journal of Environmental Management*, *225*, 75–83.

Sadhukhan, B., Mondal, N. K., & Chattoraj, S. (2016). Optimisation using central composite design (CCD) and the desirability function for sorption of methylene blue from aqueous solution onto Lemna major. *Karbala International Journal of Modern Science*, *2*(3), 145–155.

Saha, A., Bhaduri, D., Pipariya, A., & Kumar, R. (2016). Linear and Nonlinear Sorption Modelling for Adsorption of Atrazine onto Activated Peanut Husk. *Environmental Process & Sustainable Energy*, 1–11.

Saki, H., Alemayehu, E., Schomburg, J., & Lennartz, B. (2019). Halloysite Nanotubes as Adsorptive Material for Phosphate Removal from Aqueous Solution. *Water*, *11*(2), 1–10.

Samarghandi, M. R., Zarrabi, M., Amrane, A., Soori, M. M., & Sepehr, M. N. (2018). Removal of Acid Black Dye By Pumice Stone As a Low Cost Adsorbent: Kinetic, Thermodynamic and Equilibrium Studies. *Environmental Engineering and Management Journal*, *12*(11), 2137–2147.

Sellner, B. M., Hua, G., & Ahiablame, L. M. (2019). Fixed bed column evaluation of phosphate adsorption and recovery from aqueous solutions using recycled steel byproducts. *Journal of Environmental Management*, *233*, 595–602.

Shahid, M. K., Kim, Y., & Choi, Y. (2019). Magnetite synthesis using iron oxide waste and its application for phosphate adsorption with column and batch reactors. *Chemical Engineering Research and Design*, *148*, 169–179.

Shang, Y., Xu, X., Qi, S., Zhao, Y., Ren, Z., & Gao, B. (2017). Preferable uptake of phosphate by hydrous zirconium oxide nanoparticles embedded in quaternary-ammonium Chinese reed.

Journal of Colloid And Interface Science, *496*, 118-129.

Shi, Z. L., Liu, F. M., & Yao, S. H. (2011). Adsorptive removal of phosphate from aqueous solutions using activated carbon loaded with Fe(III) oxide. *Xinxing Tan Cailiao/New Carbon Materials*, *26*(4), 299–306.

Srinivasan, R. (2011). Advances in application of natural clay and its composites in removal of biological, organic, and inorganic contaminants from drinking water. *Advances in Materials Science and Engineering*, *2011*, 1–18.

Su, Y., Cui, H., Li, Q., Gao, S., & Ku, J. (2013). Strong adsorption of phosphate by amorphous zirconium oxide nanoparticles. *Water Research*, *47*, 5018-5026.

Sud, D., Mahajan, G., & Kaur, M. P. (2008). Agricultural waste material as potential adsorbent for sequestering heavy metal ions from aqueous solutions - A review. *Bioresource Technology*, *99*(14), 6017–6027.

Suresh, P., Korving, L., & Loosdrecht, M. C. M. Van. (2019). Adsorption as a technology to achieve ultra-low concentrations of phosphate : Research gaps and economic analysis. *Water Research X*, *4*, 1–17.

Tamez Uddin, M., Rukanuzzaman, M., Maksudur Rahman Khan, M., & Akhtarul Islam, M. (2009). Adsorption of methylene blue from aqueous solution by jackfruit (Artocarpus heteropyllus) leaf powder: A fixed-bed column study. *Journal of Environmental Management*, *90*(11), 3443–3450.

Tao, X., Huang, T., & Lv, B. (2020). Synthesis of Fe / Mg - Biochar Nanocomposites for Phosphate Removal. *Materials*, *13*(4).

Thomas, H. C. (1944). Hetrogeneous Ion Exchange in Flowing System. *J. Am. Chem. Soc.*, *66*(2), 1664–1666.

Tor, A., & Cengeloglu, Y. (2006). Removal of congo red from aqueous solution by adsorption onto acid activated red mud. *Journal of Hazardous Materials*, *138*(2), 409–415.

Uddin, M. K. (2017). A review on the adsorption of heavy metals by clay minerals, with special focus on the past decade. *Chemical Engineering Journal*, *308*, 438-462.

UNEP. (1997). *Water Pollution Control - A Guide to the Use of Water Quality Management Principles: Case Study I - The Ganga , India*.

UNIDO. (2019).*Supporting the improvement of the development strategy and policy for Ethiopia's Technology-Based Chemical Industry*.

Vaghetti, J. C. P., Lima, E. C., Royer, B., Brasil, J. L., Bruna, M., Simon, N. M., Cardoso, N. F., & Zapata, C. P. (2008). Application of Brazilian-pine fruit coat as a biosorbent to removal of Cr (VI) from aqueous solution - Kinetics and equilibrium study. *Biochemical Engineering Journal*, *42*, 67–76.

Vassileva, P., Detcheva, A., Uzunov, I., & Uzunova, S. (2013). Removal of Metal Ions from Aqueous Solutions Using Pyrolyzed Rice Husks: Adsorption Kinetics and Equilibria. *Chemical Engineering Communications*, *200*(12), 1578-1599.

Venezia, A. M., Floriano, M. A., Deganello, G., & Rossi, A. (1992). The structure of pumice: An XPS and 27Al MAS NMR study. *Surface and Interface Analysis*, *18*(7), 532–538.

Venkatesan, A. K., Hamdan, A.-H. M., Chavez, V. M., Brown, J. D., & Halden, R. U. (2016). Mass Balance Model for Sustainable Phosphorus Recovery in a US Wastewater Treatment Plant. *Journal of Environment Quality*, *45*(1), 84.

Vieira, M. L. G., Pinheiro, C. P., Silva, K. A., Lutke, S. F., Cadaval, T. R. S. A., Dotto, G., & Pinto, L. A. de A. (2019). Chitosan and cyanoguanidine-crosslinked chitosan coated glass beads and its application in fixed bed adsorption. *Chemical Engineering Communications*, *206*(11), 1474–1486.

Wang, J. P., Chen, Y. Z., Ge, X. W., & Yu, H. Q. (2007). Optimization of coagulation-flocculation process for a paper-recycling wastewater treatment using response surface methodology. *Colloids and Surfaces A: Physicochemical and Engineering Aspects*, *302*(1–3), 204–210.

Wang, S., Kong, L., Long, J., Su, M., Diao, Z., Chang, X., Chen, D., Song, G., & Shih, K. (2018). Adsorption of phosphorus by calcium-flour biochar: Isotherm, kinetic and transformation studies. *Chemosphere*, *195*, 666–672.

Wang, Z., Fang, W., Xing, M., & Wu, D. (2017). A bench-scale study on the removal and recovery of phosphate by hydrous zirconia-coated magnetite nanoparticles. *Journal of Magnetism and*

Magnetic Materials, *424*, 213–220.

Warner, M. (1990). Basalts, water, or shear zones in the lower continental crust? *Tectonophysics*, *173*, 163–174.

Wikipedia, the free encyclopedia. (2021). *Volcanic Rock*. https://en.wikipedia.org/wiki/Volcanic_rock (Accessed July 23,2021)

Wilkinson, B. H., McElroy, B. J., Kesler, S. E., Peters, S. E., & Rothman, E. D. (2009). Global geologic maps are tectonic speedometers - Rates of rock cycling from area-age frequencies. *Bulletin of the Geological Society of America*, *121*(5-6), 760-779.

Willett, C. B. (2015). *Color Removal From Pulp Mill Effluent Using Coal Ash Produced From Georgia Power Coal Combustion Plants* [Georgia Southern University, Ph.D Dissertation].

William, G., Eren, Y., Ayd, S., Emik, S., Tuba, A., Osra, F., & Wasswa, J. (2019). *A facile polymerisation of magnetic coal to enhanced phosphate removal from solution*. *247*(1), 356–362.

Witek-krowiak, A., Szafran, R. G., & Modelski, S. (2011). Biosorption of heavy metals from aqueous solutions onto peanut shell as a low-cost biosorbent. *Desalination*, *265*, 126–134.

Wolela, A. (2007). Fossil fuel energy resources of Ethiopia : Coal deposits. *International Journal of Coal Geology*, *72*, 293–314.

Woumfo, E. D., Siéwé, J. M., & Njopwouo, D. (2015). A fixed-bed column for phosphate removal from aqueous solutions using an andosol-bagasse mixture. *Journal of Environmental Management*, *151*, 450–460.

Wu, B., Fang, L., Fortner, J. D., Guan, X., & Lo, I. M. C. (2017). Highly efficient and selective phosphate removal from wastewater by magnetically recoverable La(OH)3/Fe3O4 nanocomposites. *Water Research*, *126*, 179-188.

Xie, J., Wang, Z., Lu, S., Wu, D., Zhang, Z., & Kong, H. (2014). Removal and recovery of phosphate from water by lanthanum hydroxide materials. *Chemical Engineering Journal*, *254*, 163–170.

Xiong, J., Zang, L., Zha, J., Mahmood, Q., & He, Z. (2019). Phosphate removal from secondary

effluents using coal gangue loaded with zirconium oxide. *Sustainability*, *11*(9), 1–10.

Xue, Y., Hou, H., & Zhu, S. (2009). Characteristics and mechanisms of phosphate adsorption onto basic oxygen furnace slag. *Journal of Hazardous Materials*, *162*(2–3), 973–980.

Yadav, D., Kapur, M., Kumar, P., & Mondal, M. K. (2015a). Adsorptive removal of phosphate from aqueous solution using rice husk and fruit juice residue. *Process Safety and Environmental Protection*, *94*(August), 402–409.

Yagub, M. T., Sen, T. K., Afroze, S., & Ang, H. M. (2015). Fixed-bed dynamic column adsorption study of methylene blue (MB) onto pine cone. *Desalination and Water Treatment*, *55*(4), 1–14.

Yang, Q., Wang, X., Luo, W., Sun, J., Xu, Q., Chen, F., Zhao, J., Wang, S., Yao, F., Wang, D., Li, X., & Zeng, G. (2018). Effectiveness and mechanisms of phosphate adsorption on iron-modified biochars derived from waste activated sludge. *Bioresource Technology, 247, 537-544*.

Yang, S., Jin, P., Wang, X., Zhang, Q., & Chen, X. (2016). Phosphate recovery through adsorption assisted precipitation using novel precipitation material developed from building waste : Behavior and mechanism. *CHEMICAL ENGINEERING JOURNAL*, *292*, 246–254.

Yang, X., Wan, Y., Zheng, Y., He, F., Yu, Z., Huang, J., Wang, H., Ok, Y. S., Jiang, Y., & Gao, B. (2019). Surface functional groups of carbon-based adsorbents and their roles in the removal of heavy metals from aqueous solutions: A critical review. *Chemical Engineering Journal*, *366*(February), 608–621.

Yang, Y., Zhao, Y. Q., Babatunde, A. O., Wang, L., Ren, Y. X., & Han, Y. (2006). Characteristics and mechanisms of phosphate adsorption on dewatered alum sludge. *Separation and Purification Technology*, *51*(2), 193–200.

Yao, Y., Gao, B., Chen, J., Zhang, M., Inyang, M., Li, Y., & Alva, A. (2013). Engineered carbon (biochar) prepared by direct pyrolysis of Mg-accumulated tomato tissues : Characterization and phosphate removal potential. *Bioresource Technology*, *138*, 8-13.

Yao, Y., Gao, B., Inyang, M., Zimmerman, A. R., Cao, X., Pullammanappallil, P., & Yang, L. (2011). Removal of phosphate from aqueous solution by biochar derived from anaerobically

digested sugar beet tailings. *Journal of Hazardous Materials*, *190*, 501-507.

Yasin, M., Ketema, T., & Bacha, K. (2015). Physico - chemical and bacteriological quality of drinking water of different sources , Jimma zone , Southwest Ethiopia. *BMC Research Notes*, *8*, 1–13.

Ye, Y., Jiao, J., Kang, D., Jiang, W., Kang, J., Ngo, H. H., Guo, W., & Liu, Y. (2019). The adsorption of phosphate using a magnesia–pullulan composite: Kinetics, equilibrium, and column tests. *Environmental Science and Pollution Research*, *26*(13), 13299–13310.

Yohannes, H., & Elias, E. (2017). Contamination of Rivers and Water Reservoirs in and Around Addis Ababa City and Actions to Combat It. *Environment Pollution and Climate Change*, *01*(02), 1–12.

Yuan, Y., Zhang, H., & Pan, G. (2016). Flocculation of cyanobacterial cells using coal fly ash modified chitosan. *Water Research*, *97*, 11–18.

Zhang, C., Zhong, Z., Feng, Y., Sun, L., & Qi, L. (2014). Potential for Phosphorus Removal in Wastewater Using Volcanic Rock as Adsorbent. *Advance Materials Research*, *1012*, 202–206.

Zhang, F. J., Zhang, H. Y., & Zhang, L. Y. (2012). The Removal of Phosphate by Coal Gangue from Wastewater. *Applied Mechanics and Materials*, *209*(211), 2005-2008.

Zhang, J., Shen, Z., Mei, Z., Li, S., & Wang, W. (2011). Removal of phosphate by Fe-coordinated amino-functionalized 3D mesoporous silicates hybrid materials. *Journal of Environmental Science*, *23*(2), 199–205.

Zhang, L., Wan, L., Chang, N., Liu, J., Duan, C., Zhou, Q., Li, X., & Wang, X. (2011). Removal of phosphate from water by activated carbon fiber loaded with lanthanum oxide. *Journal of Hazardous Materials*, *190*(1–3), 848–855.

Zhang, W., Bu, A., Ji, Q., Min, L., Zhao, S., Wang, Y., & Chen, J. (2019). P Ka-directed incorporation of phosphonates into mof-808 via ligand exchange: Stability and adsorption properties for uranium. *ACS Applied Materials and Interfaces*, *11*(37), 33931–33940.

Zheng, Y., Wang, B., Wester, A. E., Chen, J., He, F., Chen, H., & Gao, B. (2019). Reclaiming

phosphorus from secondary treated municipal wastewater with engineered biochar. *Chemical Engineering Journal*, *362*, 460–468.

Zhou, H., Bhattarai, R., Li, Y., Li, S., & Fan, Y. (2019). Utilization of coal fly and bottom ash pellet for phosphorus adsorption: Sustainable management and evaluation. *Resources, Conservation and Recycling*, *149*, 372–380.

Appendices: Supplementary materials

Annex 1: Original published papers

materials

MDPI

Article

Fixed-Bed Column Technique for the Removal of Phosphate from Water Using Leftover Coal

Dereje Tadesse Mekonnen [1,2], Esayas Alemayehu [3,4,*] and Bernd Lennartz [2,*]

[1] School of Chemical Engineering, Jimma Institute of Technology, Jimma University, Jimma P.O. Box 378, Ethiopia; getdere@gmail.com
[2] Faculty of Agricultural and Environmental Sciences, University of Rostock, Justus von-Liebig Weg 6, 18059 Rostock, Germany
[3] Faculty of Civil and Environmental Engineering, Jimma Institute of Technology, Jimma University, Jimma P.O. Box 378, Ethiopia
[4] Africa Center of Excellence for Water Management, Addis Ababa University, Addis Ababa P.O. Box 1176, Ethiopia
* Correspondence: esayas16@yahoo.com (E.A.); bernd.lennartz@uni-rostock.de (B.L.)

Abstract: The excessive discharge of phosphate from anthropogenic activities is a primary cause for the eutrophication of aquatic habitats. Several methodologies have been tested for the removal of phosphate from aqueous solutions, and adsorption in a flow-through reactor is an effective mechanism to reduce the nutrient loading of water. This research aimed to investigate the adsorption potential of leftover coal material to remove phosphate from a solution by using continuous flow fixed-bed column, and analyzes the obtained breakthrough curves. A series of column tests were performed to determine the phosphorus breakthrough characteristics by varying operational design parameters such as adsorbent bed height (5 to 8 cm), influent phosphate concentration (10–25 mg/L), and influent flow rate (1–2 mL/min). The amorphous and crystalline property of leftover coal material was studied using XRD technology. The FT-IR spectrum confirmed the interaction of adsorption sites with phosphate ions. Breakthrough time decreased with increasing flow rate and influent phosphate concentration, but increased with increasing adsorbent bed height. Breakthrough-curve analysis showed that phosphate adsorption onto the leftover coal material was most effective at a flow rate of 1 mL/min, influent phosphate concentration of 25 mg/L, and at a bed height of 8 cm. The maximal total phosphate adsorbed onto the coal material's surface was 243 mg/kg adsorbent. The Adams–Bohart model depicted the experimental breakthrough curve well, and overall performed better than the Thomas and Yoon–Nelson models did, with correlation values (R^2) ranging from 0.92 to 0.98. Lastly, leftover coal could be used in the purification of phosphorus-laden water, and the Adams–Bohart model can be employed to design filter units at a technical scale.

Keywords: breakthrough curve; fixed-bed column; bed height; adsorption; eutrophication

check for updates

Citation: Mekonnen, D.T.; Alemayehu, E.; Lennartz, B. Fixed-Bed Column Technique for the Removal of Phosphate from Water Using Leftover Coal. *Materials* **2021**, *14*, 5466. https://doi.org/10.3390/ma14195466

Academic Editors: Emmanuel Unuabonah and Andreas Taubert

Received: 15 August 2021
Accepted: 17 September 2021
Published: 22 September 2021

Publisher's Note: MDPI stays neutral with regard to jurisdictional claims in published maps and institutional affiliations.

Copyright: © 2021 by the authors. Licensee MDPI, Basel, Switzerland. This article is an open access article distributed under the terms and conditions of the Creative Commons Attribution (CC BY) license (https://creativecommons.org/licenses/by/4.0/).

1. Introduction

Increasing concern about the effect of phosphate released from different natural and human activities has resulted in more stringent environmental policies in recent years. Phosphate is one of the main nutrients for plants and aquatic lives, and is, in turn, primarily responsible for the eutrophication of water [1–6]. The eutrophication of water bodies due to phosphate discharges is a challenging issue for industrialized regions [7,8]. Domestic activities, detergent-making industries, and mining companies are the primary sources for phosphate discharged to water bodies. The uncontrolled use of fertilizers also releases phosphate and affects nearby water streams due to the runoff from agricultural activities [9,10]. Water pollution by phosphate is tremendously increasing, and demand for the removal of excess phosphate from water bodies is thereby also increasing [11].

There are numerous methods to remove phosphate from water, including chemical precipitation, biological treatment, physical process, coagulation, and adsorption [12–15].

materials

MDPI

Article

Adsorptive Removal of Phosphate from Aqueous Solutions Using Low-Cost Volcanic Rocks: Kinetics and Equilibrium Approaches

Dereje Tadesse Mekonnen [1,2], Esayas Alemayehu [3,4,*] and Bernd Lennartz [2,*]

[1] School of Chemical Engineering, Jimma Institute of Technology, Jimma University, Jimma P.O. Box 378, Ethiopia; getdere@gmail.com
[2] Faculty of Agricultural and Environmental Sciences, University of Rostock, Justus Von-Liebig Weg 6, 18059 Rostock, Germany
[3] Faculty of Civil and Environmental Engineering, Jimma Institute of Technology, Jimma University, Jimma P.O. Box 378, Ethiopia
[4] Africa Center of Excellence for Water Management, Addis Ababa University, Addis Ababa P.O. Box 1176, Ethiopia
* Correspondence: esayas16@yahoo.com (E.A.); bernd.lennartz@uni-rostock.de (B.L.); Tel.: +251-917-017-002 (E.A.); +49-381-498-3180 (B.L.)

Abstract: The contamination of surface and groundwater with phosphate originating from industrial and household wastewater remains a serious environmental issue in low-income countries. Herein, phosphate removal from aqueous solutions was studied using low-cost volcanic rocks such as pumice (VPum) and scoria (VSco), obtained from the Ethiopian Great Rift Valley. Batch adsorption experiments were conducted using phosphate solutions with concentrations of 0.5 to 25 mg·L^{-1} to examine the adsorption kinetic as well as equilibrium conditions. The experimental adsorption data were tested by employing various equilibrium adsorption models, and the Freundlich and Dubinin-Radushkevich (D-R) isotherms best depicted the observations. The maximum phosphate adsorption capacities of VPum and VSco were calculated and found to be 294 mg·kg^{-1} and 169 mg·kg^{-1}, respectively. A pseudo-second-order kinetic model best described the experimental data with a coefficient of correlation of $R^2 > 0.99$ for both VPum and VSco; however, VPum showed a slightly better selectivity for phosphate removal than VSco. The presence of competitive anions markedly reduced the removal efficiency of phosphate from the aqueous solution. The adsorptive removal of phosphate was affected by competitive anions in the order: $HCO_3^- > F^- > SO_4^{-2} > NO_3^- > Cl^-$ for VPum and $HCO_3^- > F^- > Cl^- > SO_4^{-2} > NO_3^-$ for VSco. The results indicate that the readily available volcanic rocks have a good adsorptive capacity for phosphate and shall be considered in future studies as test materials for phosphate removal from water in technical-scale experiments.

Keywords: adsorption kinetics; aqueous solution; eutrophication; isotherm models; pumice; scoria

check for updates

Citation: Mekonnen, D.T.; Alemayehu, E.; Lennartz, B. Adsorptive Removal of Phosphate from Aqueous Solutions Using Low-Cost Volcanic Rocks: Kinetics and Equilibrium Approaches. *Materials* **2021**, *14*, 1312. https://doi.org/10.3390/ma14051312

Academic Editors: Ewa Skwarek and Agnieszka Gładysz-Płaska

Received: 30 January 2021
Accepted: 1 March 2021
Published: 9 March 2021

Publisher's Note: MDPI stays neutral with regard to jurisdictional claims in published maps and institutional affiliations.

Copyright: © 2021 by the authors. Licensee MDPI, Basel, Switzerland. This article is an open access article distributed under the terms and conditions of the Creative Commons Attribution (CC BY) license (https://creativecommons.org/licenses/by/4.0/).

1. Introduction

Phosphate, a molecule consisting of the elements phosphorus (P) and oxygen [1], is an essential macronutrient for all life [2]. With nitrogen and carbon, phosphorus is the primary source of productivity and is fundamental for freshwater ecosystems' sustainability [3]. However, a high phosphate concentration above 0.1 mg·L^{-1} [4] in water bodies has serious environmental repercussions, such as eutrophication, which is associated with massive algal growth, the excessive growth of microorganisms, and the depletion of dissolved oxygen (DO) in the water bodies, and, in turn, it harmfully effects life in the aquatic ecosystems [5–9]. However, some researchers reported that a phosphate concentration as low as 0.05 mg·L^{-1} [10] or 0.02 mg·L^{-1} [11] in the water reservoir is sufficient to stimulate the growth of algae. Nowadays, the contamination of water bodies by pollutants like phosphorus has drawn attention globally. Industrialization, modern agriculture, and

water

MDPI

Article

Removal of Phosphate Ions from Aqueous Solutions by Adsorption onto Leftover Coal

Dereje Tadesse Mekonnen [1,2], Esayas Alemayehu [3,4,*] and Bernd Lennartz [2,*]

[1] School of Chemical Engineering, Jimma Institute of Technology, Jimma University, P.O. Box 378 Jimma, Ethiopia; getdere@gmail.com
[2] Faculty of Agricultural and Environmental Science, University of Rostock, Justus Von-Liebig Weg 6, 18059 Rostock, Germany
[3] Faculty of Civil and Environmental Engineering, Jimma Institute of Technology, Jimma University, P.O. Box 378 Jimma, Ethiopia
[4] Africa Center of Excellence for Water Management, Addis Ababa University, P.O. Box 1176 Addis Ababa, Ethiopia
* Correspondence: esayas16@yahoo.com (E.A.); bernd.lennartz@uni-rostock.de (B.L.); Tel.: +251-91-701-7002 (E.A.); +49-381-498-3180 (B.L.)

Received: 1 April 2020; Accepted: 10 May 2020; Published: 13 May 2020

Abstract: High loadings of wastewater with phosphors (P) require purification measures, which can be challenging to realize in regions where the technical and financial frame does not allow sophisticated applications. Simple percolation devices employing various kinds of adsorbents might be an alternative. Here, we investigated the application of leftover coal, which was collected from Ethiopian coal mining areas, as an adsorbent for the removal of phosphate from aqueous solutions in a classical slurry batch set-up. The combined effects of operational parameters such as contact time, initial concentration, and solution pH on P retention efficiency was studied employing the Response Surface Methodology (RSM). The maximum phosphate adsorption (79% removal and 198 mg kg^{-1} leftover coal) was obtained at a contact time of 200 min, an initial phosphate concentration of 5 mg/L, and a solution pH of 2.3. The Freundlich isotherm was fitted to the experimental data. The pseudo second-order equation describes the experimental data well, with a correlation value of $R^2 = 0.99$. The effect of temperature on the adsorption reveals that the process is exothermic. The results demonstrate that leftover coal material could potentially be applied for the removal of phosphate from aqueous media, but additional testing in a flow-through set-up using real wastewater is required to draw definite conclusions.

Keywords: leftover coal; phosphate; isotherms; aqueous solution; central composite design

1. Introduction

Phosphorus, generally occurring as phosphate (PO_4^{3-}) in aqueous solutions [1], is an essential amendment and nutrient for many industrial and agricultural applications and often present in water and wastewater at various concentrations [2]. For example, phosphate is highly required for the manufacturing of glass products (like glass fiber, military-grade lasers), toothpaste, pesticides and detergent among others [3]. However, the increase of phosphate in water bodies promotes the growth of algae, which results in eutrophication and eventually consumes dissolved oxygen thereby adversely affects water quality [2,4,5].

Municipal and industrial wastewaters are the main point sources for phosphate while run-off from agriculture is the dominant non-point source. Studies indicate that 4 to 15 mg/L phosphate may be contained in municipal wastewater, whereas effluent from chemical industries such as detergent

Annex 2: Supplementary materials for chapter 2

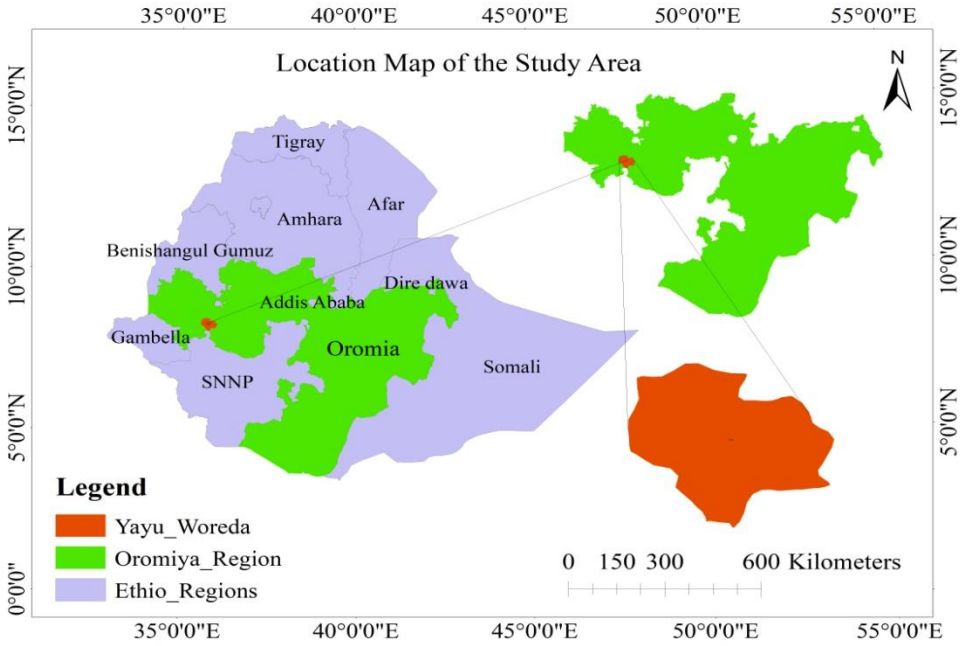

Figure A2. 1: Yayu coal mining- Oromia, Ethiopia [Latitude =(X, Y) = (8.479572, 8.069128); Longitude= (X, Y) = (35.637697, 36.098927)]

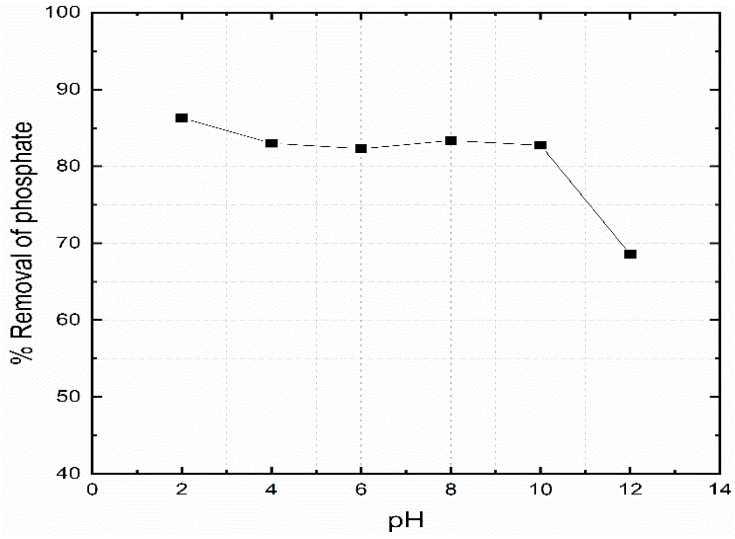

Figure A2. 2: Effect of initial pH on phosphate removal by leftover coal (Temperature: 20oC; Co: 10mg/L; dose 40g/L; adsorbent size 0.075mm-0.425mm, contact time 1440min)

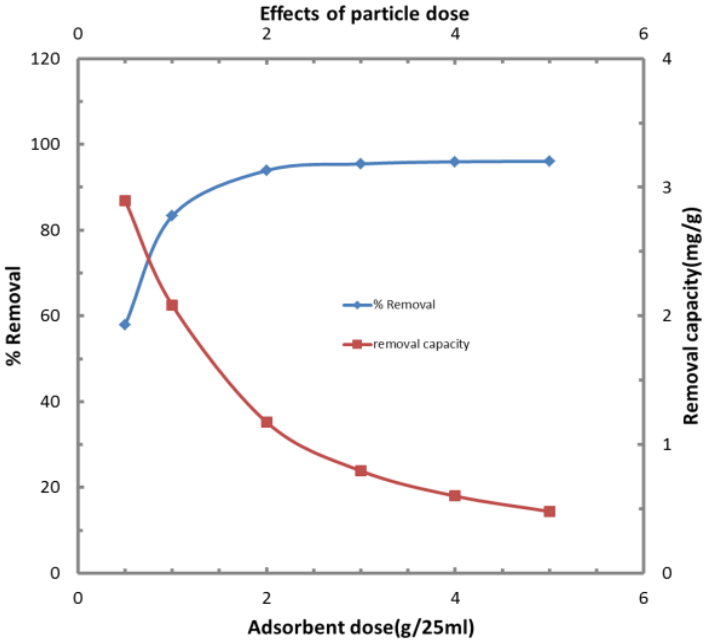

Figure A2. 3: Figure A2.3: Effect of adsorbent dose on the removal of phosphate (Temperature: 20oC; Co: 10mg/L; contact time 1440mn; adsorbent size 0.075mm-0.425mm)

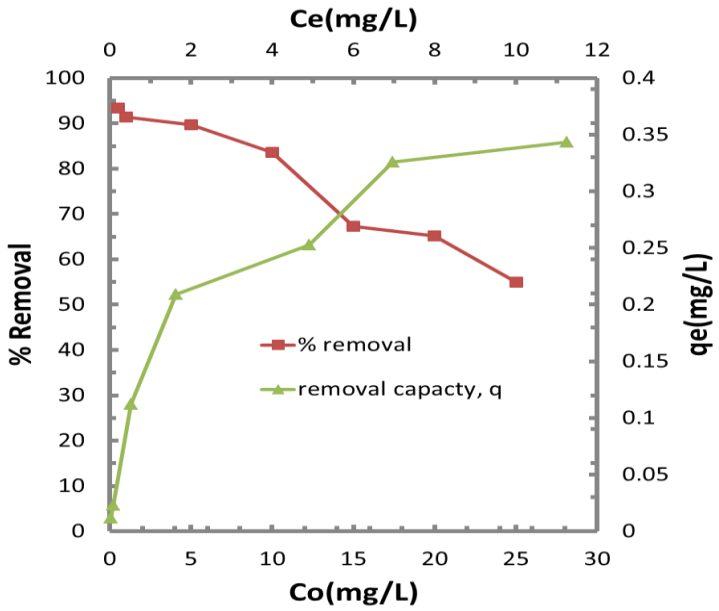

Figure A2. 4: The plot of effect of initial concentration (Co) of phosphate on the removal and uptake capacity, q (Temperature: 20oC; contact time 1440mn; dose 40g/L; adsorbent size 0.075mm-0.425mm)

Table A2. 1: Design Summary for independent and dependent variables/responses

Factor	Name	Units	Min.	Max.	Coded Low	Coded High	Mean	Std. Dev.
A	Contact Time	min	120	240	-1 = 120.00	+1=240.00	180.00	43.53
B	Concentration	mg/L	5	25	-1 = 5.00	+1=25.00	15.00	7.25
C	Solution pH	-	2	10	-1 = 2.00	+1 = 10.00	6.00	2.9
Responses								
Response	Name	Units	Minimum	Maximum	Mean	Ratio	Std. Dev.	Model
R1	% Removal	%	64.11	78.75	71.48	1.23	4.52	Quadratic
R2	Removal Capacity	mg/g	0.16	0.197	0.1787	1.23	0.191	Quadratic

Table A2. 2: Adequacy of the model tested and model summary statistics for % Removal

Source	Sum of Squares	df	Mean Square	F-value	p-value	
Mean vs Total	1.02E+05	1	1.02E+05			
Linear vs Mean	375.35	3	125.12	149.52	< 0.0001	
2FI vs Linear	1.94	3	0.6473	0.7351	0.5495	
Quadratic vs 2FI	**10.94**	**3**	**3.65**	**71.47**	**< 0.0001**	**Suggested**
Cubic vs Quadratic	0.5045	4	0.1261	137.04	< 0.0001	Aliased
Residual	0.0055	6	0.0009			
Total	1.03E+05	20	5128.83			
Model Summary						
Source	Std. Dev.	R^2	Adjusted R^2	Predicted R^2	PRESS	
Linear	0.9148	0.9656	0.9591	0.9436	21.93	
2FI	0.9384	0.9706	0.957	0.9043	37.22	
Quadratic	**0.2258**	**0.9987**	**0.9975**	**0.9852**	**5.74**	**Suggested**
Cubic	0.0303	1.000	1.000	0.9825	6.79	Aliased

Table A2. 3: Adequacy of the model tested and model summary statistics for Removal capacity, q

Source	Sum of Squares	df	Mean Square	F-value	p-value	
Mean vs Total	16.65	1	16.65			
Linear vs Mean	0.5609	3	0.1870	22.65	< 0.0001	
2FI vs Linear	0.0643	3	0.0214	4.12	0.0295	
Quadratic vs 2FI	**0.0668**	**3**	**0.0223**	**228.16**	**< 0.0001**	**Suggested**
Cubic vs Quadratic	0.0001	4	0.0000	0.2514	0.8987	Aliased
Residual	0.0008	6	0.0001			
Total	17.35	20	0.8673			

Model summary

Source	Std. Dev.	R^2	Adjusted R^2	Predicted R^2	PRESS	
Linear	0.0909	0.8094	0.7737	0.6445	0.2464	
2FI	0.0722	0.9023	0.8572	0.8588	0.0979	
Quadratic	**0.0099**	**0.9986**	**0.9973**	**0.9931**	**0.0048**	**Suggested**
Cubic	0.0118	0.9988	0.9962	-0.4809	1.03	Aliased

Table A2. 4: ANOVA, test of significance for % removal of Phosphate onto leftover coal material

Source	Sum of Squares	df[b]	Mean Square	F-value	p-value	
Model	388.23	9	43.14	845.72	< 0.0001	significant
A-Contact Time	10.32	1	10.32	202.38	< 0.0001	significant
B-Initial Concentration	364.57	1	364.57	7147.64	< 0.0001	significant
C-Solution pH	0.4580	1	0.4580	8.98	0.0134	significant
AB	0.9248	1	0.9248	18.13	0.0017	significant
AC	0.9112	1	0.9112	17.87	0.0018	significant
BC	0.1058	1	0.1058	2.07	0.1804	Not significant
A^2	3.57	1	3.57	69.96	< 0.0001	significant
B^2	7.86	1	7.86	154.15	< 0.0001	significant
C^2	0.3196	1	0.3196	6.27	0.0313	significant
Residual	0.5101	10	0.0510			
Lack of Fit	0.5101	5	0.1020			
Pure Error	0.0000	5	0.0000			
Cor Total	388.74	19				

[b] degree of freedom.

Table A2. 5: ANOVA test of significance for quadratic model of removal capacity, q

Source	Sum of Squares	df	Mean Square	F-value	p-value	
Model	0.0024	9	0.0003	845.72	< 0.0001	significant
A-Contact Time	0.0001	1	0.0001	202.38	< 0.0001	significant
B-Initial Concentration	0.0023	1	0.0023	7147.64	< 0.0001	significant
C-Solution pH	2.862E-06	1	2.862E-06	8.98	0.0134	significant

AB	5.780E-06	1	5.780E-06	18.13	0.0017	significant
AC	5.695E-06	1	5.695E-06	17.87	0.0018	significant
BC	6.613E-07	1	6.613E-07	2.07	0.1804	Not significant
A^2	0.0000	1	0.0000	69.96	< 0.0001	significant
B^2	0.0000	1	0.0000	154.15	< 0.0001	significant
C^2	1.998E-06	1	1.998E-06	6.27	0.0313	significant
Residual	3.188E-06	10	3.188E-07			
Lack of Fit	3.188E-06	5	6.376E-07			
Pure Error	0.0000	5	0.0000			
Cor Total	0.0024	19				

Table A2. 6: Experimental Design matrix and response based on actual and predicted values of % Removal and Removal capacity, q

Run Order	Factor 1 A: Contact Time (min)	Factor 2 B: Initial Concentration (mg/g)	Factor 3 C: Solution pH -	Response 1 Removal Efficiency %		Response 2 Removal Capacity mg/g	
				Actual	Predicted	Actual	Predicted
1	120	25	10	64.11	64.10	0.1603	0.1602
2	180	15	2	71.29	71.59	0.1782	0.1790
3	180	15	6	71.05	71.03	0.1776	0.1776
4	120	25	2	64.88	64.97	0.1622	0.1624
5	240	25	10	67.21	67.48	0.1680	0.1687
6	240	5	2	78.63	78.63	0.1966	0.1966
7	240	5	10	78.75	78.65	0.1969	0.1966
8	180	15	6	71.05	71.03	0.1776	0.1776
9	180	15	10	71.41	71.16	0.1785	0.1779
10	180	15	6	71.05	71.03	0.1776	0.1776
11	180	15	6	71.05	71.03	0.1776	0.1776

12	120	5	10	76.53	76.62	0.1913	0.1916
13	180	15	6	71.05	71.03	0.1776	0.1776
14	180	25	6	66.93	66.69	0.1673	0.1667
15	240	25	2	67.11	67.01	0.1678	0.1675
16	180	15	6	71.05	71.03	0.1776	0.1776
17	120	15	6	68.76	68.88	0.1719	0.1722
18	120	5	2	78.24	77.95	0.1956	0.1949
19	240	15	6	70.98	70.91	0.1774	0.1773
20	180	5	6	78.47	78.76	0.1962	0.1969

Annex 3: Supplementary materials for chapter 3

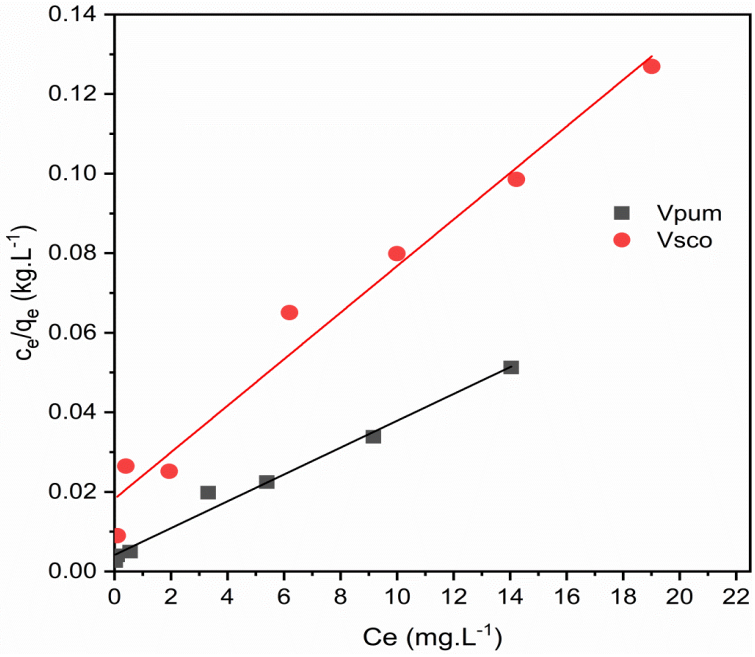

Figure A3. 1: Linear plot of Langmuir isotherm for Vpum and Vsco

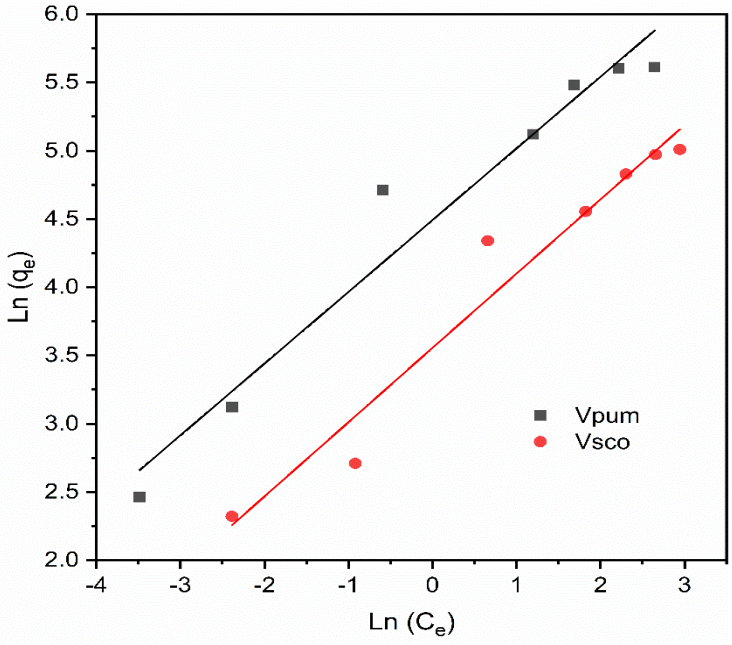

Figure A3. 2: Linear plot of Freundlich isotherm model for Vpum and Vsco

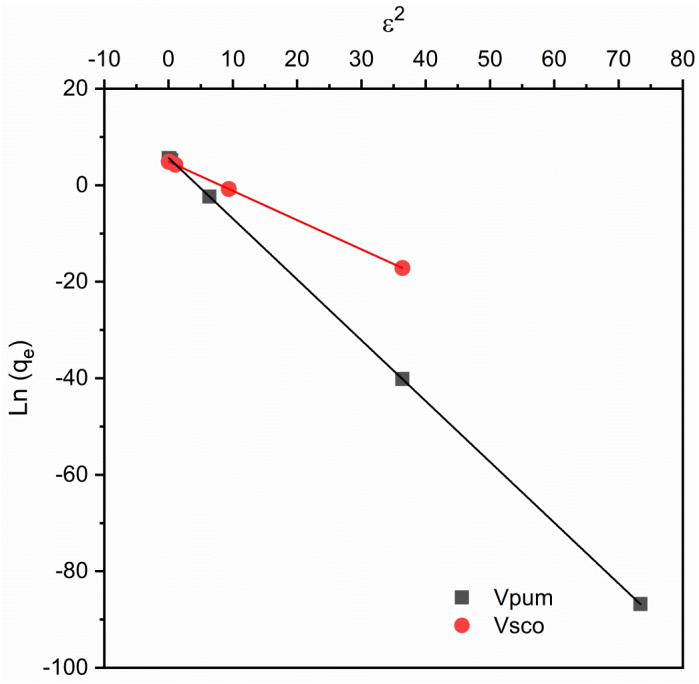

Figure A3. 3: Linear plot of Dubinin-Radushkevich isotherm model for VPum and VSco

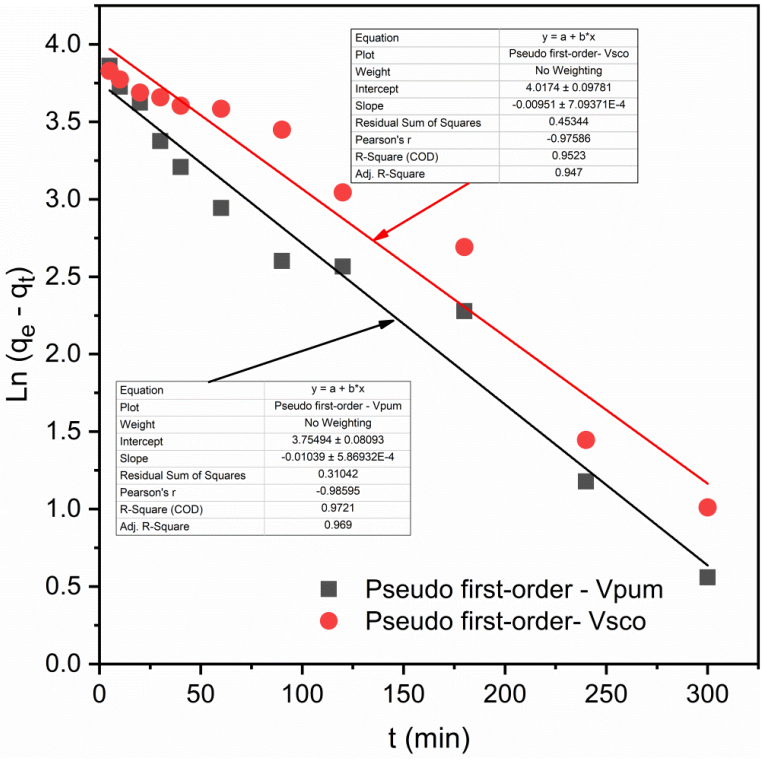

Figure A3. 4: Pseudo first-order kinetic plot for VPum and VSco

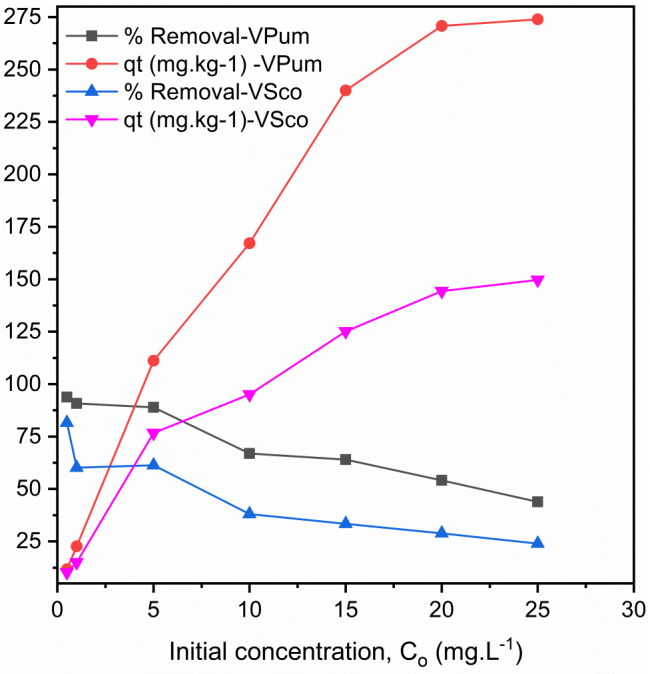

Figure A3. 5: Effects of initial concentration

Curriculum Vitae (CV)

Dereje Tadesse Mekonnen

Jimma University
P.O. Box: 378 Jimma,
Ethiopia
Mobile: +251-913140785
Personal Email: getdere@gmail.com
Institutionnel Email : dereje.tadesse@ju.edu.et
Google scholar/ResearchGate: Dereje Tadesse Mekonnen
Skype: getdereonline

Personal data

Date of Birth:	December 31, 1984
Place of birth:	Kiltu Baja/East Shewa/Oromia/Ethiopia
Sex:	Male
Marital Status:	Married
Nationality:	Ethiopian

Summary

Graduate of Chemical Engineering who has integrated academic achievement with administrative skills and capable of motivating and organizing others for research works with good interpersonal communication skills. Concrete practical and theoretical foundation supported by PhD in Environmental Engineering from University of Rostock, Germany in 2023, MSc in Chemical Engineering from Addis Ababa University, Ethiopia in 2010, and BSc in Chemical Engineering from Addis Ababa University, Ethiopia in 2008.

Software and Skills

Microsoft Office (Basic), SPSS, E-draw, ChemCAD, Origin Pro., RSM, and other basic computer operations.

Education

University of Rostock, Rostock, Germany 2023

PhD in Environmental Engineering at Faculty of Agriculture and Environmental Sciences

PhD thesis title:

Low-cost Adsorptive Technologies: Batch reactor and Fixed Bed Column Experiments for the Removal of Phosphate from Wastewater.

Addis Ababa University, Addis Ababa, Ethiopia, 2010

MSc in Chemical Engineering

MSc thesis title: Study of Domestic Solid waste management: Case Study of Jimma town, Southwestern

Ethiopia

Addis Ababa University, Addis Ababa, Ethiopia, 2008

BSc in Chemical Engineering
Final year project title**:** Starch Production form Inset.

Employment History

Assistant Professor, School of Chemical Engineering, Jimma Institute of Technology, Jimma University, Jimma, Ethiopia **Since 2010**

Achievements and responsibilities:

- Director, Academic Quality Assurance and Enhancement (from **October 2016 to September 2017**) at Jimma Institute of Technology
- Head, School of Chemical Engineering (from **July 8, 2010 to September 30, 2016**) at Jimma Institute of Technology, Jimma University, Jimma, Ethiopia
- Instructed different courses of Chemical Engineering for BSc students (Basic Environmental Engineering, Heat and Mass transfer, Thermal Unit operations, Mass Transfer, Appropriate Technology, Engineering Professions, Research Proposal, Entrepreneurship, Thermal and Mass transfer unit operations lab, Industrial Ecosystem), and for MSc students (Industrial ecosystems Engineering, Quality Control and Assurance)
- Research supervisor for postgraduate students in the area of Chemical Engineering (Process and Engineering).
- Project advisor for undergraduate as part of the BSc curriculum for the final year thesis
- Guided the revision and development of different curriculums, promotion and scholarship manuals and guidelines for Jimma Institute of Technology
- Monitored and followed up the progress and evaluation of teaching, research and community service activities within the department and across the faculty as deemed necessary.
- Reviewer at different Journals since 2020

Projects and researches

- Assessing Performance and characterization of domestic solid waste of Jimma town, Oromia, Ethiopia-Funded by JU research and publication director office, 2015-2016.
- Participated in different community-based research projects conducted by student by being as mentor at different time

Trainings and Workshops

- Participated in different workshops and leadership trainings at Ethiopia as well as abroad
- Trainer for entrepreneurship, life skill, and Work Habit

Publications and conferences

1. Mekonnen, D. T.; Alemayehu, E.; Lennartz, B. Removal of Phosphate Ions from Aqueous

Solutions by Adsorption onto Leftover Coal. Water 2020, 12, 1–15. https://doi.org/10.3390/w12051381.
2. Mekonnen, D. T.; Alemayehu, E.; Lennartz, B. Adsorptive Removal of Phosphate from Aqueous Solutions Using Low-Cost Volcanic Rocks: Kinetics and Equilibrium Approaches. Materials. 2021, 14. https://doi.org/10.3390/ma14051312
3. Mekonnen, D. T.; Alemayehu, E.; Lennartz, B. Fixed-Bed Column Technique for the Removal of Phosphate from Water Using Leftover Coal. Materials 2021, 14. https://doi.org/10.3390/ma14195466.
4. Bekele Bayu A, Mustefa Beyan S, Abeto Amibo T, Tadesse Mekonnen D. Production of fuel briquette from solid waste biomass using natural resin as a binder. Environmental Health Engineering and Management 2022; 9 (4) :321-328. https://doi.org/10.34172/EHEM.2022.34
5. Presented paper on the conference at Jimma University, April 2020 and 2019

References

1. Prof. Dr. Bernd Lennartz
Professor of Soil physics, Faculty of Agriculture and Environmental Sciences, University of Rostock
Justus Von-Liebeg Weg 6, 18051 Rostock, Germany
E-mail: bernd.lennartz@uni-rostock.de

2. Prof. Dr. -Ing Esayas Alemayehu
Professor of water and Environmental Engineering, Faculty of Civil and Environmental Engineering, Jimma Institute of Technology, Jimma University
P.O. Box 378 Jimma, Ethiopia
E-Mail: esayas16@yahoo.com

3. Dr. -Ing Berhanu Assefa (Asso. Prof.)
Addis Ababa Institute of Technology, Addis Ababa University
P.O. Box. 1176, Addis Ababa, Ethiopia
E-Mail: berassefa@yahoo.com